

The Pennsylvania State University  
The Graduate School  
Department of Civil and Environmental Engineering

**THE EFFECT OF ZINC ON THE  
BIOLOGICAL REDUCTION OF HEMATITE**

A Thesis in  
Environmental Engineering

by

James J. Stone

© 2002 James J. Stone

Submitted in Partial Fulfillment  
of the Requirements  
for the Degree of

Doctor of Philosophy

December 2002

We approve the thesis of James J. Stone.

Date of Signature

---

William D. Burgos  
Associate Professor of Environmental  
Engineering  
Thesis Advisor  
Chair of Committee

---

Susan L. Brantley  
Professor of Geosciences

---

Brian A. Dempsey  
Professor of Environmental Engineering

---

John M. Regan  
Assistant Professor of Environmental  
Engineering

---

Richard F. Unz  
Professor Emeritus of Environmental  
Microbiology

---

Paul P. Jovanis  
Professor of Civil Engineering  
Graduate Program Officer

---

---

---

---

---

---

## ABSTRACT

The impact of zinc on the reductive dissolution of hematite ( $\alpha$ -Fe<sub>2</sub>O<sub>3</sub>) by the dissimilatory metal-reducing bacterium (DMRB) *Shewanella putrefaciens* strain CN32 was studied. Experiments were conducted with a suspension of hematite (2.0 g L<sup>-1</sup>) in 10 mM PIPES (pH 6.8) and H<sub>2</sub> as an electron donor under non-growth conditions (10<sup>8</sup> cell mL<sup>-1</sup>). Experiments were also conducted with ferric citrate (2 mM) and nitrate (20 mg L<sup>-1</sup> NO<sub>3</sub>-N) to evaluate the effect of zinc with soluble electron acceptors. The net effect of zinc was measured based upon the change of rate or extent electron acceptor consumption. To further our understanding, additional hematite bioreduction experiments were performed using anthraquinone-2,6-disulfonate (AQDS), a soluble electron shuttling agent, ferrozine, a strong Fe(II) complexant, and natural organic material (NOM). All amendments were found to increase zinc inhibition compared to no-amendment biotic controls. Ferrozine and AQDS addition decreased Fe(II) sorption and increased zinc sorption. Increased zinc inhibition with ferrozine was a result of complexation of surface bound Fe(II) that subsequently allowed additional zinc sorption to cell and hematite surfaces. AQDS addition also increased surface sorbed zinc. Increased zinc inhibition during NOM addition was attributed both the Fe(II) complexation capacity and the surface sorption affinity of the NOM. Taken together, the results show that surface sorbed zinc was a more potent inhibitor of hematite bioreduction than free zinc, especially in the presence of the amendments studied.

## TABLE OF CONTENTS

ABSTRACT .....	iii
LIST OF FIGURES .....	vi
LIST OF TABLES .....	x
ACKNOWLEDGEMENTS .....	xi
<b>CHAPTER 1: Introduction .....</b>	<b>1</b>
1.1 Introduction .....	1
1.2 Research Objectives .....	2
1.3 Dissertation Layout .....	3
1.4 Literature Cited .....	3
<b>CHAPTER 2: Impact of zinc on the biological Fe(III) and NO<sub>3</sub><sup>-</sup> reduction by                     <i>Shewanella putrefaciens</i> CN32 .....</b>	<b>5</b>
2.1 Abstract .....	5
2.2 Introduction .....	6
2.3 Experimental .....	8
2.3.1 Microorganism and Culture Conditions .....	8
2.3.2 Iron Oxide .....	8
2.3.3 Bioreduction Experiment Preparation .....	9
2.3.4 Hematite Bioreduction .....	9
2.3.5 Ferric Citrate Bioreduction .....	10
2.3.6 Nitrate Bioreduction .....	11
2.3.7 DMRB Growth .....	11
2.3.8 Analytical Techniques .....	11
2.4 Results .....	12
2.4.1 Hematite Bioreduction .....	12
2.4.2 DMRB Growth .....	14
2.4.4 Variable Hematite and DMRB Concentrations .....	15
2.4.5 Ferric Citrate Bioreduction .....	17
2.4.6 Nitrate Bioreduction .....	18
2.4.7 Evaluation of Zinc Inhibition .....	18
2.5 Discussion .....	20
2.6 Acknowledgments .....	23
2.7 Literature Cited .....	24
<b>CHAPTER 3: Modes of inhibition by zinc on the biological reduction of hematite                     by <i>Shewanella putrefaciens</i> CN32 .....</b>	<b>36</b>
3.1 Abstract .....	36
3.2 Introduction .....	37
3.3 Experimental .....	40

3.3.1	Microorganism and Culture Conditions.....	40
3.2.2	Materials.....	41
3.2.3	Bioreduction Experiment Preparation.....	41
3.2.4	Hematite Bioreduction.....	42
3.2.5	Zinc and Manganese Sorption.....	42
3.2.6	Analytical Techniques.....	43
3.3	Results.....	43
3.3.1	Effect of Ferrozine and AQDS on Zinc Inhibition.....	43
3.3.2	Impact of Fe(II) Sorption with Amendment Addition.....	45
3.3.3	Impact of Zinc on Fe(II) Adsorption.....	46
3.3.4	Zn(II) Sorption.....	47
3.3.5	Impact of Amendments on Fe(II) and Zn(II) Adsorption.....	47
3.3.6	Impact of Mn(II) Addition.....	48
3.3.7	Fe(II) and Mn(II) Sorption.....	49
3.4	Discussion.....	50
3.5	Conclusion.....	55
3.6	Acknowledgments.....	56
3.7	Literature Cited.....	57

CHAPTER 4: The effect of natural organic matter on zinc inhibition of the biological Fe(III) and nitrate reduction by *Shewanella putrefaciens* CN32..... 70

4.1	Abstract.....	70
4.2	Introduction.....	71
4.3	Experimental.....	73
4.3.1	Microorganism and Culture Conditions.....	73
4.3.2	Materials.....	73
4.3.3	NOMs.....	74
4.3.4	Bioreduction Experiment Preparation.....	74
4.3.5	Hematite Bioreduction.....	75
4.3.6	Ferric Citrate Bioreduction.....	75
4.3.7	Nitrate Bioreduction.....	76
4.3.8	Analytical Techniques.....	76
4.3.9	Dialysis.....	76
4.4	Results.....	77
4.4.1	Impact of NOM on Hematite Bioreduction.....	77
4.4.2	Impact of Fe(II) Sorption with NOM Addition.....	79
4.4.3	SRNOM Equilibrium Dialysis.....	80
4.4.4	Impact on Ferric Citrate Bioreduction.....	81
4.4.5	Impact on Nitrate Bioreduction.....	82
4.4.6	Impact of Manganese Addition.....	83
4.5	Discussion.....	84
4.6	Acknowledgments.....	90
4.7	Literature Cited.....	91

## LIST OF FIGURES

- Figure 2.1 (A) Total, (B) dissolved Fe(II) production as a function of time (0 to 5 d) for the biological reduction of 2 g L<sup>-1</sup> hematite at pH 6.8 in 10 mM PIPES. Zinc addition ranged from 0 mg L<sup>-1</sup> for the biotic and abiotic controls to 15 mg L<sup>-1</sup>. *Shewanella putrefaciens* CN32 was used (10<sup>8</sup> cells mL<sup>-1</sup>) under non-growth conditions. Abiotic and biotic controls produced ≤ 0.0 and 0.2 mg L<sup>-1</sup> total Fe(II), respectively. Values are means of three replicates. .... 28
- Figure 2.2 (A) Planktonic, (B) coagulated with hematite viability percentages for BacLight LIVE/DEAD cell counts (*S. putrefaciens*) as a function of time (0 to 5 d) for variable zinc addition (0-15 mg L<sup>-1</sup>) during biological reduction of 2 g L<sup>-1</sup> hematite under non-growth conditions. Values are means of five replicates..... 29
- Figure 2.3 Inhibition of *S. putrefaciens* growth (24 h) as a function of variable free zinc addition (from 0-180 mg L<sup>-1</sup> total zinc) within M1 growth media at 20°C. Inhibition calculated as 420 nm absorbance difference between zinc containing sample and no zinc controls. Free zinc from MINTEQA2 speciation calculations..... 30
- Figure 2.4 Total Fe(II) production as a function of time (0 to 5 d) for (A) variable hematite (0.25-2.0 g L<sup>-1</sup>), (B) variable *S. putrefaciens* (10<sup>6</sup>-10<sup>8</sup> cells mL<sup>-1</sup>) as a function of time under non-growth conditions. All experiments conducted in 10 mM PIPES with no zinc addition. Variable hematite experiments used 10<sup>8</sup> cells mL<sup>-1</sup> DMRB concentrations and variable DMRB experiments used 2.0 g L<sup>-1</sup> hematite. Values are means of three replicates (± standard deviation). .... 31
- Figure 2.5 Normalized summary of (A) total Fe(II) production, (B) percent BacLight planktonic viability as a function of *S. putrefaciens* concentration per mass of hematite [cells g<sup>-1</sup>] for all results from variable hematite and variable *S. putrefaciens* hematite bioreduction experiments pH 6.8. Experiments conducted in 10 mM PIPES with no zinc. .... 32
- Figure 2.6 Dissolved Fe(II) as a function of time (0 to 6 h) for the biological reduction of 2 mM ferric citrate in 10 mM PIPES, 4 mM citric acid at pH 6.8. Zinc addition ranged from 0 mg L<sup>-1</sup> (for biotic and abiotic controls) to 90 mg L<sup>-1</sup>. Values are means of three replicates. .... 33
- Figure 2.7 (A) Percentage of total nitrate reduction relative to initial nitrate concentration, (B) percent of planktonic cells that are viable as a function of time (0 to 27 h) for the biological reduction of nitrate with variable zinc. Solution consisted of 10 mM PIPES, 144.4 mg L<sup>-1</sup> KNO<sub>3</sub> (equivalent to 20 mg NO<sub>3</sub>-N L<sup>-1</sup>), 10<sup>8</sup> cells mL<sup>-1</sup> at pH 6.8. Zinc addition ranged from 0 mg L<sup>-1</sup> for biotic and abiotic controls to 30 mg L<sup>-1</sup>. Values are means of three replicates (± standard deviation)..... 34

- Figure 2.8 Inhibition of the maximum extent of bioreduction using *S. putrefaciens* for 2 g L<sup>-1</sup> hematite, 2 mM ferric citrate, 20 mg L<sup>-1</sup> NO<sub>3</sub><sup>-</sup>N, and *S. putrefaciens* growth in M1 media as a function of (A) log total zinc, (B) log free zinc. Free zinc results determined from MINTEQA2 calculations. .... 35
- Figure 3.1 (A) Total Fe(II) production and (B) planktonic cell viability as a function of variable zinc for (■) 1.46 mM ferrozine, (Δ) 50μM ADQS, (○) no amendment control. Experiments performed using 2 g L<sup>-1</sup> hematite in 10mM PIPES, pH 6.8, 10<sup>8</sup> *S. putrefaciens* cells mL<sup>-1</sup>. All values are means of three replicates. .... 62
- Figure 3.2 Summary of percent inhibition of 5 d, total Fe(II) production as a function of total zinc concentration for (■) 1.46mM ferrozine, (Δ) 50μM ADQS, (○) no amendment control. Percent inhibition calculated from least squares estimate from no-zinc controls. Bioreduction samples included 2 g L<sup>-1</sup> hematite, 10<sup>8</sup> *S. putrefaciens* cells mL<sup>-1</sup>, 10mM PIPES, pH 6.8. Dashed lines represent 95% confidence interval. Values are means of three replicates. .... 63
- Figure 3.3 The distribution of Fe(II) during the biological reduction of 2 g L<sup>-1</sup> hematite using *S. putrefaciens* (10<sup>8</sup> cell mL<sup>-1</sup>) for (A) no-zinc, no-amendment controls, (B) variable zinc samples. Solid line is Freundlich isotherm trend line (R<sup>2</sup> = 0.890, K = 0.01156 mM Fe(II) g<sup>-1</sup>, 1/n = 0.6603) for the no-zinc, no-amendment control and dashed line represents 95% confidence interval. Results are 1-5 d composite samples. .... 64
- Figure 3.4 Langmuir zinc sorption distribution for (Δ) 2.0 g L<sup>-1</sup> hematite and 10<sup>8</sup> pasteurized cells mL<sup>-1</sup> (non-viable), (●) 2.0 g L<sup>-1</sup> hematite and 10<sup>8</sup> cells mL<sup>-1</sup> with biogenic Fe(II) (0.088 - 0.296 mM), (□) 10<sup>8</sup> pasteurized cells mL<sup>-1</sup>, and (◆) 2.0 g L<sup>-1</sup> hematite. Results are 5 d values at pH 6.8. All values are means of three replicates. .... 65
- Figure 3.5 The Freundlich sorption distribution of (A) Fe(II) and (B) zinc in the presence of (○) 50μM AQDS, (▲) 1.46 mM ferrozine during the biological reduction of 2 g L<sup>-1</sup> hematite using *S. putrefaciens* (10<sup>8</sup> cell mL<sup>-1</sup>). Solid lines represent no-amendment Fe(II) sorption (R<sup>2</sup> = 0.890, K = 0.01156 mM Fe(II) g<sup>-1</sup>, 1/n = 0.6603) and no-amendment, Fe(II) containing (0.088 - 0.296 mM) zinc sorption (R<sup>2</sup> = 0.894, K = 0.01475 mM Zn(II) g<sup>-1</sup>, 1/n = 0.532). Dashed line represents 95% confidence interval. Results are 5 d at pH 6.8. All values are means of three replicates. .... 66
- Figure 3.6 The effect of variable manganese on 5 d (A) total and dissolved Fe(II) production, (B) planktonic cell viability as a function of total manganese. Experiments performed using 2 g L<sup>-1</sup> hematite in 10mM PIPES, pH 6.8, 10<sup>8</sup> *S. putrefaciens* cells mL<sup>-1</sup>. All values are means of three replicates (± standard deviation). Error bars smaller than symbol are not shown. .... 67

- Figure 3.7 The Freundlich sorption distribution of Fe(II) during the biological reduction of 2 g L<sup>-1</sup> hematite using *S. putrefaciens* (10<sup>8</sup> cell mL<sup>-1</sup>) and variable manganese (0 – 1.82 mM). Solid line represents no-amendment Fe(II) sorption trend line in absence of manganese ( $R^2 = 0.890$ ,  $K = 0.01156 \text{ mM Fe(II) g}^{-1}$ ,  $1/n = 0.6603$ ) and dashed line represents 95% confidence interval. Results are 5 d at pH 6.8. .... 68
- Figure 3.8 Langmuir manganese sorption distribution for ( $\Delta$ ) 2.0 g L<sup>-1</sup> hematite and 10<sup>8</sup> pasteurized cells mL<sup>-1</sup> (non-viable), ( $\bullet$ ) 2.0 g L<sup>-1</sup> hematite and 10<sup>8</sup> cells mL<sup>-1</sup> with biogenic Fe(II) (0.104 – 0.200 mM). Results are 5 d values at pH 6.8. All values are means of three replicates. .... 69
- Figure 4.1 (A) Total Fe(II) production and (B) percent inhibition of Fe(II) production as a function of total zinc for ( $\circ$ ) no amendment control, ( $\blacktriangle$ ) 250 mg L<sup>-1</sup> SHA, ( $\square$ ) 150 mg L<sup>-1</sup> SHA, ( $\bullet$ ) 75 mg L<sup>-1</sup> SHA, ( $\diamond$ ) 15 mg L<sup>-1</sup> SHA. Experiments performed using 2 g L<sup>-1</sup> hematite in 10mM PIPES, pH 6.8, 10<sup>8</sup> *S. putrefaciens* cells mL<sup>-1</sup>, 5 d. Dashed line in (B) represents 95% confidence interval. All values are means of three replicates. .... 96
- Figure 4.2 (A) Total Fe(II) production and (B) percent inhibition of Fe(II) production as a function of total zinc for ( $\blacksquare$ ) 150 mg L<sup>-1</sup> SRFA, ( $\Delta$ ) 250 mg L<sup>-1</sup> SRHA. Experiments performed using 2 g L<sup>-1</sup> hematite in 10mM PIPES, pH 6.8, 10<sup>8</sup> *S. putrefaciens* cells mL<sup>-1</sup>, 5 d. Dashed line in (B) represents 95% confidence interval. All values are means of three replicates. .... 97
- Figure 4.3 The sorption distribution of (A) Fe(II) without zinc, (B) Fe(II) with variable zinc (0.020 to 0.178 mM total zinc), (C) Zn(II) with variable Fe(II) [0.012 to 0.51 mM total Fe(II)] for ( $\blacktriangle$ ) 250 mg L<sup>-1</sup> SHA, ( $\square$ ) 150 mg L<sup>-1</sup> SHA, ( $\bullet$ ) 75 mg L<sup>-1</sup> SHA, ( $\diamond$ ) 15 mg L<sup>-1</sup> SHA, ( $\blacksquare$ ) 150 mg L<sup>-1</sup> SRFA, ( $\Delta$ ) 250 mg L<sup>-1</sup> SRHA addition during the 5 d biological reduction of 2 g L<sup>-1</sup> hematite, 10<sup>8</sup> *S. putrefaciens* cells mL<sup>-1</sup>, pH 6.8. Solid line is Freundlich (non-log) isotherm trend line (for Fe(II):  $R^2 = 0.890$ ,  $K = 0.01156 \text{ mM Fe(II) g}^{-1}$ ,  $1/n = 0.6603$ ; for Zn(II):  $R^2 = 0.894$ ,  $K = 0.01475 \text{ mM Zn(II) g}^{-1}$ ,  $1/n = 0.532$ ) for the no amendment control and dashed line represents 95% confidence interval. Results are 5 d composite samples. .... 98
- Figure 4.4 The SRNOM zinc complexation isotherm using 500 MWCO dialysis separation at pH 6.8 with 0.153 mM total zinc. Results are 180 d composite samples. SRNOM concentration ranged from 0 mg L<sup>-1</sup> for controls to 200 mg L<sup>-1</sup>. All values are means of three replicates ( $\pm$  standard deviation). .... 99
- Figure 4.5 The percent of inhibition of the rate of Fe(II) production as a function of log total zinc for the addition of ( $\blacktriangle$ ) 250 mg L<sup>-1</sup> SHA, ( $\square$ ) 150 mg L<sup>-1</sup> SRFA during the biological reduction of 2 mM ferric citrate in 10 mM PIPES, 4 mM citric acid at pH 6.8. Zinc addition ranged from 0.020 to 6.88 mM total zinc.



Solid line represents the no-NOM control and dashed line the 95% confidence interval. Values are means of three replicates. .... 100

- Figure 4.6 The percent inhibition of the rate of nitrate reduction as a function of log total zinc with the addition of (○) 1000 mg L<sup>-1</sup> SRFA, (□) 150 mg L<sup>-1</sup> SRFA, (▲) 250 mg L<sup>-1</sup> SHA. Solid line represents the no-NOM control and dashed line the 95% confidence interval. Solutions contain 10 mM PIPES, 14.44 g L<sup>-1</sup> KNO<sub>3</sub> (equivalent to 20 mg NO<sub>3</sub>-N L<sup>-1</sup>), 10<sup>8</sup> cells mL<sup>-1</sup> at pH 6.8. Zinc addition ranged from 0 mM for biotic and abiotic controls to 0.459 mM total zinc. Values are means of three replicates. .... 101
- Figure 4.7 The percent inhibition of (A) total Fe(II) production during hematite reduction and (B) rate of nitrate reduction as a function of log total manganese addition for (□) no-NOM control, (Δ) 150 mg L<sup>-1</sup> SRFA, (●) 250 mg L<sup>-1</sup> SHA addition. All values are means of three replicates. .... 102
- Figure 4.8 The sorption distribution of (A) Fe(II) with variable Mn(II) (0.020 to 0.910 mM total manganese), (B) Mn(II) with variable Fe(II) [0.104 to 0.200 mM total Fe(II)] for (Δ) 150 mg L<sup>-1</sup> SRFA, (●) 250 mg L<sup>-1</sup> SHA addition during the 5 d biological reduction of 2 g L<sup>-1</sup> hematite, 10<sup>8</sup> *S. putrefaciens* cells mL<sup>-1</sup>, pH 6.8. Solid line is Freundlich (non-log) isotherm trend line (for Fe(II): R<sup>2</sup> = 0.890, K = 0.01156 mM Fe(II) g<sup>-1</sup>, 1/n = 0.6603; for Mn(II): R<sup>2</sup> = 0.780, K = 0.00452 mM Mn(II) g<sup>-1</sup>, 1/n = 0.448) for the no-amendment control and dashed line represents 95% confidence interval. Results are 5 d composite samples.... 103

## LIST OF TABLES

Table 2.1	Summary of 50% inhibition value in literature for zinc and other similar Me(II). ...	27
Table 3.1	Summary of zinc and manganese IC <sub>50</sub> <sup>a</sup> values for the biological reduction of hematite by <i>S. putrefaciens</i> CN32. All experiments were performed with 2 g L <sup>-1</sup> hematite and 10 <sup>8</sup> cells mL <sup>-1</sup> in 10mM PIPES (pH 6.8) at 20°C.....	60
Table 4.1	Characteristics of NOM.....	94
Table 4.2	Summary of zinc IC <sub>50</sub> <sup>a</sup> values for the biological reduction of hematite, ferric citrate, and nitrate by <i>S. putrefaciens</i> .....	95

## ACKNOWLEDGEMENTS

I would like to thank Bill Burgos for his outstanding guidance throughout my entire doctoral program. It was an honor to work under his tutelage. Obtaining this degree would not have materialized without his conviction that I could achieve this lofty goal. Thank you for allowing this opportunity and for believing in me. I also thank Tanja Cutting for her generous support and loyal devotion throughout the second half of my graduate school career, helping to steer my internal compass. I extend my thank you to Rich Royer for his invaluable assistance both in and out of the laboratory. I also thank Brian Dempsey and Richard Unz for their involvement and guidance throughout this project. Many thanks to numerous Kappe residents, both past and present, for their technical assistance. I extend my appreciation to the Department of Energy for funding this innovative work. And finally, I thank my parents for all of their support and encouragement that they provided during my graduate studies.

# CHAPTER 1

## INTRODUCTION

### 1.1 Introduction

The development of nuclear energy and weaponry during the cold war era resulted in a vast network of facilities engaged in manufacturing and testing of hazardous materials. As a result, “legacy” waste sites throughout the domain of the U.S. Department of Energy (DOE) remain. Many of these sites contain a complex array of heavy metal and radionuclide contaminated soil and groundwater (Riley et al. 1992). As part of its ongoing decontamination and remediation efforts, the DOE created the Natural and Accelerated Bioremediation Research (NABIR) program to investigate new and innovative remediation technologies. Results from the NABIR program research have shown that the microbial reduction of Fe(III) oxides may be a promising technology for decontaminating these waste sites. This remediation occurs primarily through the mobilization or immobilization of selected contaminants through the reductive dissolution or precipitation of metals and associated Fe(III) oxides.

While results have demonstrated that reductive dissolution may assist with remediation efforts (Arnold et al. 1988; Roden et al. 1996; Fredrickson et al. 1998; Zachara et al. 1998), relatively few studies (Cooper et al. 2000; Parmar et al. 2001; Zachara et al. 2001) have examined how effective this process will be in the presence of high metal concentrations that may be found at these sites. Metal-microbial interactions are well documented (Baath 1989; Kushner 1993; Gadd 1996; Warren et al. 2001), however the impact of metals on the biological reduction of Fe(III) oxides by dissimilar metal reducing bacteria (DMRB) is relatively unknown.

The interactions between the metals and DMRB may exert significant control on the overall effectiveness of bioremediation at these contaminated sites.

The purpose of this research was to investigate the effects of zinc on the biological reduction of hematite by DMRB *S. putrefaciens* strain CN32. Zinc is a common soil and groundwater contaminant at many DOE sites, and therefore was chosen as a representative heavy metal for this research. Heavy metals are known to adversely effect microorganisms several ways ranging from altering key enzymes that regulate intracellular transport (Welp et al. 1997) to displacement of essential cations on carboxyl and phosphoryl reactive sites on cell walls (Fein et al. 2001). It was initially thought that the presence of zinc would inhibit solid-phase biological iron reduction by at least two mechanism – via direct toxicity of the DMRB or through modification of the DMRB or iron oxide surface affecting DMRB-oxide contact or bioreduction. Experiments were conducted with both solid (hematite) and soluble-phase (nitrate, ferric citrate) terminal electron acceptors to elucidate the mechanisms of zinc inhibition. Furthermore, experiments were performed using amendments to determine if their presence could mitigate zinc inhibition during biological hematite reduction.

## 1.2 Research Objectives

- Determine the mechanisms of zinc toxicity on *S. putrefaciens* CN32;
- Ascertain the mechanisms of zinc inhibition during the biological reduction of hematite by *S. putrefaciens* CN32;
- Determine the feasibility of amendment addition for relieving the inhibitory effects of zinc. Amendments investigated included the following:
  - Ferrozine, a known Fe(II) chelating compound

- Anthraquinone-2,6-disulfonate (AQDS), a soluble electron shuttling agent
- Various aquatic and terrestrial natural organic materials (NOM), all of which promote dissolved Me(II) complexation.

### 1.3 Dissertation Layout

This dissertation consists of three manuscripts related to the study of zinc inhibition on the biological reduction of hematite by *S. putrefaciens* CN32. The dissertation is divided into the following sections:

- Chapter 2 (Manuscript 1): "Impact of zinc on the biological Fe(III) and NO<sub>3</sub><sup>-</sup> reduction by *Shewanella putrefaciens* CN32"
- Chapter 3 (Manuscript 2): "Modes of inhibition by zinc on the biological reduction of hematite by *Shewanella putrefaciens* CN32"
- Chapter 4 (Manuscript 3): "The effect of natural organic matter on zinc inhibition of the biological Fe(III) and nitrate reduction by *Shewanella putrefaciens* CN32"

### 1.4 Literature Cited

- Arnold, R. G., T. J. Dichristina, et al. (1988). "Reductive dissolution of Fe(III) oxides by *Pseudomonas* Sp 200." Biotechnology and Bioengineering 32(9): 1081-1096.
- Baath, E. (1989). "Effects of heavy-metals in soil on microbial processes and populations (a review)." Water Air and Soil Pollution 47(3-4): 335-379.
- Cooper, D. C., F. Picardal, et al. (2000). "Zinc immobilization and magnetite formation via ferric oxide reduction by *Shewanella putrefaciens* 200." Environmental Science & Technology 34(1): 100-106.
- Fein, J. B., A. M. Martin, et al. (2001). "Metal adsorption onto bacterial surfaces: Development of a predictive approach." Geochimica et Cosmochimica Acta 65(23): 4267-4273.
- Fredrickson, J. K., J. M. Zachara, et al. (1998). "Biogenic iron mineralization accompanying the dissimilatory reduction of hydrous ferric oxide by a groundwater bacterium." Geochimica et Cosmochimica Acta 62(19-20): 3239-3257.
- Gadd, G. M. (1996). "Influence of microorganisms on the environmental fate of radionuclides." Endeavour 20(4): 150-156.

- Kushner, D. J. (1993). "Effects of speciation of toxic metals on their biological activity." Water Pollution Residuals Journal of Canada 28(1): 111-128.
- Parmar, N., Y. A. Gorby, et al. (2001). "Formation of green rust and immobilization of nickel in response to bacterial reduction of hydrous ferric oxide." Geomicrobiology Journal 18(4): 375-385.
- Riley, R. G. and J. M. Zachara, Eds. (1992). Chemical contaminants on DOE lands and selection of contaminant mixtures for subsurface science research. Washington, D.C., U.S. Department of Energy.
- Roden, E. E. and J. M. Zachara (1996). "Microbial reduction of crystalline iron(III) oxides: Influence of oxide surface area and potential for cell growth." Environmental Science & Technology 30(5): 1618-1628.
- Warren, L. A. and E. A. Haack (2001). "Biogeochemical controls on metal behaviour in freshwater environments." Earth-Science Reviews 54(4): 261-320.
- Welp, G. and G. W. Brummer (1997). "Microbial toxicity of Cd and Hg in different soils related to total and water-soluble contents." Ecotoxicology and Environmental Safety 38(3): 200-204.
- Zachara, J. M., J. K. Fredrickson, et al. (1998). "Bacterial reduction of crystalline Fe<sup>3+</sup> oxides in single phase suspensions and subsurface materials." American Mineralogist 83(11-12): 1426-1443.
- Zachara, J. M., J. K. Fredrickson, et al. (2001). "Solubilization of Fe(III) oxide-bound trace metals by a dissimilatory Fe(III) reducing bacterium." Geochimica et Cosmochimica Acta 65(1): 75-93.

## CHAPTER 2

### Impact of Zinc on Biological Fe(III) and NO<sub>3</sub><sup>-</sup>

#### Reduction by *Shewanella putrefaciens* CN32

### 2.1 Abstract

The impact of zinc on the reductive dissolution of hematite ( $\alpha$ -Fe<sub>2</sub>O<sub>3</sub>) by the dissimilatory metal-reducing bacterium (DMRB) *Shewanella putrefaciens* strain CN32 was studied.

Experiments were conducted with a suspension of hematite (0.25 to 2.0 g L<sup>-1</sup>) in 10 mM PIPES (pH 6.8) and H<sub>2</sub> as an electron donor under non-growth conditions (10<sup>6</sup> to 10<sup>8</sup> cell mL<sup>-1</sup>), spiked with zinc (0 to 15 mg L<sup>-1</sup>), and incubated for 5 days. Experiments were also conducted with ferric citrate (2 mM) and nitrate (20 mg NO<sub>3</sub>-N L<sup>-1</sup>) to evaluate the effect of zinc with soluble electron acceptors. The effect of zinc was measured based on the rate and extent of consumption of the electron acceptor in the absence and presence of zinc. The toxicity of zinc was measured based on direct counts of viable cells using the LIVE/DEAD *Ba*clight staining procedure.

Results indicated that total zinc concentrations less than 6.5 mg L<sup>-1</sup> increased Fe(II) production during the bioreduction of hematite, yet decreased cell viability. No cells remained viable at total zinc concentrations greater than 15 mg L<sup>-1</sup> in the hematite suspensions. An inhibitory concentration (IC<sub>50</sub>) was defined as the zinc concentration that reduced the consumption of an electron acceptor by 50% compared to a control. The total zinc IC<sub>50</sub> for ferric citrate, hematite, and nitrate reduction were 18.6, 13.8, and 3.2 mg L<sup>-1</sup>, respectively. The free zinc IC<sub>50</sub> for hematite, ferric citrate and nitrate reduction were 8.6 mg L<sup>-1</sup>, 0.023 mg L<sup>-1</sup> and 3.2 mg L<sup>-1</sup>, respectively. The free zinc IC<sub>50</sub> for cell growth on lactate in metal containing M1 growth



medium was  $3.3 \text{ mg L}^{-1}$ . Uncertainty was associated with free zinc estimates in the ferric citrate experiments due to the high citrate (6 mM) concentration. The convergence of  $IC_{50}$  values based on free zinc suggests that free zinc was most directly related to the inhibition of anaerobic respiration.

## 2.2 Introduction

The microbial reduction of Fe(III) has been recognized as an important process for the bioremediation of heavy metals and radionuclides within contaminated aquifers. Much recent research has focused on the use of dissimilatory metal-reducing bacteria (DMRB) to promote the mobilization or immobilization of selected contaminants through the reductive dissolution or precipitation of these metals and associated iron oxides. However, few studies have examined the effects of elevated concentrations of toxic metals on biological metal reduction. Many studies have documented metal-microbe interactions (Baath 1989; Kushner 1993; Gadd 1996; Warren et al. 2001), but relatively few studies (Cooper et al. 2000; Parmar et al. 2001) have specifically focused on the impact of metals on solid-phase iron oxide reduction by the DMRB *Shewanella. putrefaciens*. This gram negative facultative anaerobe can reduce crystalline (Cooper et al. 2000; Zachara et al. 2001; Royer et al. 2002a; Royer et al. 2002b) and non-crystalline iron oxides (Fredrickson et al. 2001), soluble Fe(III) complexes (Liu et al. 2001), nitrate, and a variety of toxic metals and radionuclides including Co(III), Cr(VI), Tc(VII) and U(VI).

Heavy metals are known to affect a multitude of microbial processes ranging from altering key enzymes regulating intracellular transport (Welp et al. 1997a) to displacement of essential cations on carboxyl and phosphoryl reactive sites on the cell wall (Fein et al. 2001).

Previous studies related to heavy metal toxicity have focused on the influence of metals on microbial growth or respiration, and on metal accumulation or precipitation on microbial surfaces. Few studies related to heavy metal toxicity have examined how metals affect the biological reduction of an insoluble electron acceptor (e.g., solid-phase iron oxide). Heavy metals such as zinc, copper, and cobalt are essential micronutrients for microorganisms at low concentrations (ca.  $30 \mu\text{g L}^{-1}$ ) (Raven 1984), but when these beneficial concentrations are exceeded, microbial enzyme activity can be permanently altered. Zinc is a common ground water pollutant and has been found in ground waters at US Department of Energy (DOE) facilities at concentrations exceeding  $697 \text{ mg L}^{-1}$ , easily the highest heavy metal concentration present (Riley et al. 1992). In addition, pH-dependent sorption edge experiments (for hydrous ferric oxide) have shown that zinc sorption reaches a constant maximum value (i.e., plateau) above ca. pH 5.0 (Dzombak et al. 1990). Thus, at circumneutral and alkaline pH values, zinc will be both sorbed to mineral surfaces and in solution.

The purpose of this research was to investigate the effects of zinc on the biological reduction of hematite by the DMRB *S. putrefaciens* strain CN32. The initial hypothesis was that zinc could inhibit solid-phase biological iron reduction by at least two mechanisms – via direct toxicity/lethality to the DMRB, or via modification of the oxide and/or DMRB surfaces due to zinc sorption that would affect DMRB-oxide contact or bioreduction. Therefore, experiments were conducted with soluble electron acceptors, specifically ferric citrate and nitrate, to minimize the influence of zinc sorption to hematite for respiration by *S. putrefaciens*. The objectives of the study were to determine the effect of zinc on activity and viability of *S. putrefaciens* as a function of electron acceptor, electron donor, and complexation of zinc and Fe(II).

## 2.3 Experimental

### 2.3.1 Microorganism and Culture Conditions

*Shewanella putrefaciens* strain CN32 was provided courtesy of Dr. David Balkwill (Subsurface Microbial Culture Collection, Florida State University). *S. putrefaciens* CN32 was isolated from an anaerobic subsurface core sample (250 m below ground surface) from the Morrison Formation in northwestern New Mexico (Fredrickson et al. 1998). The cultures were grown aerobically on tryptic soy broth without dextrose (TSB-D) at 20°C (Zachara et al. 2001). Cells were harvested by centrifugation (4900 g, 10 min, 20°C) from a 16-hour-old culture (late log-decreasing growth phase). The cells were washed three times in 10 mM 1,4-piperazinediethanesulfonic acid (PIPES; pH=6.8) with the final wash made with deoxygenated solution. Cell pellets were resuspended in 5-15 ml of deoxygenated 10 mM PIPES buffer in an anaerobic chamber (Coy; Grass Lakes, MI) under a N<sub>2</sub>:H<sub>2</sub> (ca. 97.5:2.5%) atmosphere and the cell density was determined by absorbance at 420 nm.

### 2.3.2 Iron Oxide

An iron oxide powder was obtained from J.T. Baker and identified by X-ray diffraction and Mössbauer spectroscopy to be hematite ( $\alpha$ -Fe<sub>2</sub>O<sub>3</sub>) of greater than 99% purity. The hematite had an average particle diameter of 1.0  $\mu$ m measured by laser diffraction and a specific surface area of 9.04 m<sup>2</sup> g<sup>-1</sup> measured by 5-point N<sub>2</sub>-BET. The zero point of charge was pH 8.5 as determined by electrophoretic mobility and proton titrations discussed elsewhere (Jeon et al. 2001). The hematite surface site density for Fe(II) was 5.1 sites per nm<sup>2</sup> based upon adsorption of Fe(II) (Jeon et al. 2001). Hematite was heated to 550°C in air overnight before use to remove

any residual organic carbon. Hematite was added to anaerobic PIPES buffer at least 24 h prior to any experiment to allow for hydration.

### **2.3.3 Bioreduction Experiment Preparation**

A “master reactor” approach was used to prepare all experiments (Royer et al. 2002a) to ensure consistent chemical and biological conditions. All preparations were performed within a Coy anaerobic chamber (Grass Lakes, MI). A master reactor was prepared by combining the electron acceptor and the inoculum in a 120 mL serum bottle. All solutions (except the zinc stock) were prepared in 10 mM PIPES (pH 6.8). Biotic no-zinc controls were immediately prepared by transferring 10 mL of the suspension into 20 mL amber serum bottles (in at least triplicate). All 20 mL serum bottles were crimp-sealed with Teflon-faced butyl rubber stoppers and aluminum caps. Zinc was incrementally added to the master reactor in an acidified and deoxygenated  $\text{ZnCl}_2$  solution ( $1,000 \text{ mg L}^{-1}$  AAS certified standard) along with an equal volume of 0.1 N NaOH (for pH maintenance). At each concentration, 10 mL of the suspension was transferred into 20 mL amber serum bottles (in triplicate). Five to seven different zinc concentrations were usually prepared. Sealed serum bottles were incubated in the dark at  $20^\circ\text{C}$  on orbital shakers outside of the anaerobic chamber. Hydrogen from the anaerobic chamber atmosphere (97.5:2.5%  $\text{N}_2:\text{H}_2$ ) was used as the electron donor in all experiments except for the DMRB growth experiments where lactate was used.

### **2.3.4 Hematite Bioreduction**

Most experiments were performed with  $2.0 \text{ g L}^{-1}$  hematite (25 mM as Fe), a final cell density of  $10^8 \text{ cells mL}^{-1}$ , and zinc concentrations ranging from 0 to  $15 \text{ mg L}^{-1}$ . After incubation times of 1, 2, 3, 4, and 5 d, reactors were sacrificed to measure dissolved and total Fe(II), dissolved and total zinc, pH, and cell viability of both planktonic and hematite surface sorbed

cells. A series of no-zinc experiments were performed with variable concentrations of hematite and DMRB to evaluate the “baseline” effect of these experimental conditions on iron reduction and cell viability. These experiments were performed with 0.25 to 2.0 g L<sup>-1</sup> hematite, a final cell density of 10<sup>6</sup> to 10<sup>8</sup> cells mL<sup>-1</sup>, and no zinc, and reactors were sacrificed after 1, 2, 3, 4, and 5 d.

An additional hematite bioreduction experiment was performed with cells that had been exposed to zinc immediately prior to the start of the experiment. DMRB were prepared as before, however, a total zinc concentration of 5.3 mg L<sup>-1</sup> was included in a third aerobic wash of the cells (PIPES buffer) and the cell suspension was mixed aerobically on an orbital shaker for 2 h. The cell suspension was rinsed three additional times to remove all zinc, once with aerobic PIPES and twice with deoxygenated PIPES. A no-zinc un-exposed control cell suspension was also prepared, held for 2 h, and underwent the additional washings. Final cell suspensions (approximately 15 mL) were analyzed for dissolved and total zinc and no residual zinc was detected. The pre-exposed and un-exposed cell suspensions (final cell density of 10<sup>8</sup> cells mL<sup>-1</sup>) were used to inoculate hematite suspensions (2 g L<sup>-1</sup>) that were incubated for 1, 2, 3, 4, and 5 d.

### **2.3.5 Ferric Citrate Bioreduction**

Experiments were performed in 10 mM PIPES containing 2 mM ferric citrate (dissolved in 10 mM PIPES), 4 mM citric acid, a final cell density of 10<sup>8</sup> cells mL<sup>-1</sup>, and variable concentrations of zinc (0 to 90 mg L<sup>-1</sup>). Solution pH was maintained at pH 6.8 with addition of 3 N NaOH or 3 N HCl. A 3:1 molar ratio of citrate:Fe(III) was selected to prevent the formation of amorphous ferric hydroxide based on speciation calculations made with MINTEQA2 (Allison et al. 1991) using published thermodynamic data (Smith et al. 1997; Liu et al. 2001). Reactors were prepared in clear glass serum bottles (250 mL) containing between 100 to 200 mL of solution media, crimp-sealed with thick butyl rubber stoppers and aluminum caps, and sealed

serum bottles were incubated in the dark at 20°C on orbital shakers outside of the anaerobic chamber. After incubation times of 0, 1, 2.5, 3.75, and 6 h, reactors were sampled within the anaerobic chamber by piercing the septa with a sterile needle and syringe. The sample was analyzed for dissolved Fe(II), dissolved zinc, viable planktonic cells, and pH.

### **2.3.6 Nitrate Bioreduction**

Experiments were performed in 10 mM PIPES (pH 6.8) containing 144.4 mg L<sup>-1</sup> KNO<sub>3</sub> (20 mg NO<sub>3</sub>-N L<sup>-1</sup>), a final cell density of 10<sup>8</sup> cells mL<sup>-1</sup>, and variable concentrations of zinc (0 to 30 mg L<sup>-1</sup>). Reactor preparation and reactor sampling were performed using the same techniques as the ferric citrate experiments. Samples were collected after incubation times of ca. 0, 5, 10, 21, and 27 h, and were used to measure nitrate-nitrogen, dissolved zinc, viable planktonic cells, and pH.

### **2.3.7 DMRB Growth**

Cells were prepared as above, however, M1 growth medium (Myers et al. 1988) was used for the final two aerobic rinses to remove residual TSB-D. Rinsed cells were inoculated into reactors containing M1 medium, 30 mM lactate, and variable concentrations of zinc (0 to 200 mg L<sup>-1</sup> total zinc) and were grown aerobically. Cell concentrations were measured after incubation times of 0 and 21 h. Aseptic techniques were used in all steps.

### **2.3.8 Analytical Techniques**

Fe(II) was reported as dissolved, total, and adsorbed. For dissolved Fe(II), samples were filtered (0.2 µm cellulose acetate) and Fe(II) was measured by ferrozine (1.96 mM ferrozine in 50 mM HEPES, pH 8.0) in the anaerobic chamber. Solution pH of the filtrate was determined in the anaerobic chamber using a combination pH electrode. For total Fe(II), an unfiltered sample was acidified with HCl to achieve a final solution normality of 0.5 N. The solution was mixed

for ca. 24 h, filtered (0.2  $\mu\text{m}$ ) and Fe(II) in the filtrate was measured by ferrozine. Adsorbed Fe(II) was calculated as the difference between dissolved and total Fe(II). Dissolved and total zinc were measured from the corresponding dissolved and total Fe(II) filtrate samples by flame atomic absorption spectrometry (AAS) after preservation with conc.  $\text{HNO}_3$ . Nitrate was measured using a Hach 2010 spectrometer (Hach Company; Loveland, CO) using the high range nitrate (0-30  $\text{mg L}^{-1}$ ) Test 'n Tube method 322.

The LIVE/DEAD<sup>®</sup> *Baclight*<sup>™</sup> bacterial viability kit (Molecular Probes, Eugene, OR) includes mixtures of the green fluorescent nucleic acid stain SYTO 9 and the red fluorescent nucleic acid stain propidium iodide. The SYTO 9 stain generally labels all bacteria while the propidium iodide penetrates only bacteria with damaged membranes causing a displacement of the SYTO 9 stain (Boulos et al. 1999). Non-viable (assumed damaged) cells were counted by their fluorescent red color while viable cells were counted by their fluorescent green color. An unfiltered 10  $\mu\text{L}$  sample aliquot was removed from a reactor, stained, and placed on a glass slide beneath a 4.84  $\text{cm}^2$  cover slip. Cell viability was calculated as the average from 5 field counts (within  $2.64 \times 10^{-4} \text{ cm}^2$  for 64x objective lens) for each sample aliquot (one reactor). Planktonic cells were counted as cells not visibly attached to hematite particles (free swimming) while sorbed cells were counted as physically attached to the hematite surface. The differentiation between planktonic and sorbed cells was readily discernible throughout the counting procedure.

## **2.4 Results**

### **2.4.1 Hematite Bioreduction**

In this study, the assessment of zinc toxicity was quantified as the inhibition of the biological reduction of the provided electron acceptor (either hematite, ferric citrate, or nitrate)

by *S. putrefaciens* CN32. This effect was based upon a decrease of both dissolved and total Fe(II) produced during the reduction of the hematite over a 5 d period. Total and dissolved Fe(II) production as a function of added zinc (Figs. 1A, 1B) reveal that the rate and 5 d extent of biogenic Fe(II) production was dependent on the total zinc concentration. Abiotic controls resulted in no Fe(II) production (results not shown). Total zinc concentrations less than 6.5 mg L<sup>-1</sup> increased Fe(II) production relative to the biotic no-zinc control, resulting in a stimulatory effect of zinc. Total zinc concentrations higher than 6.5 mg L<sup>-1</sup> decreased Fe(II) production relative to the biotic no-zinc control. At 15.0 mg L<sup>-1</sup> total zinc, the highest zinc concentration used in the hematite experiments, the final 5 d total Fe(II) concentration was 36% of the biotic no-zinc control.

To quantify the effect of zinc on *S. putrefaciens* CN32, cell viability was measured throughout these experiments using *Ba*clight viability stains. In the biotic no-zinc control, most planktonic cells showed green fluorescence which indicated cells had intact cell membranes (Sani et al. 2001). The percentage of the total number of cells within the medium (planktonic) that were viable is presented in Figure 2A, while the percent of viable cells coagulated to the surface of the hematite particles is presented in Figure 2B. For this study we utilize the definition where planktonic cells are cells that are free swimming (Langley et al. 1999) and not coagulated with any surface, specifically the hematite surface. As seen in Figure 2A, an increase in zinc decreased the number of viable planktonic cells over time. In the biotic no-zinc control, 82% of the cells were viable after 5 d, while essentially 100% of the cells were non-viable after 5 d in the system with 15 mg L<sup>-1</sup> zinc.

The viability of cells sorbed to the hematite surface decreased as the zinc concentration increased (Fig. 2B). These results indicate that non-viable cells appeared to adhere to hematite



more so than viable cells. Proton titrations performed with suspensions of *S. putrefaciens* CN32 have shown that the outer membrane of this organism would possess a negative charge at pH 6.8 due to dissociated carboxyl and phosphoryl groups (Plette et al. 1996; Sarret et al. 1998; Fein et al. 2001). Proton titrations performed with the same hematite as used in this study have shown that the hematite surface would possess a positive charge at pH 6.8 ( $\text{pH}_{\text{zpc}} = 8.5$ ) (Jeon et al. 2001). Thus, there would be an electrostatic attraction between the cell and hematite surfaces that non-viable/non-motile cells would not be able to overcome. The highest zinc concentrations tested (all  $>6.5 \text{ mg L}^{-1}$ ) produced the greatest percentage of non-viable cells found on the hematite surface, where after 48 h,  $>95\%$  of the sorbed cells were non-viable. In the biotic no-zinc control only 22% of the sorbed cells were viable after 5 d.

#### **2.4.2 DMRB Growth**

Aerobic growth experiments were conducted to directly determine if zinc would inhibit the growth of *S. putrefaciens* CN32, and if growth inhibition under aerobic conditions and the inhibition of hematite bioreduction occurred at the same zinc concentration. Growth experiments were performed in a defined growth medium (M1), (Myers et al. 1988) so that free zinc concentrations could be calculated with MINTEQA2. Growth inhibition was defined as the percent difference in cell density ( $A_{420}$ ) of zinc-containing growth media relative to a biotic no-zinc control (Sani et al. 2001), and was based on the extent of growth after 21 h incubation. Growth inhibition of *S. putrefaciens* CN32 in M1 media after 21 h for total zinc concentrations ranging from 0 to  $180 \text{ mg L}^{-1}$  (with corresponding free zinc concentrations displayed) is shown in Figure 3. Growth inhibition increased with increased free zinc concentrations. The highest level of inhibition (90%) occurred at the highest free zinc concentration ( $55.4 \text{ mg L}^{-1}$  or  $180 \text{ mg L}^{-1}$  total zinc). The solid line in Figure 3 represents the least square regression ( $R^2 = 0.939$ ) for

growth inhibition versus free zinc concentration (log values). The zinc concentration resulting in 50% inhibition of the maximum specific growth ( $IC_{50, \text{growth}}$ ) occurred at  $3.3 \text{ mg L}^{-1}$  free zinc based on this regression equation.

### **2.4.3 Pre-Exposure of DMRB to Zinc**

This experiment was designed to isolate the biological/toxic effect of zinc on *S. putrefaciens* CN32 from the physical effect of zinc caused by zinc sorption to hematite or *S. putrefaciens* CN32 that may interfere with cell attachment to the oxide (in some cases a prerequisite for iron reduction). The results from this experiment revealed that the rate and extent of biogenic Fe(II) production were not statistically separable between cells pre-exposed to  $5.3 \text{ mg L}^{-1}$  zinc and the un-exposed controls (data not shown). However, cell viability data revealed that pre-exposed cells were only 30% viable after 24 h compared to 92% viable for the un-exposed cells (results for planktonic cells). Taken together, these results show that even though zinc was acutely toxic during the pre-exposure period, the rate and extent of hematite bioreduction was relatively insensitive to the number of viable cells. Since there are likely limited cell binding sites to the hematite, bioreduction may only be limited below a certain viable cell-to-hematite ratio.

### **2.4.4 Variable Hematite and DMRB Concentrations**

To further investigate these results in the absence of zinc, experiments were performed using either variable hematite or cell concentrations. Total Fe(II) production-versus-time for variable hematite concentrations are shown in Figure 4A. These experiments were conducted with hematite concentrations of  $0.25 \text{ g L}^{-1}$  to  $2.0 \text{ g L}^{-1}$  with a constant cell concentration of  $10^8$  cells  $\text{mL}^{-1}$ . The results show that total Fe(II) production was similar for the two highest hematite concentrations tested. Fe(II) production decreased substantially at hematite concentrations

below  $1.5 \text{ g L}^{-1}$ , with the lowest hematite concentration ( $0.25 \text{ g L}^{-1}$ ) generating  $3.7 \text{ mg L}^{-1}$  total Fe(II) after 5 d, 73% less than the greatest 5 d extent of Fe(II) production. Total Fe(II) production-versus-time for variable cell concentrations are shown in Figure 4B. These experiments were performed with cell concentrations of  $10^6$  to  $10^8$  cells  $\text{mL}^{-1}$  with a constant hematite concentration of  $2.0 \text{ g L}^{-1}$ . A 50% decrease in cell concentration (from  $10^8$  to  $5 \times 10^7$  cells  $\text{mL}^{-1}$ ) resulted in a 30% decrease in Fe(II) production after 5 d. A 75% decrease in cell concentration (from  $10^8$  to  $2.5 \times 10^7$  cells  $\text{mL}^{-1}$ ) resulted in a 89% decrease in Fe(II) production after 5 d. At cell concentrations below  $5 \times 10^6$  cells  $\text{mL}^{-1}$  essentially no iron reduction occurred. Variability between the two experiments using identical conditions ( $1 \times 10^8$  cells  $\text{mL}^{-1}$  and  $2.0 \text{ g L}^{-1}$  hematite) in Figs. 4A and 4B was within the expected range. In general, these experiments demonstrated that the rate and extent of iron reduction was proportional to the hematite concentration but not directly proportional to the DMRB concentration.

The results from both the variable hematite and variable DMRB experiments were combined by normalizing the values for 5 d extent of total Fe(II) production based on cells per mass of hematite (Figure 5). In Figure 5A, an increase in the DMRB-to-hematite ratio (cells  $\text{g}^{-1}$ ) increased total Fe(II) production up to  $5 \times 10^{10}$  cells  $\text{g}^{-1}$ . DMRB-to-hematite ratios higher than this value decreased total Fe(II) production. The DMRB-to-hematite ratio of  $5 \times 10^{10}$  cells  $\text{g}^{-1}$  corresponds to the experimental conditions previously used within our experiments ( $10^8$  cells  $\text{mL}^{-1}$  and  $2.0 \text{ g L}^{-1}$  hematite). The corresponding viability of planktonic cells with these DMRB-to-hematite ratios are shown in Figure 5B. A dramatic decrease in planktonic cell viability occurred at DMRB-to-hematite ratios greater than  $5 \times 10^{10}$  cells  $\text{g}^{-1}$ . Planktonic cell viability was between 90-100% for DMRB-to-hematite ratios up to  $5 \times 10^{10}$  cells  $\text{g}^{-1}$ , whereas higher ratios resulted in significant decreases in cell viability. Most importantly, these results demonstrate

that for the four conditions of greatest Fe(II) production (ranged from 10.5 to 13.5 mg L<sup>-1</sup> after 5 d) the experimental system was relatively insensitive to cell viability (ranged from 23 to 93%). Thus, these results are in agreement with the results obtained with cells pre-exposed or un-exposed to zinc.

#### **2.4.5 Ferric Citrate Bioreduction**

Experiments were performed with ferric citrate to evaluate the effect of zinc on a soluble electron acceptor and to determine if the inhibitory effect would be different than those effects observed with hematite. MINTEQA2 calculations using published thermodynamic data (Smith et al. 1997; Liu et al. 2001) indicated that ferrihydrite formation would be thermodynamically favorable in 10 mM PIPES (pH 6.8) with a 1:1 molar ratio of citrate:Fe(III) (2 mM ferric citrate), therefore, a 3:1 molar ratio was used by addition of 4 mM citric acid. MINTEQA2 calculations indicated that ferrihydrite could form with a 3:1 molar ratio of citrate:Fe(III). At pH 6.8 in 10 mM PIPES with 4 mM citrate and 2 mM Fe(III), the free zinc concentrations calculated with MINTEQA2 were only 0.113 to 0.204% of the total zinc concentration for lowest and highest total zinc concentrations tested (1.3 and 90 mg L<sup>-1</sup>, respectively). The dominant species in this system was Fe(III)citrate, similar to the ASM-I model results presented by Liu et al. (Liu et al. 2001).

The results shown in Figure 6 demonstrate that zinc addition did not stimulate ferric citrate bioreduction, as observed with hematite (Fig. 1). Total zinc concentrations greater than 15.0 mg L<sup>-1</sup> resulted in significantly less Fe(II) production compared to lower zinc concentrations and the biotic no-zinc control. Because of the high citrate concentration (6 mM), even the highest total zinc concentration (90 mg L<sup>-1</sup>) resulted in a relatively low free zinc concentration (0.184 mg L<sup>-1</sup>) based on MINTEQA2 calculations. *Ba*clight counts (data not

shown) revealed that cell viability was not significantly affected up to a total zinc concentration of 90 mg L<sup>-1</sup>. However, an ancillary experiment using 450 mg L<sup>-1</sup> total zinc under identical experimental conditions (results not shown) yielded no viable cells.

#### 2.4.6 Nitrate Bioreduction

Experiments were performed with nitrate to evaluate the effect of zinc with another soluble electron acceptor, in this case with one that did not include a high ligand concentration (i.e., citrate). *S. putrefaciens* can reduce nitrate in the absence of oxygen with hydrogen as the electron donor (Kim et al. 1999; Cooper et al. 2000). Results with nitrate and variable concentrations of zinc are shown in Figure 7. The highest rate and extent of nitrate consumption (with initial nitrate-nitrogen concentrations of ca. 20 mg L<sup>-1</sup>) occurred with the biotic no-zinc control and the 1.3 mg L<sup>-1</sup> zinc concentration (Fig. 7A). Low concentrations of zinc did not stimulate nitrate bioreduction. Zinc concentrations greater than 1.3 mg L<sup>-1</sup> reduced the rate and extent of nitrate reduction compared to the biotic no-zinc control. Cell viability measurements showed a steady decrease over time with increasing zinc concentrations (Fig. 7B).

#### 2.4.7 Evaluation of Zinc Inhibition

Zinc inhibited aerobic cell growth and the anaerobic respiration of hematite, ferric citrate and nitrate by *S. putrefaciens* CN32. To quantify zinc inhibition in these different experimental systems, we have modified the definition developed by Sani et al. (Sani et al. 2001). Specifically, we define inhibition as the percent change in biological respiration rate or extent of the system due to zinc addition relative to the biotic no-zinc control. This definition can be expressed as:

$$\%Inhibition = \left( 1 - \frac{\text{Bioreduction Extent with Zinc}}{\text{Bioreduction Extent with no Zinc}} \right) \times 100 \quad (1)$$

where bioreduction extent is either the 5 d (hematite) or 6 h (ferric citrate) total Fe(II) production, 27 h nitrate consumption, or 21 h cell growth. The concentration causing a 50% decrease in biological output ( $IC_{50}$ ) is expressed as:

$$IC_{50} = 10^{\left(\frac{50 - \beta_0}{\beta_1}\right)} \quad (2)$$

Where  $\beta_0$  is the intercept of the log zinc-linear percent inhibition regression line and  $\beta_1$  is the slope of the log zinc-linear percent inhibition regression line. By using these definitions, total zinc was more inhibitory with the two soluble electron acceptors, ferric citrate and nitrate, compared to solid-phase hematite (Fig. 8A). Decreased biological respiration (i.e., consumption of electron acceptors) occurring at lower zinc concentrations indicates a greater inhibitory effect. Nitrate bioreduction was most sensitive to zinc, with an  $IC_{50}$  value of 3.2 mg L<sup>-1</sup> total zinc. The  $IC_{50}$  values for ferric citrate, hematite, and cell growth were 18.6, 13.8, and 19.6 mg L<sup>-1</sup> total zinc, respectively.

The  $IC_{50}$  values were also calculated using Eq. 1 based on free zinc concentrations (Fig. 8B). In the nitrate bioreduction experiments, the total zinc concentrations were equal to the dissolved zinc concentrations and the free zinc concentrations were equal to ca. 99.4% of the dissolved zinc concentrations (based on MINTEQA2 calculations), thus the  $IC_{50}$  value based on free zinc was also 3.2 mg L<sup>-1</sup> free zinc. In the hematite bioreduction experiments, the dissolved zinc concentrations were less than the total zinc concentrations because of sorption to hematite and cells, and the free zinc concentrations were equal to ca. 99.7% of the dissolved zinc concentrations (based on MINTEQA2 calculations). The  $IC_{50}$  value based on free zinc for hematite bioreduction was 8.6 mg L<sup>-1</sup>. In the ferric citrate experiments the free zinc concentrations were significantly less than the total zinc concentrations because of the high citrate concentration. Based on MINTEQA2 calculations of the free zinc concentrations, the

IC<sub>50</sub> value based on free zinc for ferric citrate bioreduction was 0.023 mg L<sup>-1</sup>. Lastly, for the cell growth experiments, MINTEQA2 calculations found zinc preferentially associated with lactate and SeO<sub>4</sub><sup>2-</sup> present in the M1 growth media, reducing the IC<sub>50</sub> value for free zinc to 3.3 mg L<sup>-1</sup>.

## 2.5 Discussion

Growth of *S. putrefaciens* CN32 was found to be very sensitive to zinc at free zinc concentrations exceeding 3.3 mg L<sup>-1</sup>. Previous growth studies related to filamentous bacteria (Shuttleworth et al. 1991), sulfate reducing bacteria (Utgikar et al. 2001; Utgikar et al. 2002), and DMRB (Poulson et al. 1997; Sani et al. 2001) have also shown that zinc inhibited cell growth. The summary of zinc toxicity results presented in Table 1 is in agreement with our free zinc results. Microbial toxicity has previously been associated with free metal activity (Knight et al. 1995; Chaudri et al. 1999; Chaudri et al. 2000; Ritchie et al. 2001), with B-type metal cations (Stumm et al. 1996) such as zinc complexation with carboxyl and phosphoryl surface sites on cell walls (Fein et al. 2001). Metal sorption affinities appear to be similar across a wide range of species (Fein et al. 2001), allowing comparisons to be made for a variety of DMRB. In addition to growth inhibition, zinc toxicity was evident during both hematite and nitrate bioreduction experiments, and through zinc pre-exposure experiments based on cell viability measurements.

While being directly toxic above certain concentrations, zinc was also shown to stimulate hematite bioreduction at total zinc concentrations below 6.5 mg L<sup>-1</sup>. Stimulation of activity (at sub-toxic concentrations) may be due to relieving nutrient deficiencies (Welp et al. 1997b), increasing soil nitrification rates (Fruhling et al. 2001), escalating rates of methanogenesis (Mishra et al. 1999), increasing algae respiration rates (Webster et al. 1996), and increasing microbial growth (Shuttleworth et al. 1991). Our results were consistent with the Type II dose-

response effects described by Welp et al. (Welp et al. 1997b) where zinc stimulates a biological response at low concentrations while subsequently inhibiting the response at higher concentrations. Zinc stimulation appears to either be related to a microbial response due to metabolic damage (Fruhling et al. 2001) or from a localized shift in pH allowing trace nutrients to become more bioavailable (Welp et al. 1997b).

Neither of these explanations, however, can account for our observations in which hematite bioreduction increased while cell viability decreased compared to the biotic no-zinc controls. For example, 3.3 mg L<sup>-1</sup> total zinc increased the 5 day Fe(II) production in the hematite system by 14% relative to the biotic no-zinc control (Fig. 1A) while the planktonic viable cell population decreased by 39% (Fig. 2A). Additionally, cells pre-exposed to zinc prior to hematite bioreduction produced the same amount of Fe(II) with a significantly less number of viable cells (87% viable cells for the un-exposed control compared to 26% for the pre-exposed cells). Based on these results, we believe the system was usually not often limited by viable cell numbers. This position is supported by the results obtained from the variable concentrations of hematite and DMRB (Fig. 5). For the four trials that produced the greatest amount of Fe(II), the DMRB-to-hematite ratios were 5x10<sup>10</sup> (duplicated), 7x10<sup>10</sup>, and 1x10<sup>11</sup> cells g<sup>-1</sup>, while the corresponding planktonic cell viabilities were 82, 93, 72, and 24%, respectively. DMRB-to-iron oxide ratios calculated by Roden and Zachara (Roden et al. 1996) for *S. algae* BrY and goethite were 1x10<sup>9</sup> cells m<sup>-2</sup> of iron oxide, which for our hematite suspension (N<sub>2</sub>-BET surface area of 9.04 m<sup>2</sup> g<sup>-1</sup>) was calculated to be 9x10<sup>9</sup> cells g<sup>-1</sup>. Both values demonstrated that the rate of bioreduction was proportional to the hematite concentration and not the DMRB concentration. This correlation to hematite supports the presumption that rate was proportional to the available free surface sites on the hematite.



The bioreduction of soluble electron acceptors (nitrate and ferric citrate) was more sensitive to free zinc than the bioreduction of solid-phase hematite (Fig. 8B). Bioreduction of ferric citrate was found to be most sensitive to free zinc ( $IC_{50}$  of  $0.023 \text{ mg L}^{-1}$ ), however, the calculation of free zinc concentrations in the presence of 6 mM citrate may be imprecise because of uncertainties regarding the formation and stability constants of the zinc-citrate complexes (Liu et al. 2001). MINTEQA2 calculations were likely more precise for the nitrate bioreduction experiments and predicted only minor solution complexation within the solution ( $ZnNO_3^+$  and  $ZnOH^+$  were 0.244% and 0.316% of the total zinc concentrations, respectively, for all conditions). The free zinc  $IC_{50}$  for nitrate reduction was  $3.2 \text{ mg L}^{-1}$  while the free zinc  $IC_{50}$  for growth inhibition was  $3.2 \text{ mg L}^{-1}$ . The strong similarity between these  $IC_{50}$  values for nitrate bioreduction and growth inhibition suggests that both processes were affected by zinc by similar mechanisms. The only sorption sites available within these experiments were those associated with either the cell surface or through cellular uptake, thus sorption and subsequent cellular toxicity appear to be the primary mode of inhibition for these soluble phase experiments.

The free zinc  $IC_{50}$  value for hematite bioreduction was  $8.6 \text{ mg L}^{-1}$ , or 160% greater than the  $IC_{50}$  values for nitrate bioreduction and growth inhibition. The  $IC_{50}$  value was higher for hematite bioreduction even though sorption of zinc to hematite and DMRB was taken into account to calculate the free zinc concentration. The higher  $IC_{50}$  for hematite bioreduction (i.e., zinc is less toxic) could have been caused by a competitive sorption effect between Zn(II) and Fe(II). The sorption of biogenic Fe(II) to hematite likely affects the rate and extent of bioreduction of solid-phase iron oxides. Previous studies (Urrutia et al. 1998; Roden et al. 1999) suggested that surface coverage or “passivation” of the oxide surface by sorbed Fe(II) inhibited bioreduction by decreasing the number of reactive surface sites available and either preventing

DMRB-oxide contact or increasing the passive resistance of electron transport. Competition between Zn(II) and Fe(II) for hematite sorption sites was found to decrease sorbed Fe(II) compared to biotic no-zinc controls (Stone et al. 2002). By decreasing Fe(II) sorption, surface passivation is decreased and hematite reduction can proceed to a further extent. Thus, because zinc can stimulate hematite bioreduction, its corresponding  $IC_{50}$  is higher in these systems.

The results of this study further our understanding of the inhibitory effects of zinc on the biological reduction of hematite, ferric citrate, and nitrate by the DMRB *S. putrefaciens* CN32. Zinc inhibition was observed through decreasing the rate and extent of biogenic Fe(II) production while decreasing cell viability. Zinc toxicity to *S. putrefaciens* was apparent during both cell growth experiments and nitrate bioreduction experiments by reduction in cell growth rates and decreased cell viability. The similarity between the free zinc  $IC_{50}$  for cell growth and nitrate reduction indicated that cellular toxicity due to free zinc may be an important factor in respiratory inhibition. However, the differences in the free zinc  $IC_{50}$  observed between soluble (ferric citrate and nitrate) and solid phase (hematite) electron acceptors indicated that biogenic Fe(II) and zinc surface complexation may contribute to the inhibitory effects observed, mainly through surface passivation of the hematite surface.

## **2.6 Acknowledgments**

Research supported by the Natural and Accelerated Bioremediation Research Program (NABIR), Office of Biological and Environmental Research (OBER), Office of Energy Research, U.S. Department of Energy (DOE), Grants no. DE-FG02-98ER62691 and No. DE-FG02-01ER63180 is gratefully acknowledged.

## 2.7 Literature Cited

- Allison, J. D., D. S. Brown, et al. (1991). MINTEQA2/PRODEFA2, a geochemical assessment model for environmental systems: Version 3.0 users manual. Athens, GA, U.S. Environmental Protection Agency.
- Baath, E. (1989). "Effects of heavy-metals in soil on microbial processes and populations (a review)." Water Air and Soil Pollution **47**(3-4): 335-379.
- Boulos, L., M. Prevost, et al. (1999). "LIVE/DEAD (R) BacLight (TM): application of a new rapid staining method for direct enumeration of viable and total bacteria in drinking water." Journal of Microbiological Methods **37**(1): 77-86.
- Chaudri, A. M., B. P. Knight, et al. (1999). "Determination of acute Zn toxicity in pore water from soils previously treated with sewage sludge using bioluminescence assays." Environmental Science & Technology **33**(11): 1880-1885.
- Chaudri, A. M., K. Lawlor, et al. (2000). "Response of a Rhizobium-based luminescence biosensor to Zn and Cu in soil solutions from sewage sludge treated soils." Soil Biology & Biochemistry **32**(3): 383-388.
- Cooper, D. C., F. Picardal, et al. (2000). "Zinc immobilization and magnetite formation via ferric oxide reduction by *Shewanella putrefaciens* 200." Environmental Science & Technology **34**(1): 100-106.
- Dzombak, D. A. and M. M. Francis (1990). Surface complexation modeling: Hydrous Ferric Oxide. New York, John Wiley and Sons.
- Fein, J. B., A. M. Martin, et al. (2001). "Metal adsorption onto bacterial surfaces: Development of a predictive approach." Geochimica et Cosmochimica Acta **65**(23): 4267-4273.
- Fredrickson, J. K., J. M. Zachara, et al. (1998). "Biogenic iron mineralization accompanying the dissimilatory reduction of hydrous ferric oxide by a groundwater bacterium." Geochimica et Cosmochimica Acta **62**(19-20): 3239-3257.
- Fredrickson, J. K., J. M. Zachara, et al. (2001). "Biotransformation of Ni-substituted hydrous ferric oxide by an Fe(III)-reducing bacterium." Environmental Science & Technology **35**(4): 703-712.
- Fruhling, W., K. Ronnpage, et al. (2001). "Effect of zinc and benzalkonium chloride on *Nitrosomonas communis* and potential nitrification in soil." Environmental Toxicology **16**(5): 439-443.
- Gadd, G. M. (1996). "Influence of microorganisms on the environmental fate of radionuclides." Endeavour **20**(4): 150-156.
- Jeon, B. H., B. A. Dempsey, et al. (2001). "Reactions of ferrous iron with hematite." Colloids and Surfaces a-Physicochemical and Engineering Aspects **191**(1-2): 41-55.
- Kim, S. and F. W. Picardal (1999). "Enhanced anaerobic biotransformation of carbon tetrachloride in the presence of reduced iron oxides." Environmental Toxicology and Chemistry **18**(10): 2142-2150.
- Knight, B. and S. P. McGrath (1995). "A method to buffer the concentrations of free Zn and Cd ions using a cation-exchange resin in bacterial toxicity studies." Environmental Toxicology and Chemistry **14**(12): 2033-2039.
- Kushner, D. J. (1993). "Effects of speciation of toxic metals on their biological activity." Water Pollution Residuals Journal of Canada **28**(1): 111-128.

- Langley, S. and T. J. Beveridge (1999). "Metal binding by *Pseudomonas aeruginosa* PAO1 is influenced by growth of the cells as a biofilm." Canadian Journal of Microbiology **45**(7): 616-622.
- Liu, C. G., J. M. Zachara, et al. (2001). "Microbial reduction of Fe(III) and sorption/precipitation of Fe(II) on *Shewanella putrefaciens* strain CN32." Environmental Science & Technology **35**(7): 1385-1393.
- Mishra, S. R., K. Bharati, et al. (1999). "Effects of heavy metals on methane production in tropical rice soils." Ecotoxicology and Environmental Safety **44**(1): 129-136.
- Myers, C. R. and K. H. Nealson (1988). "Bacterial manganese reduction and growth with manganese oxide as the sole electron-acceptor." Science **240**(4857): 1319-1321.
- Parmar, N., Y. A. Gorby, et al. (2001). "Formation of green rust and immobilization of nickel in response to bacterial reduction of hydrous ferric oxide." Geomicrobiology Journal **18**(4): 375-385.
- Plette, A. C. C., M. F. Benedetti, et al. (1996). "Competitive binding of protons, calcium, cadmium, and zinc to isolated cell walls of a gram-positive soil bacterium." Environmental Science & Technology **30**(6): 1902-1910.
- Poulson, S. R., P. J. S. Colberg, et al. (1997). "Toxicity of heavy metals (Ni,Zn) to *Desulfovibrio desulfuricans*." Geomicrobiology Journal **14**(1): 41-49.
- Raven, J. A. (1984). Energetics and transport in aquatic plants. New York.
- Riley, R. G. and J. M. Zachara, Eds. (1992). Chemical contaminants on DOE lands and selection of contaminant mixtures for subsurface science research. Washington, D.C., U.S. Department of Energy.
- Ritchie, J. M., M. Cresser, et al. (2001). "Toxicological response of a bioluminescent microbial assay to Zn, Pb and Cu in an artificial soil solution: relationship with total metal concentrations and free ion activities." Environmental Pollution **114**(1): 129-136.
- Roden, E. E. and M. M. Urrutia (1999). "Ferrous iron removal promotes microbial reduction of crystalline iron(III) oxides." Environmental Science & Technology **33**(11): 1847-1853.
- Roden, E. E. and J. M. Zachara (1996). "Microbial reduction of crystalline iron(III) oxides: Influence of oxide surface area and potential for cell growth." Environmental Science & Technology **30**(5): 1618-1628.
- Royer, R. A., W. D. Burgos, et al. (2002a). "Enhancement of hematite bioreduction by natural organic matter." Environmental Science & Technology **36**(13): 2897-2904.
- Royer, R. A., W. D. Burgos, et al. (2002b). "Enhancement of biological reduction of hematite by electron shuttling and Fe(II) complexation." Environmental Science & Technology **36**(9): 1939-1946.
- Sani, R. K., B. M. Peyton, et al. (2001). "Copper-induced inhibition of growth of *Desulfovibrio desulfuricans* G20: Assessment of its toxicity and correlation with those of zinc and lead." Applied and Environmental Microbiology **67**(10): 4765-4772.
- Sarret, G., A. Manceau, et al. (1998). "Structural determination of Zn and Pb binding sites in *Penicillium chrysogenum* cell walls by EXAFS spectroscopy." Environmental Science & Technology **32**(11): 1648-1655.
- Shuttleworth, K. L. and R. F. Unz (1991). "Influence of metals and metal speciation on the growth of filamentous bacteria." Water Research **25**(10): 1177-1186.
- Smith, R. A. and A. E. Martell (1997). NIST critically selected stability constants of metal complexes database. Version 3.0. User's guide and database software. NIST Standard Reference and Database no. 46. Gathersburg, Maryland, U.S. Department of Commerce.

- Stone, J. J., W. D. Burgos, et al. (2002). "Modes of inhibition by zinc on the biological reduction of hematite by *Shewanella putrefaciens* CN32." To be submitted for publication.
- Stumm, W. and J. J. Morgan (1996). Aquatic chemistry: chemical equilibria and rates in natural waters. New York, John Wiley and Sons, Inc.
- Urrutia, M. M., E. E. Roden, et al. (1998). "Microbial and surface chemistry controls on reduction of synthetic Fe(III) oxide minerals by the dissimilatory iron-reducing bacterium *Shewanella alga*." Geomicrobiology Journal **15**(4): 269-291.
- Utgikar, V. P., B. Y. Chen, et al. (2001). "Acute toxicity of heavy metals to acetate-utilizing mixed cultures of sulfate-reducing bacteria: EC100 and EC50." Environmental Toxicology and Chemistry **20**(12): 2662-2669.
- Utgikar, V. P., S. M. Harmon, et al. (2002). "Inhibition of sulfate-reducing bacteria by metal sulfide formation in bioremediation of acid mine drainage." Environmental Toxicology **17**(1): 40-48.
- VanGestel, C. A. M. and P. J. Hensbergen (1997). "Interaction of Cd and Zn toxicity for *Folsomia candida* Willem (Collembola: Isotomidae) in relation to bioavailability in soil." Environmental Toxicology and Chemistry **16**(6): 1177-1186.
- Warren, L. A. and E. A. Haack (2001). "Biogeochemical controls on metal behaviour in freshwater environments." Earth-Science Reviews **54**(4): 261-320.
- Webster, E. A. and G. M. Gadd (1996). "Stimulation of respiration in *Ulva lactuca* by high concentrations of cadmium and zinc: Evidence for an alternative respiratory pathway." Environmental Toxicology and Water Quality **11**(1): 7-12.
- Welp, G. (1999). "Inhibitory effects of the total and water-soluble concentrations of nine different metals on the dehydrogenase activity of a loess soil." Biology and Fertility of Soils **30**(1-2): 132-139.
- Welp, G. and G. W. Brummer (1997a). "Microbial toxicity of Cd and Hg in different soils related to total and water-soluble contents." Ecotoxicology and Environmental Safety **38**(3): 200-204.
- Welp, G. and G. W. Brummer (1997b). "Toxicity of increased amounts of chemicals and the dose-response curves for heterogeneous microbial populations in soil." Ecotoxicology and Environmental Safety **37**(1): 37-44.
- Zachara, J. M., J. K. Fredrickson, et al. (2001). "Solubilization of Fe(III) oxide-bound trace metals by a dissimilatory Fe(III) reducing bacterium." Geochimica et Cosmochimica Acta **65**(1): 75-93.

Table 2.1 Summary of 50% inhibition value in literature for zinc and other similar Me(II).

Species	Evaluation Process	Zinc 50% inhibition <sup>a</sup>	Source
<i>E. coli</i>	Bioluminescence in artificial soil solution	3.35 mg L <sup>-1</sup>	(Ritchie et al. 2001)
<i>E. coli</i>	Bioluminescence in sewage sludge	5.6 <sup>b</sup> , 2.5 <sup>c</sup> mg L <sup>-1</sup>	(Chaudri et al. 1999)
<i>P. fluorescens</i>	Bioluminescence in sewage sludge	22.5 <sup>b</sup> , 9.6 <sup>c</sup> mg L <sup>-1</sup>	(Chaudri et al. 1999)
<i>Rhizotox-c</i>	Bioluminescence in sewage sludge	16 <sup>b</sup> , 6 <sup>c</sup> mg L <sup>-1</sup>	(Chaudri et al. 2000)
<i>D. desulfuricans</i>	Cell growth	1.05 mg L <sup>-1 d</sup>	(Sani et al. 2001)
<i>Thiothrix</i>	Cell growth	0.124 <sup>b</sup> , 3.27 <sup>c</sup> mg L <sup>-1</sup>	(Shuttleworth et al. 1991)
<i>Nitrosomonas communis</i>	Ammonium oxidation in soil	171 mg kg <sup>-1</sup> soil	(Fruhling et al. 2001)
<i>F. candida</i>	Reproduction in soil	683 µg g <sup>-1</sup> soil	(VanGestel et al. 1997)
SRB <sup>e</sup>	Microbial community sulfate reduction in acid mine drainage	16.5 mg L <sup>-1</sup>	(Utgikar et al. 2001)
Heterogeneous soil microbial population	Microbial community dehydrogenase activity in contaminated soil	115 mg kg <sup>-1 b,f</sup> , 0.19 mg L <sup>-1 c</sup>	(Welp 1999)
<i>D. desulfuricans</i>	Microbial sulfidogenesis	13 mg L <sup>-1 g</sup>	(Poulson et al. 1997)

<sup>a</sup> Dose response relationship where 50% reduction in microbial activity or response occurred relative to a no Me(II) control.

<sup>b</sup> Total zinc within the soil.

<sup>c</sup> Soluble zinc measured within the soil solution

<sup>d</sup> Total Cu(II)

<sup>e</sup> Unidentified culture of sulfate reducing bacteria found within acid mine drainage

<sup>f</sup> Differences between metals soil and pore water concentrations occur due to variable affinity of metals to soil materials.

<sup>g</sup> Concentration where inhibition of sulfidogenic activity started

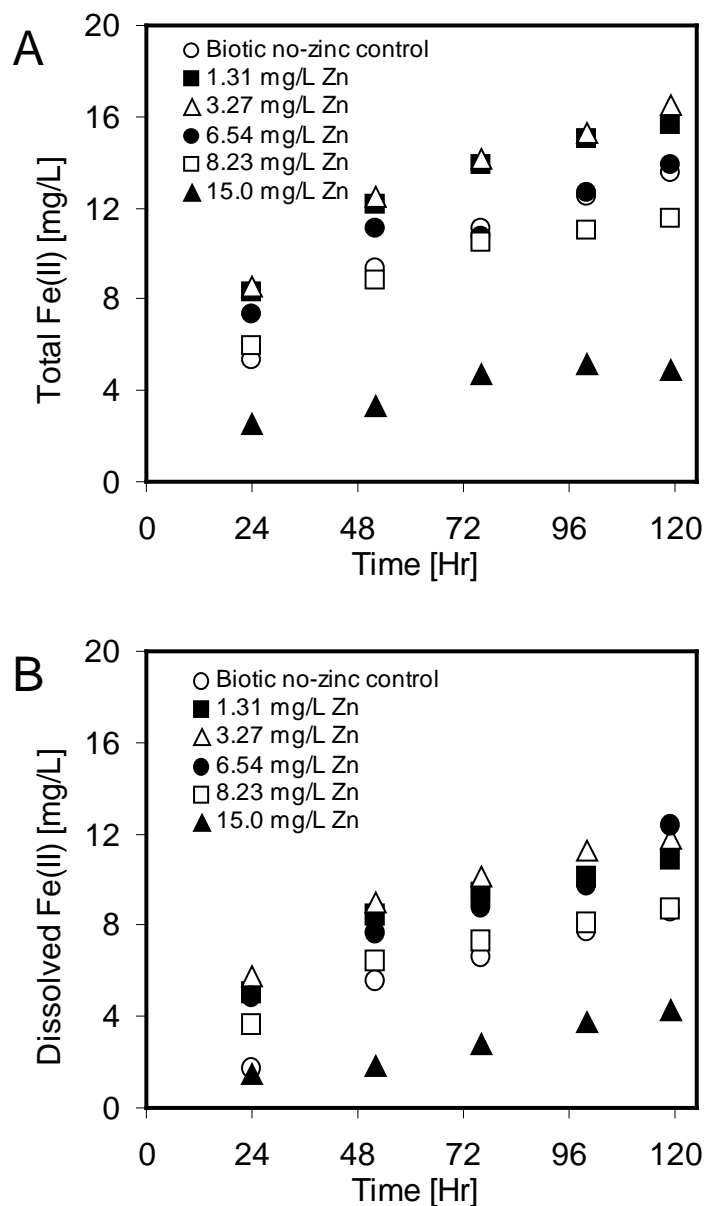


Figure 2.1 (A) Total, (B) dissolved Fe(II) production as a function of time (0 to 5 d) for the biological reduction of  $2 \text{ g L}^{-1}$  hematite at pH 6.8 in 10 mM PIPES. Zinc addition ranged from  $0 \text{ mg L}^{-1}$  for the biotic and abiotic controls to  $15 \text{ mg L}^{-1}$ . *Shewanella putrefaciens* CN32 was used ( $10^8 \text{ cells mL}^{-1}$ ) under non-growth conditions. Abiotic and biotic controls produced  $\leq 0.0$  and  $0.2 \text{ mg L}^{-1}$  total Fe(II), respectively. Values are means of three replicates.

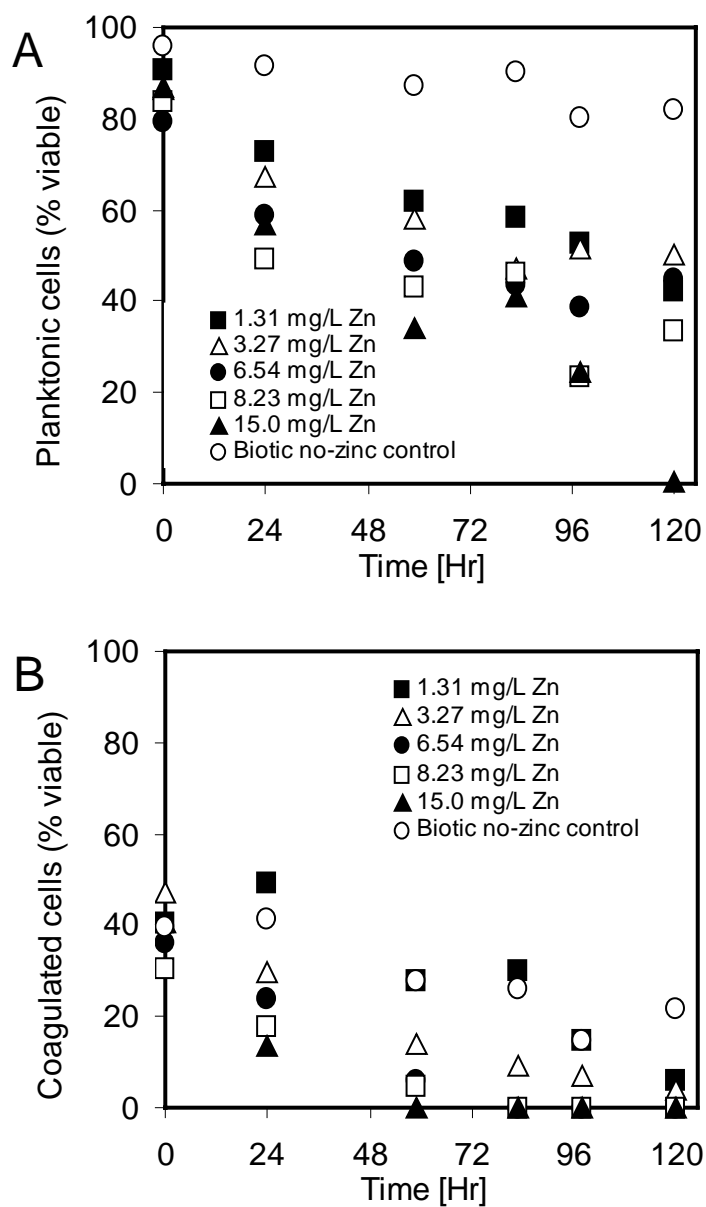


Figure 2.2 (A) Planktonic, (B) coagulated with hematite viability percentages for Baclight LIVE/DEAD cell counts (*S. putrefaciens*) as a function of time (0 to 5 d) for variable zinc addition (0-15 mg L<sup>-1</sup>) during biological reduction of 2 g L<sup>-1</sup> hematite under non-growth conditions. Values are means of five replicates.



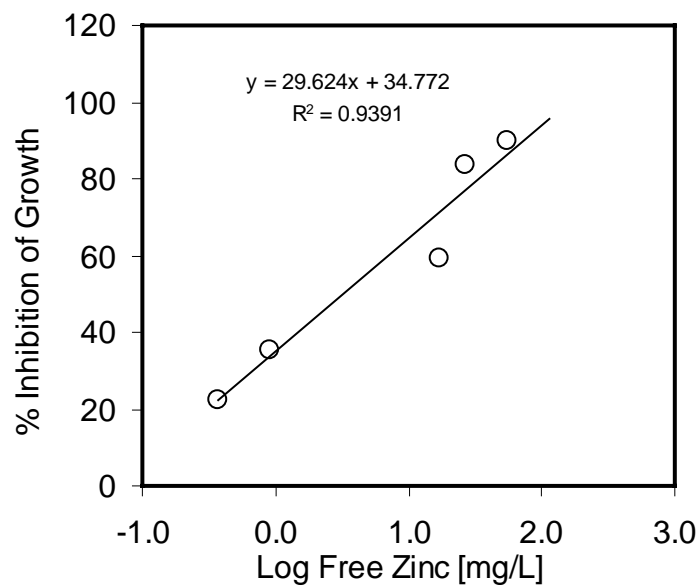


Figure 2.3 Inhibition of *S. putrefaciens* growth (24 h) as a function of variable free zinc addition (from 0-180 mg L<sup>-1</sup> total zinc) within M1 growth media at 20°C. Inhibition calculated as 420 nm absorbance difference between zinc containing sample and no zinc controls. Free zinc from MINTEQA2 speciation calculations.

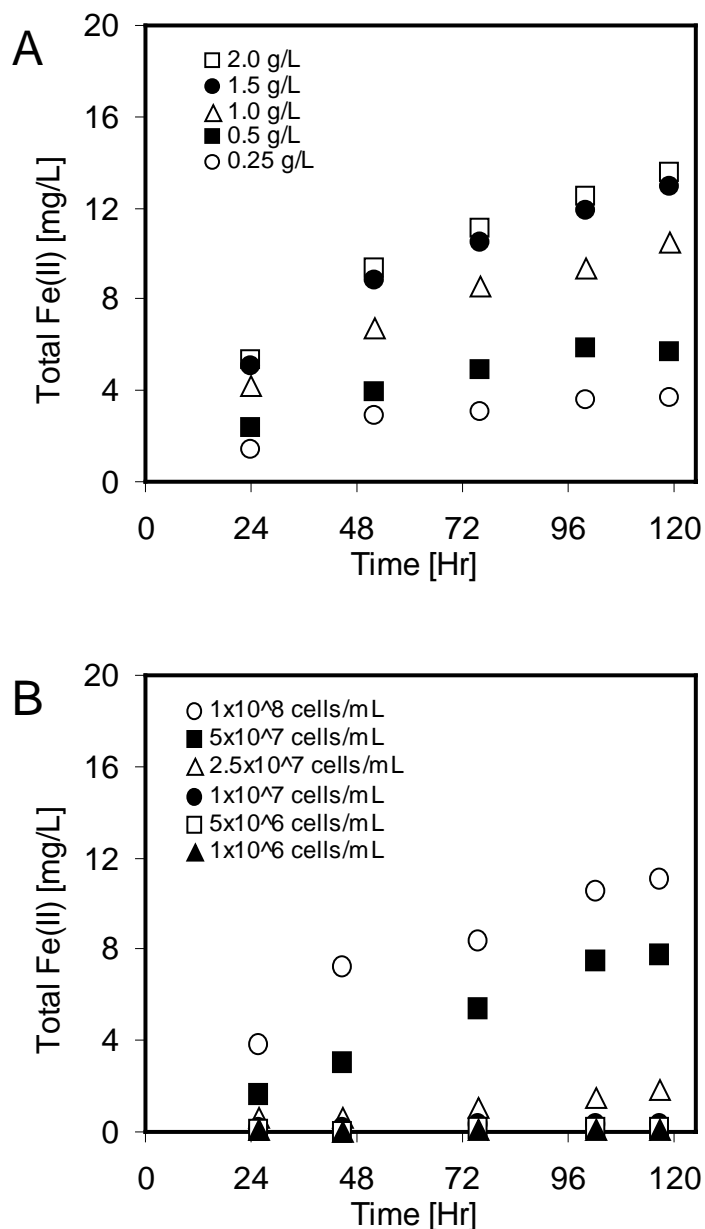


Figure 2.4 Total Fe(II) production as a function of time (0 to 5 d) for (A) variable hematite ( $0.25\text{-}2.0\text{ g L}^{-1}$ ), (B) variable *S. putrefaciens* ( $10^6\text{-}10^8\text{ cells mL}^{-1}$ ) as a function of time under non-growth conditions. All experiments conducted in 10 mM PIPES with no zinc addition. Variable hematite experiments used  $10^8\text{ cells mL}^{-1}$  DMRB concentrations and variable DMRB experiments used  $2.0\text{ g L}^{-1}$  hematite. Values are means of three replicates ( $\pm$  standard deviation).

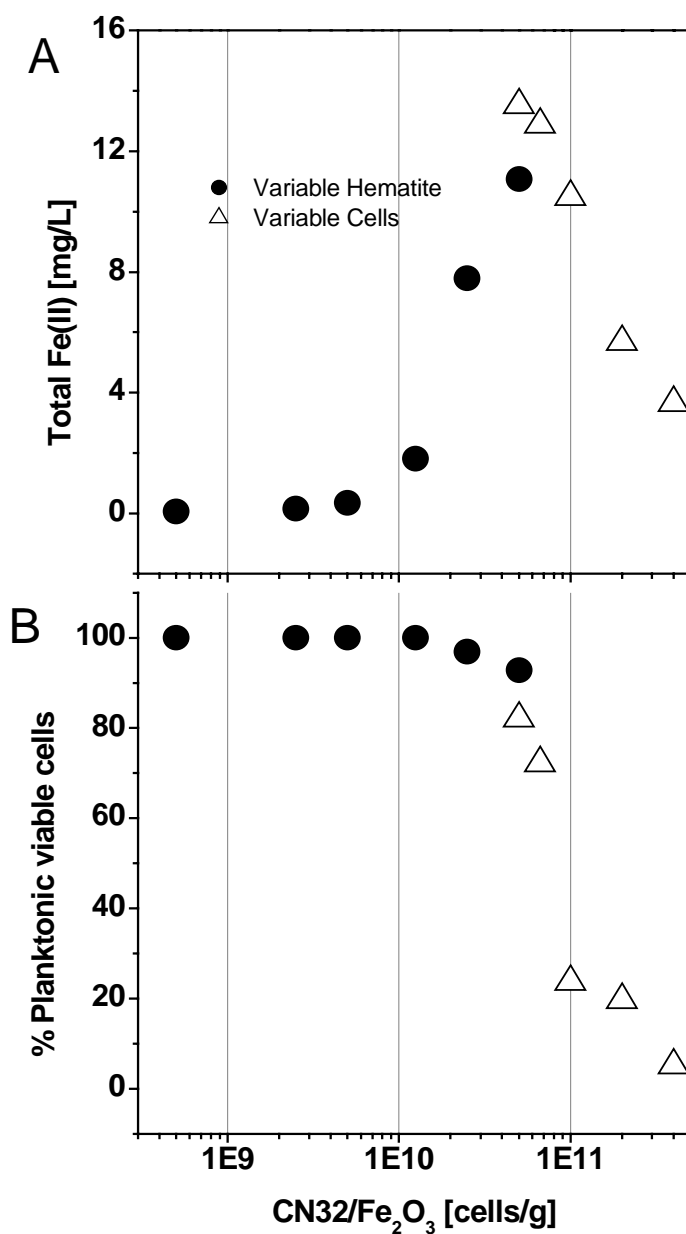


Figure 2.5 Normalized summary of (A) total Fe(II) production, (B) percent *Ba*light planktonic viability as a function of *S. putrefaciens* concentration per mass of hematite [cells g<sup>-1</sup>] for all results from variable hematite and variable *S. putrefaciens* hematite bioreduction experiments pH 6.8. Experiments conducted in 10 mM PIPES with no zinc.

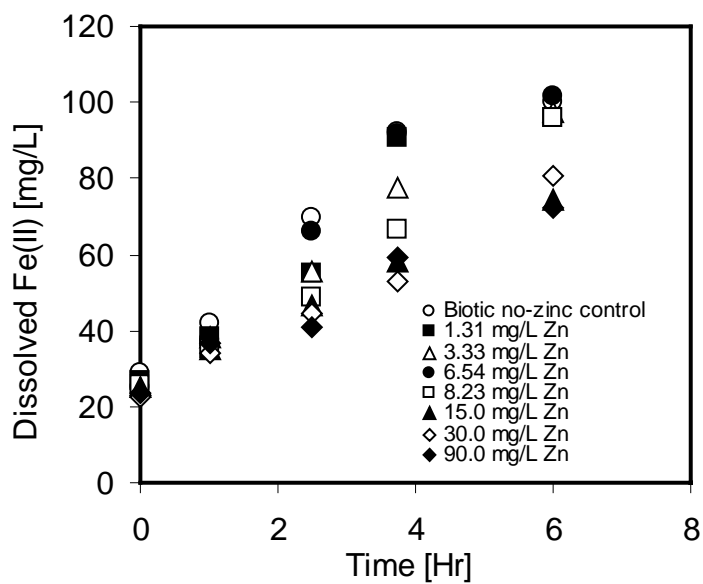


Figure 2.6 Dissolved Fe(II) as a function of time (0 to 6 h) for the biological reduction of 2 mM ferric citrate in 10 mM PIPES, 4 mM citric acid at pH 6.8. Zinc addition ranged from 0 mg L<sup>-1</sup> (for biotic and abiotic controls) to 90 mg L<sup>-1</sup>. Values are means of three replicates.

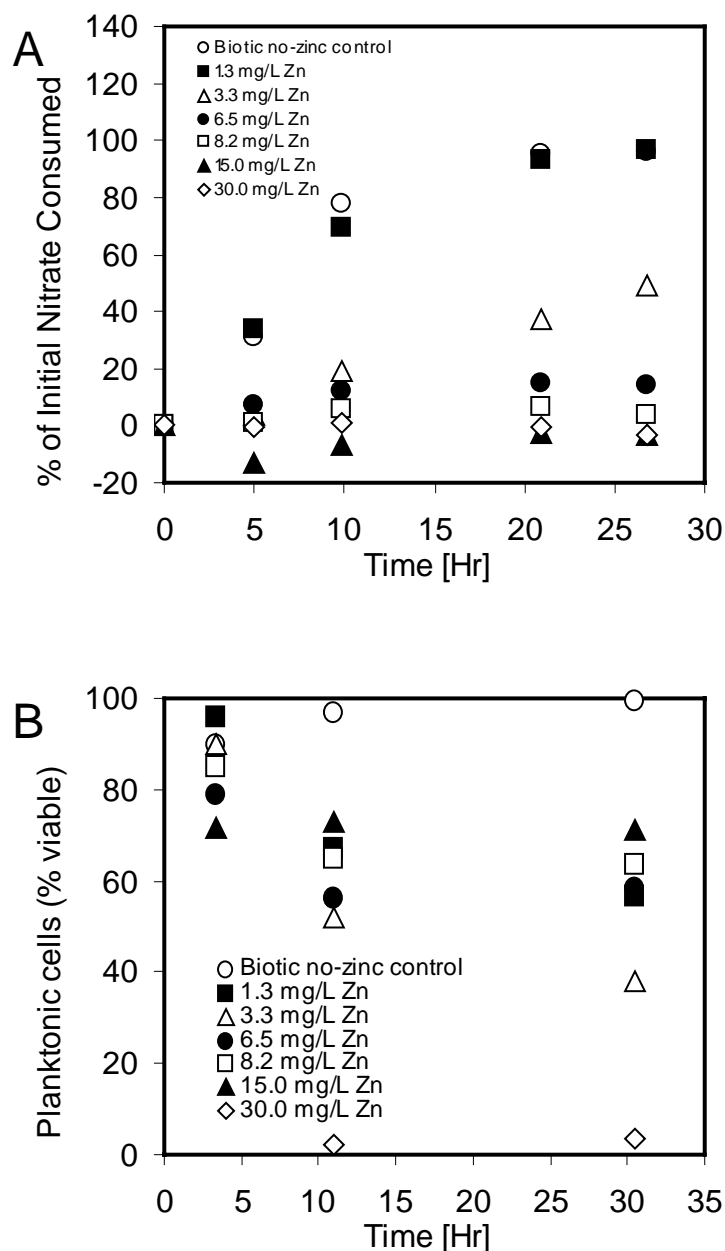


Figure 2.7 (A) Percentage of total nitrate reduction relative to initial nitrate concentration, (B) percent of planktonic cells that are viable as a function of time (0 to 27 h) for the biological reduction of nitrate with variable zinc. Solution consisted of 10 mM PIPES,  $144.4 \text{ mg L}^{-1} \text{ KNO}_3$  (equivalent to  $20 \text{ mg NO}_3\text{-N L}^{-1}$ ),  $10^8 \text{ cells mL}^{-1}$  at pH 6.8. Zinc addition ranged from  $0 \text{ mg L}^{-1}$  for biotic and abiotic controls to  $30 \text{ mg L}^{-1}$ . Values are means of three replicates ( $\pm$  standard deviation).

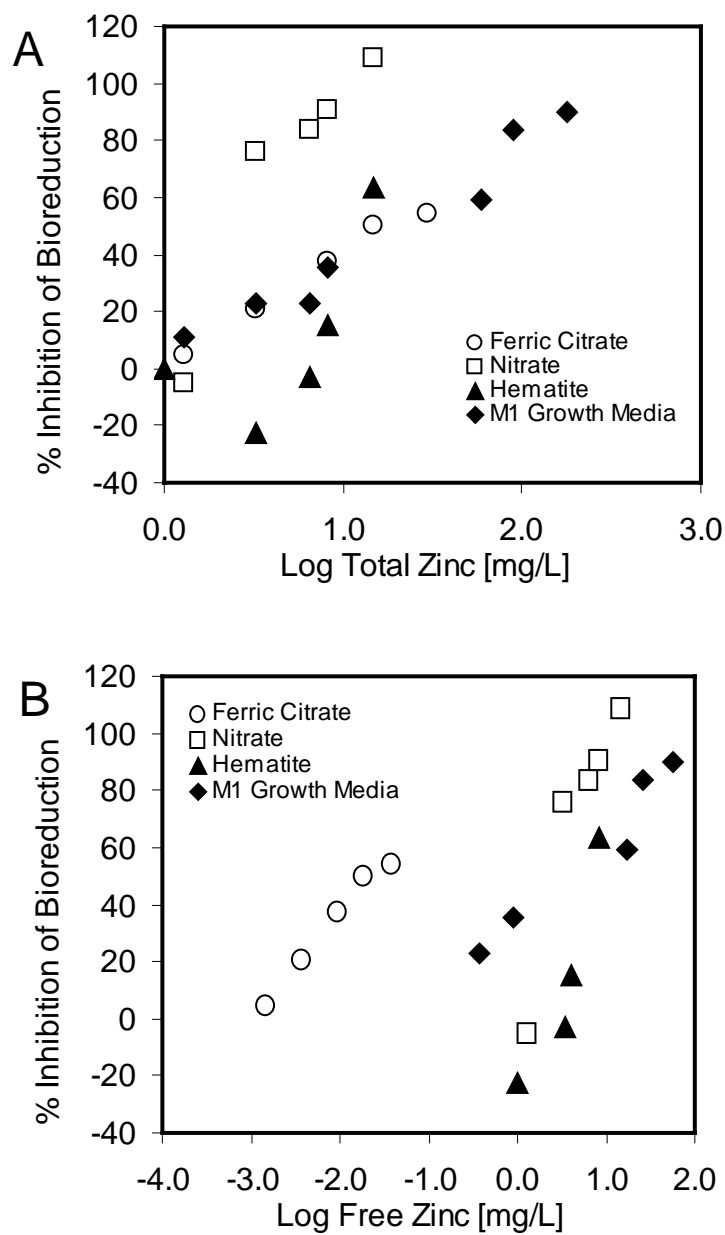


Figure 2.8 Inhibition of the maximum extent of bioreduction using *S. putrefaciens* for 2 g L<sup>-1</sup> hematite, 2 mM ferric citrate, 20 mg L<sup>-1</sup> NO<sub>3</sub><sup>-</sup>N, and *S. putrefaciens* growth in M1 media as a function of (A) log total zinc, (B) log free zinc. Free zinc results determined from MINTEQA2 calculations.

## CHAPTER 3

### Modes of Inhibition by Zinc on the Biological

#### Reduction of Hematite by *Shewanella putrefaciens* CN32

##### 3.1 Abstract

The reductive dissolution of hematite ( $\alpha\text{-Fe}_2\text{O}_3$ ) in the presence of zinc by the dissimilatory metal-reducing bacterium (DMRB) *Shewanella putrefaciens* strain CN32 was studied using anthraquinone-2,6-disulfonate (AQDS), a soluble electron shuttling agent, and ferrozine, a strong Fe(II) complexant, to better understand how zinc affects the system. Both AQDS and ferrozine had previously been shown to enhance the 5 day extent of hematite bioreduction. Experiments were conducted with a suspension of hematite ( $2.0 \text{ g L}^{-1}$ ) in 10 mM PIPES (pH 6.8) and  $\text{H}_2$  as an electron donor under non-growth conditions ( $10^8 \text{ cell mL}^{-1}$ ), spiked with zinc (0 to 0.229 mM) or manganese (0 to 1.86 mM) and incubated for 5 days. The net effect of zinc (i.e., inhibition) was measured based on the rate and extent of consumption of the electron acceptor in the absence and presence of zinc. The toxicity of zinc was measured based on direct counts of viable cells using the LIVE/DEAD *Ba*clight staining procedure. Results indicated that both AQDS and ferrozine increased zinc inhibition compared to no-amendment biotic controls. Fe(II) sorption decreased in the presence of zinc for both amendments indicating that Fe(II) and zinc compete for cell and oxide surface sorption sites. Zinc sorption decreased in the presence of Fe(II), yet increased with AQDS and ferrozine addition. Zinc sorbed to cell and hematite surfaces appeared to be a more potent inhibitor of hematite bioreduction than free zinc. Increased zinc inhibition with ferrozine was caused by complexation of surface bound Fe(II) that subsequently allowed additional zinc sorption to cell and hematite surfaces. The increased zinc

inhibition with AQDS indicated that electron shuttling between cells and hematite does not overcome the toxic effects of zinc. Hematite bioreduction was not affected by manganese addition below ca. 0.91 mM. The extent of manganese sorption was minimal compared to zinc and was unaffected by the presence of Fe(II), suggesting that surface passivation was not a primary inhibition mechanism by manganese during hematite bioreduction. The results indicated that surface sorbed zinc, especially zinc sorbed to the cell surface, was a potent inhibitor and provided greater insight towards resolving the inhibitory mode of zinc than the free zinc concentration.

### **3.2 Introduction**

The dissimilatory reduction of Fe(III) appears to be an important process for the cleanup of contaminated sediments and aquifers. The wealth of ferric containing minerals found within these contaminated sediments can heavily influence the fate and transport of organic and inorganic contaminants. While microbial iron reduction appears to be a promising remediation process, little is known regarding its performance in the presence of high concentrations of contaminants such as heavy metals. Previous studies have shown that the rate and extent of microbial Fe(III) reduction were influenced by the presence of metals (Markwiese et al. 2000; Fredrickson et al. 2001; Parmar et al. 2001; Zachara et al. 2001), mainly due to metal toxicity to the dissimilatory metal-reducing bacteria (DMRB). While metal-microbe interactions are well documented, (Baath 1989; Kushner 1993; Gadd 1996; Warren et al. 2001), only a few studies have specifically focused on solid-phase iron oxide reduction by the DMRB *Shewanella spp* (Royer et al. 2002a; Royer et al. 2002b). These interactions may exert significant control on the effectiveness of bioremediation at contaminated sites.



In a previous study investigating zinc inhibition of Fe(III) and nitrate bioreduction with *S. putrefaciens* strain CN32, Stone et al. (Stone et al. 2002) found that the rate and extent of bioreduction was strongly controlled by the “free” zinc concentration. The concentration of zinc that inhibited growth by 50% compared to the no-zinc control (IC<sub>50</sub>) was similar for both nitrate reduction (soluble phase) and *S. putrefaciens* growth (with lactate in M1 medium), indicating that the mode of inhibition was related to microbial toxicity and not a surface sorption mechanism. However, the inhibition of hematite did not correlate directly to cell viability, partially because the bioreduction of hematite was insensitive to the number of viable cells, but also partially because zinc sorbed to hematite and DMRB surfaces may exert another mode of inhibition.

The two mechanisms initially thought to control metal inhibition during solid-phase bioreduction were surface site saturation and direct microbial toxicity. Surface sorption of biogenic Fe(II) on Fe(III) oxide and DMRB surfaces has been proposed as a mechanism which inhibits bioreduction (Urrutia et al. 1998; Roden et al. 1999). Inhibition occurs when biogenic Fe(II) produced during reduction occupies or saturates surface hydroxyl groups, preventing DMRB-oxide contact and/or forming an electrostatic barrier that may impede electron transfer from the DMRB to the oxide (Roden et al. 2002). The second proposed mechanism, microbial toxicity, has previously been associated with free metal activity (Knight et al. 1995; Chaudri et al. 1999; Chaudri et al. 2000; Ritchie et al. 2001), with B-type metal cations (Stumm et al. 1996) such as zinc complexing with carboxyl and phosphoryl surface sites on cell walls (Fein et al. 2001).

The enhancement of solid-phase iron bioreduction by two soluble amendments, anthraquinone-2,6-disulfonate (AQDS) and ferrozine, was reported by Royer et al. (Royer et al.

2002a). AQDS can serve as an alternative electron acceptor and shuttle electrons between DMRB and solid-phase ferric oxides (Fredrickson et al. 1998; Zachara et al. 1998; Fredrickson et al. 2001; Hacherl et al. 2001; Zachara et al. 2001), while ferrozine can complex both surface sorbed and free Fe(II) (Royer et al. 2002b). Both amendments have previously been shown to stimulate hematite bioreduction under conditions similar to those employed within this study (Royer et al. 2002a).

The role of AQDS as an electron shuttling quinone has been well documented, however, the mechanisms related to electron shuttling in the presence of divalent metals other than biogenic Fe(II) are relatively unknown. Fredrickson et al. (Fredrickson et al. 2001) reported that AQDS did not enhance the bioreduction of Ni(II)- or Co(III)-substituted goethite by *S. putrefaciens* CN32. This lack of enhancement, compared to increased reduction in the absence of metals, was attributed to Ni<sup>2+</sup> or Co (II/III) blockage of goethite surface sites that could slow re-oxidation of AH<sub>2</sub>DS by goethite. These metal cations may have sorbed to the oxides, forming bi- or multi-nuclear surface complexes that inhibited bioreduction through “surface passivation” (Zachara et al. 2001). Surface passivation mechanisms may also promote the formation of metal-substituted magnetite which formed in the presence of AQDS (Fredrickson et al. 2001).

The addition of manganese instead of zinc during hematite bioreduction was used in the current study to distinguish between surface sorption effects and those effects associated with toxicity. Manganese addition had no effect on hematite bioreduction under conditions similar to those employed in the current study (Royer et al. 2002c) and was non-toxic to cyanobacteria *Anacystis nidulans* growth at ca. less than 1.82 mM total manganese (Lee et al. 1994). Therefore, by using manganese at ca. less than 1.82 mM, any inhibitory effects observed during

hematite bioreduction could be attributed to a surface passivation mechanisms and not cell lethality.

While our previous work (Stone et al. 2002) showed that zinc inhibits both Fe(III) and nitrate reduction, the specific modes of zinc inhibition were unresolved. For this study, additional experiments using ferrozine and AQDS were performed to further our understanding of the inhibitory role of zinc during hematite bioreduction. In addition, manganese addition at sub-toxic concentrations was studied to separate surface sorption effects from effects related to microbial toxicity.

### **3.3 Experimental**

#### **3.3.1 Microorganism and Culture Conditions**

*Shewanella putrefaciens* strain CN32 was provided courtesy of Dr. David Balkwill (Subsurface Microbial Culture Collection, Florida State University). *S. putrefaciens* CN32 was isolated from an anaerobic subsurface core sample (250 m below ground surface) from the Morrison Formation in northwestern New Mexico (Fredrickson et al. 1998). The cultures were grown aerobically on tryptic soy broth without dextrose (TSB-D) at 20°C. Cells were harvested by centrifugation (4900x g, 10 min, 20°C) from a 16-hour-old culture (late log-decreasing growth phase). The cells were washed three times in 10 mM 1,4-piperazinediethanosulfonic acid (PIPES; pH=6.8) with the final wash made with deoxygenated solution to remove residual oxygen. Cell pellets were re-suspended in 5-15 ml of deoxygenated 10 mM PIPES buffer in an anaerobic chamber (Coy; Grass Lakes, MI) under a N<sub>2</sub>:H<sub>2</sub> (ca. 97.5:2.5%) atmosphere and the cell density was determined by absorbance at 420 nm.

### 3.2.2 Materials

An iron oxide powder was obtained from J.T. Baker and identified by X-ray diffraction and Mössbauer spectroscopy to be hematite ( $\alpha$ -Fe<sub>2</sub>O<sub>3</sub>) of greater than 99% purity. The hematite had an average particle diameter of 1.0  $\mu\text{m}$  measured by laser diffraction and a specific surface area of 9.04  $\text{m}^2 \text{g}^{-1}$  measured by 5-point N<sub>2</sub>-BET. The zero point of charge was pH 8.5 as determined by electrophoretic mobility and proton titrations. The hematite surface site density for Fe(II) was 5.1 sites per  $\text{nm}^2$  based upon the adsorption of Fe(II) (Jeon et al. 2001). Hematite was heated to 550°C in air overnight before use to remove any residual organic carbon. Hematite was added to the anaerobic PIPES buffer at least 24 h prior to any experiment to allow for hydration. Anthraquinone-2,6-disulfonate (AQDS, Sigma-Aldrich, St. Louis, MO) and ferrozine (J. T. Baker) was used as received and a filtered (0.2  $\mu\text{m}$ ) stock solution was prepared in PIPES buffer.

### 3.2.3 Bioreduction Experiment Preparation

A “master reactor” approach was used to prepare all experiments (Royer et al. 2002a) to ensure consistent chemical and biological conditions. All preparations were performed within a Coy anaerobic chamber. A master reactor was prepared by combining the electron acceptor and the inoculum in a 250 mL serum bottle. All solutions (except the zinc and manganese stocks) were prepared in 10 mM PIPES (pH 6.8). Biotic no-amendment (i.e., AQDS or ferrozine) controls were immediately prepared by transferring 10 mL of the suspension into 20 mL amber serum bottles (in at least triplicate). All 20 mL serum bottles were crimp-sealed with Teflon-faced butyl rubber stoppers and aluminum caps. For AQDS and ferrozine treatments, biotic with-amendment no-metal controls were also prepared. Afterwards, zinc or manganese was incrementally added to the master reactor in an acidified and deoxygenated ZnCl<sub>2</sub> or MnCl<sub>2</sub>

solution (1,000 mg/L AAS certified standards) along with an equal volume of 0.1 N NaOH (for pH maintenance). At each concentration, 10 mL of the suspension was transferred into 20 mL amber serum bottles (in triplicate). Five to seven different metal concentrations were usually prepared. Sealed serum bottles were incubated in the dark at 20°C on orbital shakers outside of the anaerobic chamber. Hydrogen from the anaerobic chamber atmosphere (97.5:2.5% N<sub>2</sub>:H<sub>2</sub>) was used as the electron donor in all experiments.

### **3.2.4 Hematite Bioreduction**

Experiments were performed with 2.0 g L<sup>-1</sup> hematite (0.0125 mol Fe<sub>2</sub>O<sub>3</sub> L<sup>-1</sup>), a final cell density of 10<sup>8</sup> cells mL<sup>-1</sup>, metal concentrations ranging from 0 to 0.229 mM total zinc or 0 to 1.82 mM total manganese, and amendment concentrations of 50 μM AQDS and 1.46 mM ferrozine. After incubation times of 5 d, reactors were sacrificed to measure dissolved and total Fe(II), dissolved and total metal, viable planktonic cells, and pH.

### **3.2.5 Zinc and Manganese Sorption**

Experiments were performed to determine the sorption of zinc and manganese to 10<sup>8</sup> cells mL<sup>-1</sup>, 2.0 g L<sup>-1</sup> hematite, and sterilized suspensions containing 10<sup>8</sup> cells mL<sup>-1</sup> and 2.0 g L<sup>-1</sup> hematite. Metal concentrations ranged from 0 to 0.910 mM manganese, and 0 to 0.688 mM zinc. Cells for all sorption experiments were pasteurized at 63°C for 30 min. The effectiveness of this sterilization procedure and cell wall integrity of the sterilized cells were confirmed using the LIVE/DEAD<sup>®</sup> *BaCl*light<sup>™</sup> bacterial viability kit (Molecular Probes; Eugene, OR). All sorption experiments were performed at pH 6.8 in the anaerobic chamber using the master reactor method described above. Individual serum vials in triplicate were incubated on an orbital shaker outside the anaerobic chamber. Total and dissolved metal concentrations were measured using methods described below.

### 3.2.6 Analytical Techniques

Fe(II) was reported as dissolved, total, and adsorbed. For dissolved Fe(II), samples were filtered (0.2  $\mu\text{m}$  cellulose acetate) and Fe(II) was measured by ferrozine (1.96 mM ferrozine in 50 mM HEPES, pH 8.0) in the anaerobic chamber. Solution pH of the filtrate was determined in the anaerobic chamber using a combination pH electrode. For total Fe(II), an unfiltered sample was acidified with HCl to achieve a final solution normality of 0.5 N. The solution was mixed for ca. 24 h, filtered (0.2  $\mu\text{m}$ ) and Fe(II) in the filtrate was measured by ferrozine. Adsorbed Fe(II) was calculated as the difference between dissolved and total Fe(II). Dissolved and total metal concentrations were measured from the corresponding dissolved and total Fe(II) filtrate samples by flame atomic absorption spectrometry (AAS) after preservation with conc.  $\text{HNO}_3$ . Previously described methods (Stone et al. 2002) were employed to determine cell viability using the *Baclight* viability kit.

## 3.3 Results

### 3.3.1 Effect of Ferrozine and AQDS on Zinc Inhibition

In a previous study zinc was shown to inhibit hematite bioreduction (Stone et al. 2002), however, the specific mode(s) of inhibition were unresolved. To better understand the mechanisms of zinc inhibition, two soluble amendments known to stimulate hematite bioreduction (Royer et al. 2002b) were added to these experiments. Total Fe(II) production after 5 d as a function of zinc addition for 1.46 mM ferrozine, 50  $\mu\text{M}$  AQDS and the biotic no-amendment controls are presented in Figure 1A. These two amendment concentrations were selected because they both enhanced hematite bioreduction by similar amounts compared to biotic no-amendment controls (Royer et al. 2002a). For each amendment, biotic no-amendment

no-zinc controls and biotic with-amendment no-zinc controls were prepared and these data are distributed along the y-axis of Figure 1A. In the absence of zinc, all amendment concentrations significantly stimulated hematite bioreduction compared to their corresponding no-amendment controls. Note that the no-amendment with-zinc controls shown in Figures 1A and 2 (open circle series) were prepared independently from all amendment experiments. Variability between the no-amendment and the no-amendment controls (low data cluster on y-axis in Fig. 1A) is within expected ranges for these biogeochemical systems.

Low concentrations of zinc stimulated Fe(II) production in the presence of ferrozine and for the no-amendment control. In the no-amendment control, Fe(II) production increased relative to its corresponding no-zinc control with total zinc concentrations up to 0.05 mM. Fe(II) production for ferrozine increased relative to the no-zinc control at a total zinc concentration of 0.05 mM. No stimulatory effect of zinc was observed in the presence of AQDS. The results for the ferrozine and no-amendment control Fe(II) production conform to a Type II dose-response curve (Welp et al. 1997) with maximum Fe(II) production occurring at a low zinc concentration and decreasing Fe(II) production at higher zinc concentrations.

*Ba*clight cell viability counts (planktonic, Fig. 1B) for the ferrozine and no-amendment control experiments show that zinc addition decreased cell viability with 100% lethality occurring at 0.229 mM total zinc for both experiments. The decrease in cell viability was more dramatic for ferrozine, with only 4% of cells remaining viable at 0.126 mM total zinc. Cell viability counts were not performed for the AQDS experiments. Cell viability was the greatest for the no-zinc controls (75 and 82% viable cells after 5 d for the ferrozine and no-amendment controls, respectively). The slight stimulation in viability (7%) observed for the no-amendment control at 0.050 mM total zinc corresponded to stimulation in Fe(II) production (Fig. 1A).

Conversely, the stimulation of Fe(II) production for ferrozine at 0.050 mM total zinc did not correspond with increased cell viability.

Amendment addition increased the inhibition of zinc during hematite bioreduction (Fig. 2). Inhibition was quantified using methods discussed previously (Stone et al. 2002) where inhibition was defined as the percent change in the biological output of the system due to zinc addition relative to the corresponding biotic no-zinc control (Sani et al. 2001). The zinc concentration corresponding to a 50% decrease in biological output compared to the no-zinc control was defined as the  $IC_{50}$ . The  $IC_{50}$  value was 0.202 mM total zinc for hematite bioreduction with no amendment. Amendment addition decreased the  $IC_{50}$  to 0.0806 and 0.101 mM total zinc for AQDS and ferrozine, respectively. The results presented in Figure 2 may be interpreted as decreased biological output (i.e., consumption of electron acceptor) occurring at lower zinc concentrations, indicative of a greater inhibitory effect.  $IC_{50}$  values could not be calculated based on free zinc concentrations because zinc-amendment complexation constants were not available. A summary of all zinc  $IC_{50}$  values is presented in Table 1.

### **3.3.2 Impact of Fe(II) Sorption with Amendment Addition**

Sorbed Me(II) concentrations were calculated as the difference between the total and dissolved Me(II) concentrations. This difference included Me(II) sorbed to both hematite and DMRB; however, there was no means to measure the distribution of Me(II) between these two sorbents. Therefore, sorbed Me(II) concentrations are reported as mM Me(II) per g  $Fe_2O_3$  in all sorption isotherms. A “baseline” Fe(II) sorption isotherm (Fig. 3A) was developed from a series of hematite bioreduction experiments (Stone et al. 2002) performed in the absence of any amendment (e.g., zinc, manganese, AQDS, ferrozine). Experiments were performed with



variable hematite concentrations and a constant initial DMRB concentration of  $10^8$  cells  $\text{mL}^{-1}$ . All data presented in Fig. 3A were calculated from 5 d incubations.

A Freundlich sorption isotherm ( $R^2 = 0.890$ ) was selected over a Langmuir isotherm (results not shown;  $R^2 = 0.735$ ) because of its higher correlation coefficient (i.e.,  $R^2$  value). Conceptually, this sorption isotherm should be viewed as a “distribution diagram” for biogenic Fe(II) between solid (hematite and DMRB surfaces) and solution phases in a dynamic system. Note that local equilibrium is assumed with any isotherm equation, however, the nature of both the cell and hematite surfaces could be changing during these experiments. The dashed lines in Fig. 3A represent 95% confidence intervals associated with the Freundlich isotherm. The sorption isotherm for Fe(II) was similar to abiotic results reported by Jeon et al. (Jeon et al. 2002). Freundlich isotherms were used to describe metal sorption calculated from most bioreduction experiments [Fe(II) and Zn(II)] while Langmuir isotherms were used to describe Zn(II) and Mn(II) sorption onto the cells and hematite measured in separate abiotic sorption experiments.

### **3.3.3 Impact of Zinc on Fe(II) Adsorption**

The effect of zinc on the sorption of Fe(II) during the bioreduction of hematite is presented in Fig. 3B. The solid line represents the “baseline” no-zinc sorption isotherm (Fig. 3A) while the dashed lines represents the 95% confidence interval associated with the Freundlich isotherm. The Fe(II) sorption measurements were from 1 through 5 d incubations for each zinc concentration. The highest dissolved Fe(II) concentration for each zinc addition corresponded to the 5 d incubation. For the majority of the zinc concentrations, the addition of zinc lowered the extent of Fe(II) sorption. Zinc concentrations greater than 0.050 mM decreased Fe(II) sorption the most (28% to 78%) relative to the no-zinc control.

### 3.3.4 Zn(II) Sorption

Experiments were performed to determine the zinc sorption capacity of *S. putrefaciens* CN32, hematite, and sterile cells and hematite. Experiments with sterile cells and hematite were performed with and without Fe(II). The samples containing Fe(II) [0.012 to 0.51 mM total Fe(II)] were taken from the no-amendment control results presented in Figure 1A. Cells were pasteurized prior to inoculation for all the sorption experiments with no Fe(II) to ensure that no Fe(II) would be generated due to hematite bioreduction. Langmuir sorption isotherms for zinc are presented in Fig. 3B. The data points indicate measured sorption values and the solid (no-Fe(II)-control) and dashed [biotic results with Fe(II)] lines represent the calculated Langmuir isotherms. Sorption isotherms are also presented for the individual components (i.e., cells or hematite) to show the relative distribution of zinc between these sorbents in the absence of Fe(II). A summary of the Langmuir sorption isotherm parameters is presented in Table 1. For 2 g L<sup>-1</sup> hematite and 10<sup>8</sup> cells mL<sup>-1</sup> as used in our experiments (with cell mass assumed to equal 6.4 x 10<sup>-10</sup> mg dry wt. cell<sup>-1</sup> (Liu et al. 2002)), the maximum concentration of sorbed metal ( $C_{\max}$ ) was calculated for each test condition (Table 1). Zinc sorption was greatest for the combined hematite and cell isotherm ( $C_{\max}$  of 0.115 mM) without Fe(II). The presence of Fe(II) lowered zinc sorption to  $C_{\max}$  of 0.109 mM for the biotic reduction experiments. The individual components sorbed 0.0812 and 0.0643 mM total zinc onto hematite and cells, respectively, and these values appeared to be directly additive when the components were combined.

### 3.3.5 Impact of Amendments on Fe(II) and Zn(II) Adsorption

The change of Fe(II) sorption to the hematite and cells due to ferrozine and AQDS is presented in Figure 5A. The solid line represents the “baseline” Fe(II) sorption isotherm in the absence of the amendments (from Fig. 3A) and the dashed line represents 95% confidence

intervals associated with the Fe(II) isotherm. A greater amount of ferrozine data is presented due to the additional number of experiments performed using ferrozine. These data show that 1.46 mM ferrozine eliminates Fe(II) sorption to the hematite and cells for all dissolved Fe(II) concentrations. Ferrozine has a maximum Fe(II) complexation capacity of  $0.33 \text{ mol Fe(II) mol}^{-1}$  ferrozine (Stookey 1970), thus the Fe(II) complexation capacity associated with 1.46 mM ferrozine would be equal to 0.48 mM Fe(II). This complexation capacity exceeded the concentration of biogenic Fe(II) produced in all but one experiment. Ferrozine-complexed Fe(II) did not sorb to the hematite and cell surfaces. The addition of 50  $\mu\text{M}$  AQDS lowered Fe(II) sorption by 30 to 59% compared to the no-amendment controls. In summary, these results show that each amendment decreased the sorption of Fe(II) to hematite and cells.

The effects of the amendments on zinc sorption to the hematite and cells are presented in Fig. 5B. The “baseline” no-amendment with-biogenic-Fe(II) sorption isotherm (dark circles from Fig. 4) was developed from no-amendment hematite bioreduction experiments (Stone et al. 2002). The dashed lines represent 95% confidence interval associated with this isotherm. Both AQDS and ferrozine increased zinc sorption for less than ca. 0.0459 mM dissolved zinc. Dissolved zinc concentrations greater than 0.0459 mM increased zinc sorption only with AQDS.

### **3.3.6 Impact of Mn(II) Addition**

Hematite bioreduction experiments using manganese instead of zinc were performed to determine whether Mn(II), which has similar charge and chemical properties as both Zn(II) and Fe(II), may inhibit hematite bioreduction at similar concentrations as those observed with zinc. The results for the manganese-amended hematite bioreduction experiments are presented in Figure 6A. Total Fe(II) was typically twice the dissolved Fe(II) concentration for each manganese concentration, similar to sorption distributions observed with zinc (Stone et al. 2002).

Total Fe(II) production was consistent up to ca. 1.82 mM total manganese where total Fe(II) decreased to 0.104 mM. Cell viability results (planktonic, Fig. 6B) show that manganese addition was not lethal to cells. Final 5 d viable counts ranged from 55 to 90% for all manganese concentrations. The highest manganese concentration (1.82 mM) decreased Fe(II) production by 40% with a 31% decrease in cell viability compared to the no-manganese control.

### 3.3.7 Fe(II) and Mn(II) Sorption

The effect of manganese on the sorption of Fe(II) onto hematite and the cells is presented in Figure 7. The solid line represents the “baseline” Fe(II) sorption in the absence of manganese (from Fig. 3A) with the dashed line indicating the 95% confidence interval for the isotherm. Total manganese concentrations for these Fe(II) sorption data ranged from 0 to 1.82 mM. The results show that manganese did not consistently increase or decrease Fe(II) sorption. The relatively small range of dissolved and sorbed Fe(II) concentrations was due to the relatively consistent levels of total Fe(II) produced during 5 d hematite bioreduction. These Fe(II) sorption results suggest that manganese does not interfere or compete with Fe(II) for hematite and cell sorption sites.

Langmuir sorption isotherms for manganese sorption onto hematite and cells in the presence and absence of Fe(II) is presented in Fig. 8. The data presented for manganese sorption with Fe(II) [between 0.10 - 0.20 mM total Fe(II)] was developed from the manganese bioreduction results presented in Fig. 6A. Pasteurized cells were used for the sorption results in the absence of Fe(II) to prevent biogenic Fe(II) production. The results show that manganese sorption was not influenced by the presence of Fe(II). The maximum manganese sorption ( $C_{\max}$ ) was 0.0583 and 0.0457 mM total manganese for experiments performed with and without Fe(II). A summary of the manganese sorption results is presented in Table 1.

### 3.4 Discussion

Zinc inhibition during hematite bioreduction was initially thought to be controlled by two mechanisms: direct microbial lethality due to the presence of zinc, or an increase in zinc sorption decreasing available hematite surface sites for DMRB contact. Free metal activity has been well correlated to microbial toxicity in many environmental systems (Shuttleworth et al. 1993; Poulson et al. 1997; Chaudri et al. 1999; Ritchie et al. 2001). Indeed,  $IC_{50}$  values based on free zinc for nitrate bioreduction and cell growth (using lactate in M1 medium) with *S. putrefaciens* CN32 were essentially identical (Stone et al. 2002). In addition to free dissolved zinc, sorbed zinc species may also inhibit the bioreduction of solid-phase oxides. As noted above, sorbed zinc may interfere with DMRB-oxide contact, however, we speculate that sorbed zinc species may also be potent biochemical inhibitors.

The extent of zinc sorption onto the hematite and cell surfaces was influenced by the presence of divalent cations such as Fe(II), consistent with the findings by Jeon et al. (Jeon et al. 2002). The impact of Fe(II) on zinc sorption was most apparent in Figure 4 where Fe(II) reduced the extent of zinc sorption onto both cells and hematite by 5% (from 0.115 to 0.109 mM total zinc). Zinc sorption (Fig. 4) was consistently higher than manganese sorption (Fig. 8) for all conditions [cells, hematite, and composite systems with and without Fe(II)]. More importantly, however, was the large difference between zinc and manganese sorption on non-viable cells. Zinc binding to the cells ( $1.005 \text{ mM g}^{-1}$  dry weight cells) was much higher than manganese ( $0.330 \text{ mM g}^{-1}$  dry weight cells), indicating that zinc was preferentially sorbed to the cells. While metal binding affinities have been reported as proportional to hydraulic radius, waters of hydration, and valance (Trivedi et al. 2000), the level zinc binding we observed was much

greater than the binding capacity reported for *B. subtilis* ( $0.701 \text{ mM g}^{-1}$ ) (Beveridge et al. 1976). The high binding capacity for zinc indicated that for our experimental conditions (pH 6.8, 10mM PIPES, anoxic), zinc sorption to cells was very prominent. While cellular sorption accounted for only a small percentage of the overall mass of zinc sorbed (Table 2), the results indicated that even the slightest increased zinc sorption provoked a more dramatic inhibitory response to the presence of zinc.

Ferrozine enhanced hematite bioreduction by its ability to complex biogenic Fe(II), preventing surface passivation of Fe(II) on the hematite or DMRB surfaces (Royer et al. 2002b). The premise for adding ferrozine was to determine if zinc inhibition would increase in a system where zinc sorption was anticipated to increase [because of decreased competition with Fe(II)]. While increased zinc sorption would decrease free zinc concentrations, zinc sorbed to hematite or cells could still be a significant exposure pathway. Furthermore, zinc concentrations could be greatly magnified in localized regions at the point of contact between the hematite and cells.

Similar to the no-amendment control, ferrozine stimulated Fe(II) production at a total zinc concentration of 0.05 mM zinc followed by decreased Fe(II) production for higher zinc concentrations (Fig. 1A). Although Fe(II) production was higher for the low zinc concentrations, the increased sensitivity of zinc resulted in lowering the total zinc  $IC_{50}$  (0.101 mM) compared to the untreated control. The cell viability results (Fig. 1B) confirm that ferrozine provoked greater cell lethality compared to the no-amendment control for ca. 0.010 mM total zinc and above. The mechanisms for zinc inhibition for the ferrozine treatment were thought to be attributed to the Fe(II) scavenging ability of ferrozine. Evidence of Fe(II) scavenging were apparent with the sharp reduction of Fe(II) sorption for the ferrozine addition (Fig. 5A). This decrease was expected because the theoretical complexation capacity of Fe(II) ( $0.333 \text{ mol Fe(II) mol}^{-1}$ )

ferrozine; or 0.486 mM Fe(II) for 1.46 mM ferrozine) was not exceeded due to increased Fe(II) production at any time of the experiment (Royer et al. 2002b). The decrease in Fe(II) sorption, mainly attributed to ferrozine chelating surface bound Fe(II), resulted in additional zinc sorption (Fig. 5B) for dissolved zinc concentrations below 0.0387 mM zinc. For these conditions, ferrozine increased zinc sorption by 11 to 33% compared to the no-amendment control. Further, knowing that ferrozine complexed nearly all of the surface bound Fe(II) (Fig. 5A) leaving little Fe(II) to compete with zinc for sorption sites, we could assume that zinc sorption under these conditions would be best described using the composite cells and hematite Langmuir sorption isotherm without Fe(II) (Fig. 4, open triangles). The sorption maximum for this no Fe(II) condition was 5% higher than the bioreduction results containing Fe(II). While cell growth inhibition was previously attributed to free zinc, these results indicate that zinc sorption to the cells and hematite observed for ferrozine may be responsible for the increased cell lethality and zinc sensitivity compared to the no-amendment controls.

AQDS enhanced hematite bioreduction by its ability to serve as an alternative soluble electron acceptor and shuttle electrons to areas previously inaccessible to DMRB (Hacherl et al. 2001; Zachara et al. 2001). Previous studies have shown that AQDS could overcome the inhibition caused by Co(III)- and Ni(II)-substituted into a series of goethites (Zachara et al. 2001). The premise for adding AQDS was to determine if zinc would still be inhibitory under conditions where the DMRB and hematite were not required to be within direct contact. In other words, if the DMRB preferentially used AQDS over hematite as an electron acceptor and the re-oxidation of AH<sub>2</sub>DS by hematite was unaffected by zinc, then an electron shuttle may effectively overcome Me(II) inhibition.

AQDS stimulated bio-reduction in the absence of zinc (Fig. 1B) by increasing Fe(II) production by 145% compared to the no-amendment control. However, unlike the ferrozine or no-amendment control results, no additional stimulation of Fe(II) production at low zinc concentrations occurred. Instead, Fe(II) production decreased with increasing zinc for AQDS. The absence of Fe(II) stimulation at lower zinc concentrations may be attributed to the increased resistance of AH<sub>2</sub>DS re-oxidation in the presence of zinc or the formation a passive film (Roden et al. 2002), both of which may contribute lowering the microbial reducibility of the hematite. The decrease in Fe(II) sorption in the presence of zinc (Fig. 5A) was consistent with the no-amendment Fe(II) sorption results (Fig. 3B) where zinc decreased Fe(II) sorption, indicating that AQDS does not alter Fe(II) sorption. However, AQDS increased zinc sorption by 10% (Fig. 5B), providing further evidence that surface sorbed zinc was a significant pathway for cellular zinc exposure. Taken together, the AQDS results show that electron shuttling from the oxidation/reduction reaction of AQDS does not overcome the toxic mechanisms of zinc. Even though electron shuttling minimized contact between the cells and hematite which subsequently reduced cellular exposure to hematite bound zinc, the increased surface sorption of zinc on both the cells and hematite appeared to overcome the electron shuttling mechanisms of AQDS.

The hematite bio-reduction experiments with manganese were performed to separate surface coverage mechanisms from mechanisms attributed to direct lethality. Manganese concentrations were previously shown to be non-toxic to DMRB below 1.82 mM total manganese (Lee et al. 1994; Royer et al. 2002c), therefore any inhibitory effects observed during hematite bio-reduction in the presence of manganese could be attributed to mechanisms related to surface sorption and not direct toxicity of the cells. Manganese addition did not affect Fe(II) production for total manganese ca. below 0.910 mM (Fig. 6A) while the IC<sub>50</sub> increased to 3.06



mM compared to the  $IC_{50}$  for zinc (0.202 mM total zinc). The maximum manganese sorption for the composite samples (cells and hematite) in the presence of Fe(II) (Fig. 8, dashed line) was 0.0583 mM total manganese. Manganese sorption in the absence of Fe(II) (Fig. 8, solid line) was only slightly less, indicating that manganese and Fe(II) do not compete for sorption sites. The maximum concentration of manganese sorbed to cells and hematite (0.0583 mM total manganese) was significantly less than the manganese concentration where inhibition was first observed (1.82 mM). Had manganese inhibition occurred at a concentration closer to the sorption maxima, one could conclude that surface saturation by sorbed manganese would be the primary inhibition mode.

To further our understanding of inhibition mode for manganese, a comparison between the maximum sorption of manganese (0.0583 mM) and the corresponding effect of zinc at the same concentration was made. According to the sorption results for zinc in the presence of Fe(II) (Fig. 4, open circles with dashed line), 0.0583 mM sorbed zinc resulted in approximately 0.015 mM dissolved zinc during hematite bioreduction. This dissolved zinc concentration was consistently measured as the matching dissolved zinc concentration measured for the addition of 0.050 mM total zinc during bioreduction experiments presented in Figure 1A (controls, dissolved results not shown). At 0.050 mM total zinc, Fe(II) production was stimulated for the no-amendment controls (open-circles). However, at this same zinc concentration, evidence of metal toxicity to the DMRB was observed (Fig. 1B) as only 50% of the cell population remained viable. By comparison, manganese addition did not result in additional cell lethality (Fig. 6B) until 1.82 mM total manganese was present, which was the concentration previously shown as toxic to cells (Lee et al. 1994). Taken together, these results demonstrate that manganese and zinc affected hematite bioreduction using different mechanisms. The lower degree of manganese

sorption compared to zinc implied that manganese inhibition was related to toxicity by free manganese only at high (> 0.91 mM) total manganese concentrations and was not related to surface sorption or “passivation” by sorbed manganese. On the contrary, surface sorbed zinc appeared to control zinc inhibition during hematite bioreduction, as demonstrated by the sorption and Fe(II) production results for AQDS and ferrozine addition.

### **3.5 Conclusion**

In summary, the addition of the soluble amendments AQDS and ferrozine increased zinc inhibition of hematite bioreduction by *S. putrefaciens* CN32. Increased inhibition was attributed to several factors, most importantly the increased sorption of zinc onto hematite and cell surfaces. The complexation of Fe(II) by ferrozine allowed free zinc to sorb to surfaces that would otherwise have been occupied by Fe(II), leading to increased zinc sorption onto hematite and cell surfaces. The elevated and localized zinc concentrations were proven toxic to the cells through greater cell lethality counts which further lowered the rate and extent of hematite bioreduction compared to the no-amendment control. Zinc inhibition proved to be insurmountable for AQDS and its electron shuttling capabilities, negating the benefits of non-contact between the cells and oxides. Zinc was found to also have a very high cell sorption affinity compared to manganese, providing further evidence that the slight increase in zinc sorption measured for both AQDS and ferrozine could result in even greater zinc sorption onto the cells, leading to greater cell lethality.

### **3.6 Acknowledgments**

Research supported by the Natural and Accelerated Bioremediation Research Program (NABIR), Office of Biological and Environmental Research (OBER), Office of Energy Research, U.S. Department of Energy (DOE), Grants no. DE-FG02-98ER62691 and No. DE-FG02-01ER63180 is gratefully acknowledged.

### 3.7 Literature Cited

- Baath, E. (1989). "Effects of heavy-metals in soil on microbial processes and populations (a review)." Water Air and Soil Pollution 47(3-4): 335-379.
- Beveridge, T. J. and R. G. E. Murray (1976). "Uptake and retention by cell walls of *Bacillus subtilis*." Journal of Bacteriology 127(3): 1502-1518.
- Chaudri, A. M., B. P. Knight, et al. (1999). "Determination of acute Zn toxicity in pore water from soils previously treated with sewage sludge using bioluminescence assays." Environmental Science & Technology 33(11): 1880-1885.
- Chaudri, A. M., K. Lawlor, et al. (2000). "Response of a Rhizobium-based luminescence biosensor to Zn and Cu in soil solutions from sewage sludge treated soils." Soil Biology & Biochemistry 32(3): 383-388.
- Fein, J. B., A. M. Martin, et al. (2001). "Metal adsorption onto bacterial surfaces: Development of a predictive approach." Geochimica et Cosmochimica Acta 65(23): 4267-4273.
- Fredrickson, J. K., J. M. Zachara, et al. (1998). "Biogenic iron mineralization accompanying the dissimilatory reduction of hydrous ferric oxide by a groundwater bacterium." Geochimica et Cosmochimica Acta 62(19-20): 3239-3257.
- Fredrickson, J. K., J. M. Zachara, et al. (2001). "Biotransformation of Ni-substituted hydrous ferric oxide by an Fe(III)-reducing bacterium." Environmental Science & Technology 35(4): 703-712.
- Gadd, G. M. (1996). "Influence of microorganisms on the environmental fate of radionuclides." Endeavour 20(4): 150-156.
- Hacherl, E. L., D. S. Kosson, et al. (2001). "Measurement of Iron(III) bioavailability in pure iron oxide minerals and soils using anthraquinone-2,6-disulfonate oxidation." Environmental Science & Technology 35(24): 4886-4893.
- Jeon, B. H., B. A. Dempsey, et al. (2001). "Reactions of ferrous iron with hematite." Colloids and Surfaces a-Physicochemical and Engineering Aspects 191(1-2): 41-55.
- Jeon, B. H., B. A. Dempsey, et al. (2002). "Sorption Kinetics of Fe(II) ion onto Hematite: Effect of Divalent Metal Ions (Zn, Co, Ni, and Cd) in Single and Competitive Binary Systems." To be submitted for publication.
- Knight, B. and S. P. McGrath (1995). "A method to buffer the concentrations of free Zn and Cd ions using a cation-exchange resin in bacterial toxicity studies." Environmental Toxicology and Chemistry 14(12): 2033-2039.
- Kushner, D. J. (1993). "Effects of speciation of toxic metals on their biological activity." Water Pollution Residuals Journal of Canada 28(1): 111-128.
- Lee, L. H., B. Lustigman, et al. (1994). "Effect of manganese and zinc on the growth of *Anacystis- Nidulans*." Bulletin of Environmental Contamination and Toxicology 53(1): 158-165.
- Liu, C. X., J. M. Zachara, et al. (2002). "Modeling the inhibition of the bacterial reduction of U(VI) by beta-MnO<sub>2</sub>(S)(g)." Environmental Science & Technology 36(7): 1452-1459.
- Markwiese, J. T. and P. J. S. Colberg (2000). "Bacterial reduction of copper-contaminated ferric oxide: Copper toxicity and the interaction between fermentative and iron-reducing bacteria." Archives of Environmental Contamination and Toxicology 38(2): 139-146.

- Parmar, N., Y. A. Gorby, et al. (2001). "Formation of green rust and immobilization of nickel in response to bacterial reduction of hydrous ferric oxide." Geomicrobiology Journal 18(4): 375-385.
- Poulson, S. R., P. J. S. Colberg, et al. (1997). "Toxicity of heavy metals (Ni,Zn) to *Desulfovibrio desulfuricans*." Geomicrobiology Journal 14(1): 41-49.
- Ritchie, J. M., M. Cresser, et al. (2001). "Toxicological response of a bioluminescent microbial assay to Zn, Pb and Cu in an artificial soil solution: relationship with total metal concentrations and free ion activities." Environmental Pollution 114(1): 129-136.
- Roden, E. E. and M. M. Urrutia (1999). "Ferrous iron removal promotes microbial reduction of crystalline iron(III) oxides." Environmental Science & Technology 33(11): 1847-1853.
- Roden, E. E. and M. M. Urrutia (2002). "Influence of biogenic Fe(II) on bacterial crystalline Fe(III) oxide reduction." Geomicrobiology Journal 19(2): 209-251.
- Royer, R. A., W. D. Burgos, et al. (2002a). "Enhancement of hematite bioreduction by natural organic matter." Environmental Science & Technology 36(13): 2897-2904.
- Royer, R. A., W. D. Burgos, et al. (2002b). "Enhancement of biological reduction of hematite by electron shuttling and Fe(II) complexation." Environmental Science & Technology 36(9): 1939-1946.
- Royer, R. A., B. H. Jeon, et al. (2002c). "Inhibition of biological reductive dissolution of hematite by ferrous iron." To be submitted for publication.
- Sani, R. K., B. M. Peyton, et al. (2001). "Copper-induced inhibition of growth of *Desulfovibrio desulfuricans* G20: Assessment of its toxicity and correlation with those of zinc and lead." Applied and Environmental Microbiology 67(10): 4765-4772.
- Shuttleworth, K. L. and R. F. Unz (1993). "Sorption of Heavy-Metals to the Filamentous Bacterium *Thiothrix* Strain A1." Applied and Environmental Microbiology 59(5): 1274-1282.
- Stone, J. J., W. D. Burgos, et al. (2002). "Impact of zinc on biological Fe(III) and  $\text{NO}_3^-$  reduction by *Shewanella putrefaciens* CN32." To be submitted for publication.
- Stookey, L. L. (1970). "Ferrozine - A new spectrophotometric reagent for iron." Analytical Chemistry 42(7): 779-781.
- Stumm, W. and J. J. Morgan (1996). Aquatic chemistry: chemical equilibria and rates in natural waters. New York, John Wiley and Sons, Inc.
- Trivedi, P. and L. Axe (2000). "Modeling Cd and Zn sorption to hydrous metal oxides." Environmental Science & Technology 34(11): 2215-2223.
- Urrutia, M. M., E. E. Roden, et al. (1998). "Microbial and surface chemistry controls on reduction of synthetic Fe(III) oxide minerals by the dissimilatory iron-reducing bacterium *Shewanella* alga." Geomicrobiology Journal 15(4): 269-291.
- Warren, L. A. and E. A. Haack (2001). "Biogeochemical controls on metal behaviour in freshwater environments." Earth-Science Reviews 54(4): 261-320.
- Welp, G. and G. W. Brummer (1997). "Microbial toxicity of Cd and Hg in different soils related to total and water-soluble contents." Ecotoxicology and Environmental Safety 38(3): 200-204.
- Zachara, J. M., J. K. Fredrickson, et al. (1998). "Bacterial reduction of crystalline  $\text{Fe}^{3+}$  oxides in single phase suspensions and subsurface materials." American Mineralogist 83(11-12): 1426-1443.

Zachara, J. M., J. K. Fredrickson, et al. (2001). "Solubilization of Fe(III) oxide-bound trace metals by a dissimilatory Fe(III) reducing bacterium." Geochimica et Cosmochimica Acta 65(1): 75-93.

Table 3.1 Summary of zinc and manganese  $IC_{50}^a$  values for the biological reduction of hematite by *S. putrefaciens* CN32. All experiments were performed with  $2 \text{ g L}^{-1}$  hematite and  $10^8 \text{ cells mL}^{-1}$  in 10mM PIPES (pH 6.8) at  $20^\circ\text{C}$ .

Experimental Condition	Total Me(II) $IC_{50}$
Hematite, no amendments	0.202 mM total zinc 3.06 mM total manganese
Hematite, 1.46 mM ferrozine	0.101 mM total zinc
Hematite, 50 $\mu\text{M}$ AQDS	0.0806 mM total zinc

- a. Defined as inhibitory concentration of Me(II) where a 50% reduction of the biological process occurs relative to a no Me(II) control. The  $IC_{50}$  was calculated from a least squares line obtained from the data.

Table 3.2 Summary of Langmuir isotherm parameters<sup>a</sup> for 5 d variable Me(II) sorption in 10mM PIPES, pH 6.8.

Metal	Sorbent [g L <sup>-1</sup> ]	Q <sub>max</sub> <sup>b</sup> [mM Me(II) g <sup>-1</sup> sorbent]	C <sub>max</sub> <sup>c</sup> [mM Me(II)]	b <sup>d</sup> [mM Me(II)]
Zinc	2.0 g L <sup>-1</sup> hematite	0.0406	0.0812	0.152
Zinc	0.064 g L <sup>-1</sup> <i>S. putrefaciens</i> <sup>e,f</sup>	1.005	0.0643	0.0209
Zinc	2.0 g L <sup>-1</sup> hematite + 0.064 g L <sup>-1</sup> <i>S. putrefaciens</i> <sup>e,f</sup>	0.0555	0.115	0.00618
Zinc	2.0 g L <sup>-1</sup> hematite + 0.064 g L <sup>-1</sup> <i>S. putrefaciens</i> <sup>e,g</sup>	0.0527	0.109	0.0379
Manganese	2.0 g L <sup>-1</sup> hematite	0.0372	0.0745	0.868
Manganese	0.064 g L <sup>-1</sup> <i>S. putrefaciens</i> <sup>e,f</sup>	0.330	0.0211	0.0464
Manganese	2.0 g L <sup>-1</sup> hematite + 0.064 g L <sup>-1</sup> <i>S. putrefaciens</i> <sup>e,f</sup>	0.0221	0.0457	0.107
Manganese	2.0 g L <sup>-1</sup> hematite + 0.064 g L <sup>-1</sup> <i>S. putrefaciens</i> <sup>e,h</sup>	0.0282	0.0583	0.186

a. Values derived using Langmuir sorption equation  $q = Q_{\max} C_{\text{Me(II)}} C_{\text{sorbent}} / (b + C_{\text{Me(II)}})$  (Liu et al. 2002).

b. Langmuir Me(II) sorption maxima per mass of sorbent.

c. Langmuir Me(II) sorption maxima.

d. Calculated from Langmuir equation  $b = (\text{y-intercept of Langmuir regression line}) / (Q_{\max})$

e. Estimated from  $10^8$  cells mL<sup>-1</sup> concentration of cells with  $6.4 \times 10^{-10}$  mg cell<sup>-1</sup> (Liu et al. 2002).

f. Cells pasteurized to ensure non-viability and no biogenic Fe(II).

g. Results from bioreduction of hematite experiments with variable zinc. Contained variable total Fe(II) ranging from 0.088 - 0.296 mM.

h. Results from bioreduction of hematite experiments with variable manganese. Contained variable total Fe(II) ranging from 0.104 – 0.200 mM.



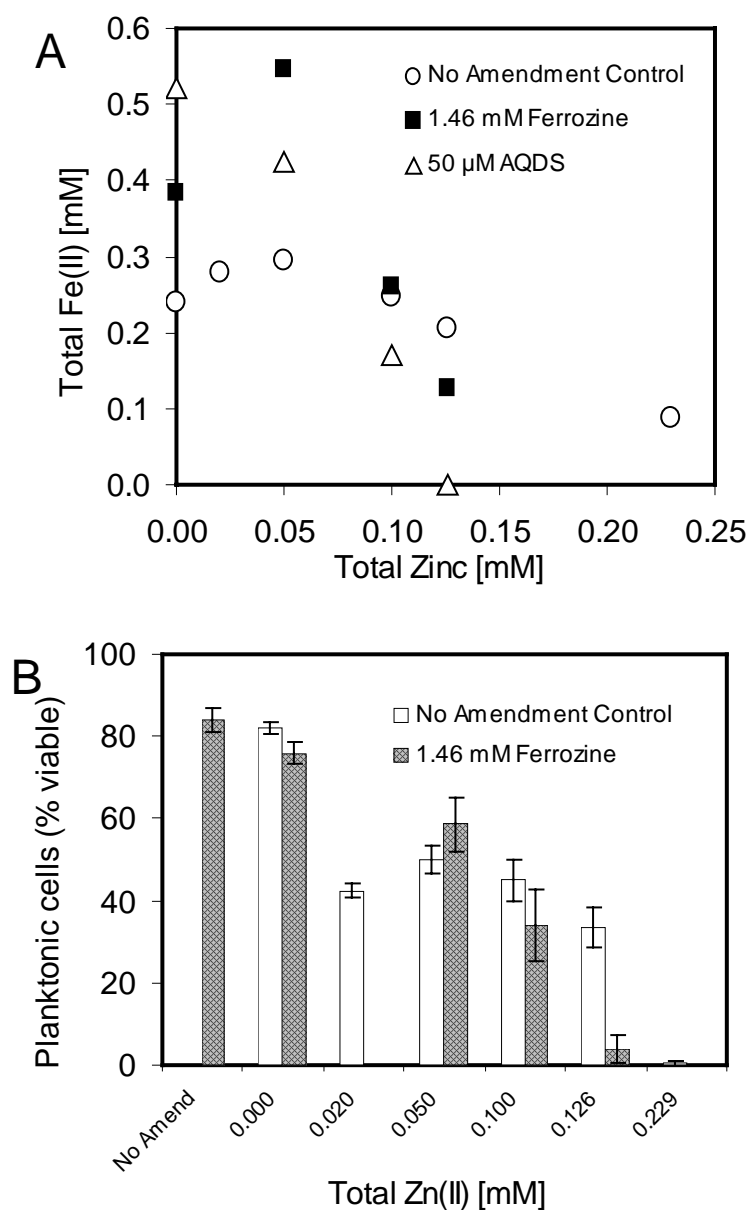


Figure 3.1 (A) Total Fe(II) production and (B) planktonic cell viability as a function of variable zinc for (■) 1.46 mM ferrozine, (Δ) 50 $\mu$ M ADQS, (○) no amendment control. Experiments performed using 2 g L<sup>-1</sup> hematite in 10mM PIPES, pH 6.8, 10<sup>8</sup> *S. putrefaciens* cells mL<sup>-1</sup>. All values are means of three replicates.

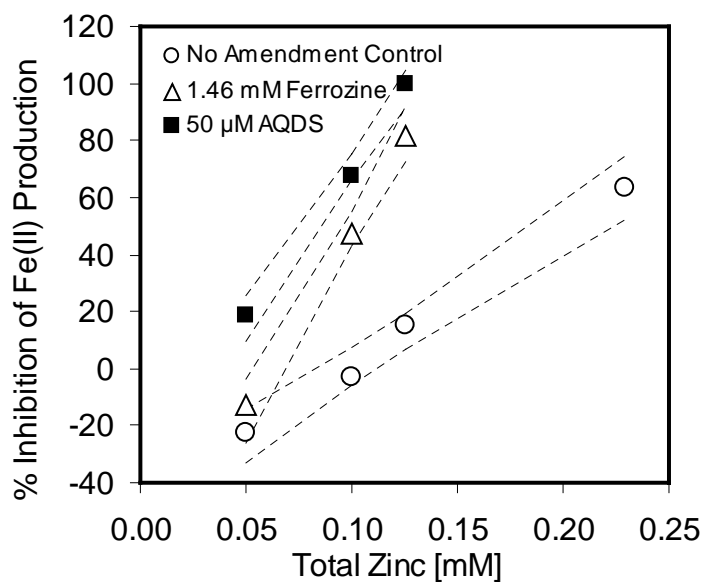


Figure 3.2 Summary of percent inhibition of 5 d, total Fe(II) production as a function of total zinc concentration for (■) 1.46mM ferrozine, (Δ) 50μM ADQS, (○) no amendment control. Percent inhibition calculated from least squares estimate from no-zinc controls. Bioreduction samples included  $2 \text{ g L}^{-1}$  hematite,  $10^8$  *S. putrefaciens* cells  $\text{mL}^{-1}$ , 10mM PIPES, pH 6.8. Dashed lines represent 95% confidence interval. Values are means of three replicates.

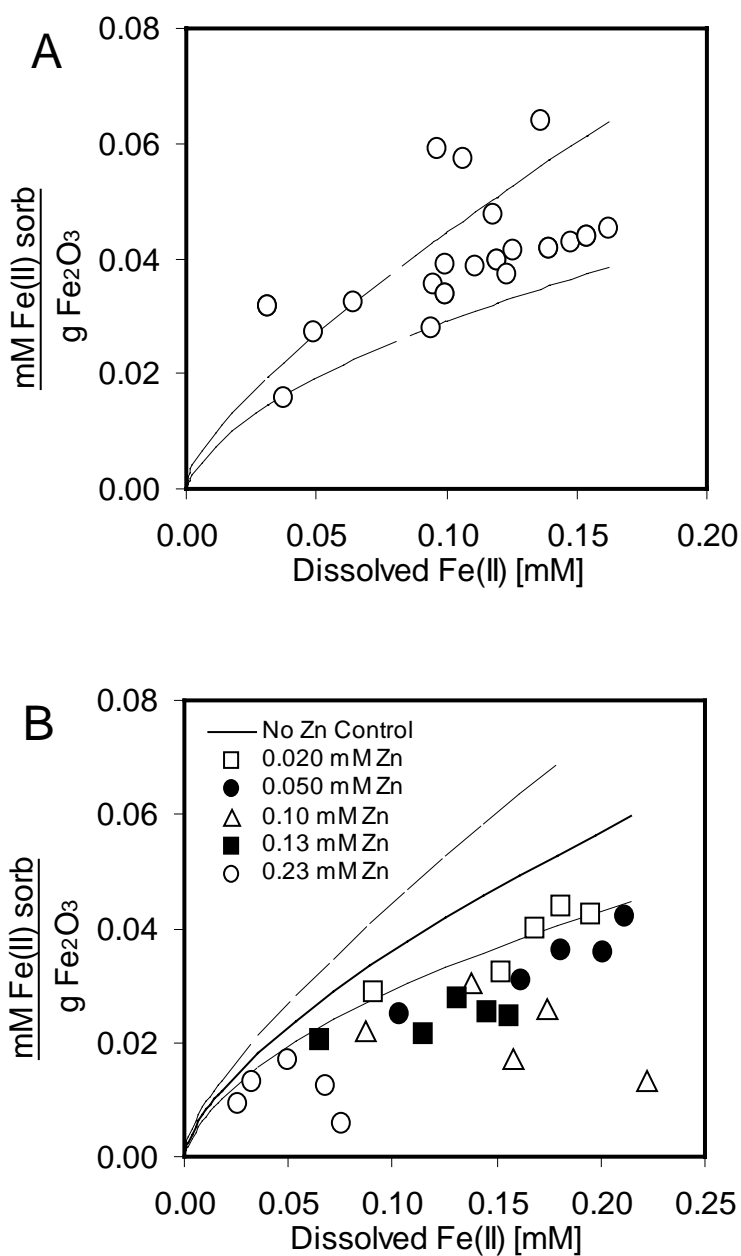


Figure 3.3 The distribution of Fe(II) during the biological reduction of  $2 \text{ g L}^{-1}$  hematite using *S. putrefaciens* ( $10^8 \text{ cell mL}^{-1}$ ) for (A) no-zinc, no-amendment controls, (B) variable zinc samples. Solid line is Freundlich isotherm trend line ( $R^2 = 0.890$ ,  $K = 0.01156 \text{ mM Fe(II) g}^{-1}$ ,  $1/n = 0.6603$ ) for the no-zinc, no-amendment control and dashed line represents 95% confidence interval. Results are 1-5 d composite samples.

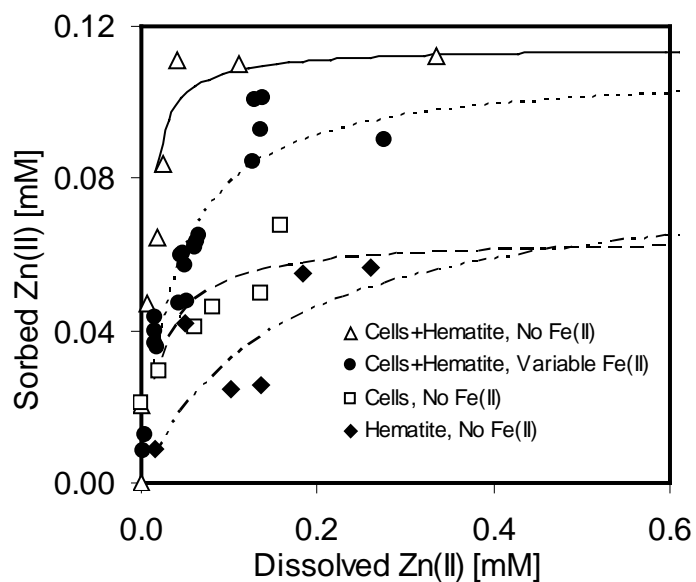


Figure 3.4 Langmuir zinc sorption distribution for ( $\Delta$ )  $2.0 \text{ g L}^{-1}$  hematite and  $10^8$  pasteurized cells  $\text{mL}^{-1}$  (non-viable), ( $\bullet$ )  $2.0 \text{ g L}^{-1}$  hematite and  $10^8$  cells  $\text{mL}^{-1}$  with biogenic Fe(II) (0.088 - 0.296 mM), ( $\square$ )  $10^8$  pasteurized cells  $\text{mL}^{-1}$ , and ( $\blacklozenge$ )  $2.0 \text{ g L}^{-1}$  hematite. Results are 5 d values at pH 6.8. All values are means of three replicates.

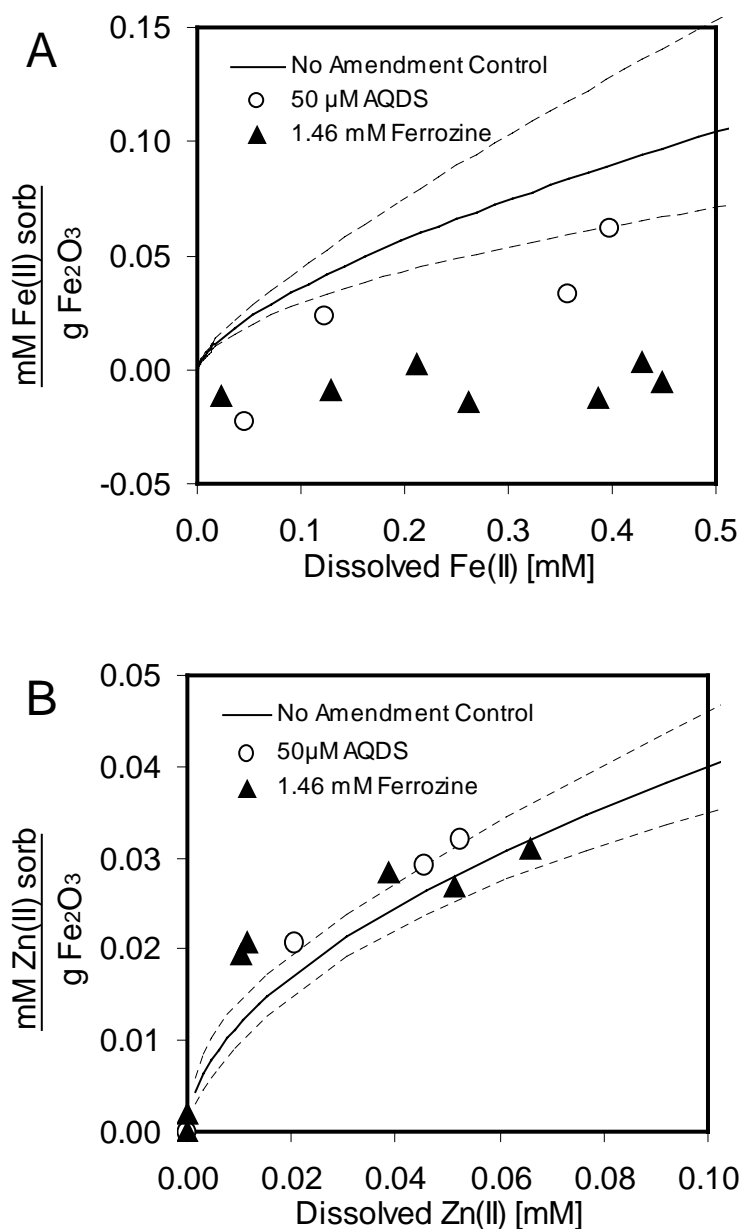


Figure 3.5 The Freundlich sorption distribution of (A) Fe(II) and (B) zinc in the presence of (○) 50 μM AQDS, (▲) 1.46 mM ferrozine during the biological reduction of 2 g L<sup>-1</sup> hematite using *S. putrefaciens* (10<sup>8</sup> cell mL<sup>-1</sup>). Solid lines represent no-amendment Fe(II) sorption ( $R^2 = 0.890$ ,  $K = 0.01156 \text{ mM Fe(II) g}^{-1}$ ,  $1/n = 0.6603$ ) and no-amendment, Fe(II) containing (0.088 - 0.296 mM) zinc sorption ( $R^2 = 0.894$ ,  $K = 0.01475 \text{ mM Zn(II) g}^{-1}$ ,  $1/n = 0.532$ ). Dashed line represents 95% confidence interval. Results are 5 d at pH 6.8. All values are means of three replicates.

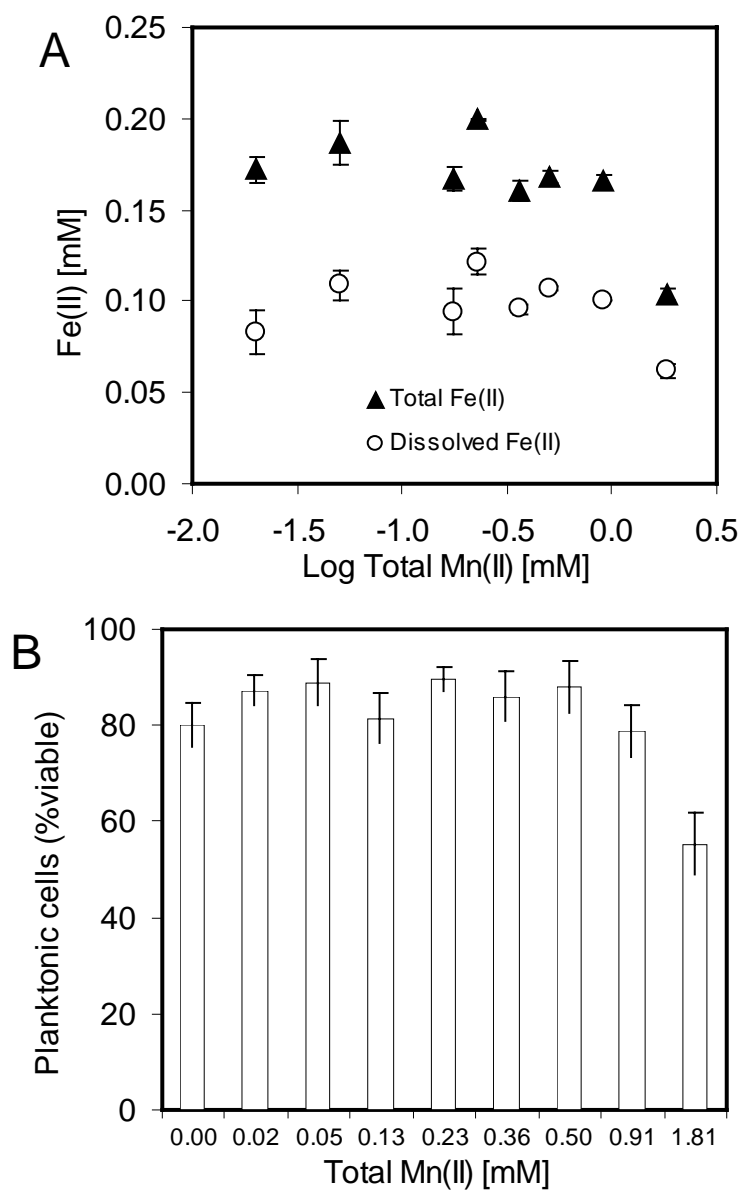


Figure 3.6 The effect of variable manganese on 5 d (A) total and dissolved Fe(II) production, (B) planktonic cell viability as a function of total manganese. Experiments performed using 2 g L<sup>-1</sup> hematite in 10mM PIPES, pH 6.8, 10<sup>8</sup> *S. putrefaciens* cells mL<sup>-1</sup>. All values are means of three replicates ( $\pm$  standard deviation). Error bars smaller than symbol are not shown.

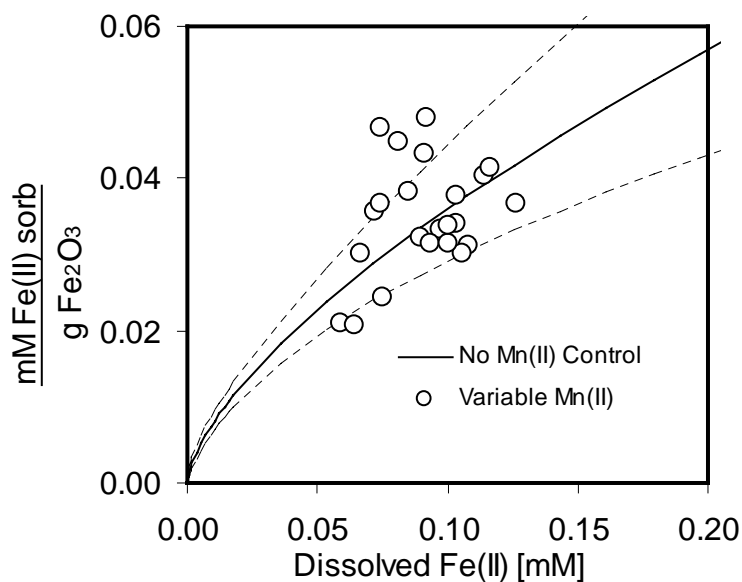


Figure 3.7 The Freundlich sorption distribution of Fe(II) during the biological reduction of 2 g L<sup>-1</sup> hematite using *S. putrefaciens* (10<sup>8</sup> cell mL<sup>-1</sup>) and variable manganese (0 – 1.82 mM). Solid line represents no-amendment Fe(II) sorption trend line in absence of manganese ( $R^2 = 0.890$ ,  $K = 0.01156 \text{ mM Fe(II) g}^{-1}$ ,  $1/n = 0.6603$ ) and dashed line represents 95% confidence interval. Results are 5 d at pH 6.8.

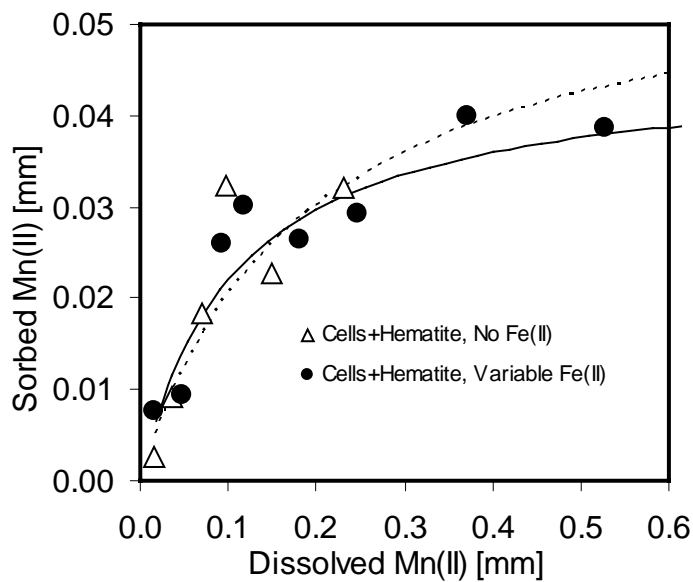


Figure 3.8 Langmuir manganese sorption distribution for ( $\Delta$ )  $2.0 \text{ g L}^{-1}$  hematite and  $10^8$  pasteurized cells  $\text{mL}^{-1}$  (non-viable), ( $\bullet$ )  $2.0 \text{ g L}^{-1}$  hematite and  $10^8$  cells  $\text{mL}^{-1}$  with biogenic Fe(II) (0.104 – 0.200 mM). Results are 5 d values at pH 6.8. All values are means of three replicates.



## CHAPTER 4

### The Effect of Natural Organic Matter on Zinc Inhibition of Biological Fe(III) and Nitrate Reduction by *Shewanella putrefaciens* CN32

#### 4.1 Abstract

The effect of zinc on the biological reduction of hematite ( $\alpha\text{-Fe}_2\text{O}_3$ ) by the dissimilatory metal-reducing bacterium (DMRB) *Shewanella putrefaciens* CN32 was studied in the presence of natural organic materials (NOMs). Experiments were performed under non-growth conditions with  $\text{H}_2$  as the electron donor and zinc inhibition was quantified as the decrease in electron acceptor consumption and as the decrease in planktonic cell viability as compared to no-zinc controls. NOMs were shown to significantly increase zinc inhibition during hematite bioreduction. NOMs were shown to alter the distribution of both biogenic Fe(II) and Zn(II) between sorbed (hematite and DMRB surfaces) and solution phases. To better evaluate the mechanism(s) of NOM-promoted zinc inhibition, similar bioreduction experiments were conducted with the soluble electron acceptors ferric citrate and nitrate, and hematite bioreduction experiments were conducted with variable concentrations of Mn(II). NOMs did not increase zinc inhibition with the soluble electron acceptors, but instead zinc inhibition decreased in four of five treatments. For manganese, NOM addition initiated hematite bioreduction inhibition for manganese concentrations that previously exhibited no effect. Taken together these results indicated that the formation of ternary surface complexes between NOM, zinc, and either the cell or hematite surface were responsible for the inhibition of hematite bioreduction. These ternary complexes inhibited hematite bioreduction by either passivating the hematite surface as a result of

NOM sorption which subsequently reduced the availability of reactive surface sites, or through increased cellular toxicity due to increased zinc sorption.

## 4.2 Introduction

The dissimilatory reduction of Fe(III) has been recognized as an important process for the bioremediation of contaminated soil and ground waters. While these processes appear very promising for the cleanup of Department of Energy (DOE) waste sites, few researchers have studied the impact of high concentrations of inorganic metals during this process. In our ongoing effort to determine the role metals may have during Fe(III) bioreduction, we investigated the role that natural organic matter (NOM) may have during hematite bioreduction. The presence of NOM has previously been shown to stimulate the reduction of hematite by both biotic and abiotic processes (Fredrickson et al. 2001; Royer et al. 2002a; Royer et al. 2002b). Microbial toxicity has previously been associated with free metal activity (Knight et al. 1995; Chaudri et al. 1999; Chaudri et al. 2000; Ritchie et al. 2001) and the presence of NOM may influence metal activity through complexation reactions with the reactive functional groups associated with the NOM. NOM has been found to significantly influence metal ion sorption onto oxides and DMRB (Ali et al. 1996), while metal sorption [in particular Fe(II)] has previously been shown to control the rate and extent of inhibition of Fe(III) bioreduction through metal complexation reactions of surface bound Fe(II) (Roden et al. 1999; Urrutia et al. 1999; Roden et al. 2002).

The theory behind NOM relieving the effects of metal inhibition observed previously (Stone et al. 2002a; b) was based upon the ability of NOM to sequester or complex free or surface bound metals which would reduce the free metal activity in solution. Synthetic metal

chelating compounds such as EDTA and NTA may mitigate metal microbial toxicity (Shuttleworth et al. 1991; 1993) or prevent or delay surface attenuation of biogenic Fe(II) (Roden et al. 1999; Urrutia et al. 1999; Roden et al. 2002) through metal complexation reactions. Likewise, the ability of metal complexation with NOM is inherently based upon its diverse array of physical and chemical properties. Of the NOM properties reported in the literature, aromaticity, oxygen-to-carbon ratio, and molecular weight appear to best describe NOM metal complexation performance (Murphy et al. 1990; Stevenson 1994; Duker et al. 1995). For example, humic substances containing a very high percentage of carboxylic acids can readily exchange protons for divalent metals during ligand exchange reactions. The carboxylic acid content for a particular NOM represents the number of ligand exchange sites available for metal complexation reactions (Stevenson 1994). The ability of NOM to enhance hematite bioreduction was found to best correlate with the aromaticity of the compound (Royer et al. 2002a), defined as the percentage of the NOM structure associated with aromatics. Organic radical content and acidity did not correlate with hematite bioreduction enhancement (Royer et al. 2002a), however others have found these properties, in addition to the oxygen-to-carbon ratio and molecular weight, to be good indicators of the sorption affinity of NOM to cells and oxide surfaces (Murphy et al. 1990).

The purpose of this research was to investigate whether or not the addition of natural organic material (NOM) could augment the effect(s) of zinc during the biological reduction of hematite by the DMRB *Shewanella putrefaciens* strain CN32. Our hypothesis proposed that NOM would control zinc inhibition by one of two mechanisms: through complexation of free zinc which would reduce the free zinc activity previously thought to control microbial toxicity, or through complexation reactions involving Fe(II) which would decrease surface sorption

competition with zinc and allow additional zinc sorption on the hematite and cells. Studies were undertaken to improve the understanding of the inhibitory effects of zinc during bioreduction for both soluble and aqueous phase electron donors in the presence of NOM.

### **4.3 Experimental**

#### **4.3.1 Microorganism and Culture Conditions**

*Shewanella putrefaciens* strain CN32 was provided courtesy of Dr. David Balkwill (Subsurface Microbial Culture Collection, Florida State University). *S. putrefaciens* CN32 was isolated from an anaerobic subsurface core sample (250 m below ground surface) from the Morrison Formation in northwestern New Mexico (Fredrickson et al. 1998). The cultures were grown aerobically on tryptic soy broth without dextrose (TSB-D) at 20°C. Cells were harvested by centrifugation (4900x g, 10 min, 20°C) from a 16-hour-old culture (late log-decreasing growth phase). The cells were washed three times in 10 mM 1,4-piperazinediethanesulfonic acid (PIPES; pH=6.8) with the final wash made with deoxygenated solution. Cell pellets were re-suspended in 5-15 ml of deoxygenated 10 mM PIPES buffer in an anaerobic chamber (Coy; Grass Lakes, MI) under a N<sub>2</sub>:H<sub>2</sub> (ca. 97.5:2.5%) atmosphere and the cell density was determined by absorbance at 420 nm.

#### **4.3.2 Materials**

An iron oxide powder was obtained from J.T. Baker and identified by X-ray diffraction and Mössbauer spectroscopy to be hematite ( $\alpha$ -Fe<sub>2</sub>O<sub>3</sub>) of greater than 99% purity. The hematite had an average particle diameter of 1.0  $\mu$ m measured by laser diffraction and a specific surface area of 9.04 m<sup>2</sup> g<sup>-1</sup> measured by 5-point N<sub>2</sub>-BET. The zero point of charge was pH 8.5 as determined by electrophoretic mobility and proton titrations. The hematite surface site density

for Fe(II) was 5.1 sites per nm<sup>2</sup> based upon the adsorption of Fe(II) (Jeon et al. 2001). Hematite was heated to 550°C in air overnight before use to remove any residual organic carbon.

Hematite was added to the anaerobic PIPES buffer at least 24 h prior to any experiment to allow for hydration.

### **4.3.3 NOMs**

The four NOMs tested from the International Humic Substances Society (IHSS) included: Suwannee River NOM (SRNOM), Suwannee River humic acid (SRHA), Suwannee River fulvic acid (SRFA), and soil humic acid (SHA). NOM suspensions dissolved in 10 mM PIPES were added to each master reactor at the appropriate concentration. Aromaticity values for the NOMs were determined from <sup>13</sup>C NMR spectra from a published report for the IHSS materials (Thorn et al. 1989). Proton titration data (NOM at 400 mg L<sup>-1</sup> in 0.1 M NaCl) for all materials were provided courtesy of Dr. M. Perdue (Georgia Institute of Technology, personal communication). Characteristics of the NOM materials used are provided in Table 1.

### **4.3.4 Bioreduction Experiment Preparation**

A “master reactor” approach was used to prepare all experiments (Royer et al. 2002a) in order to ensure consistent chemical and biological conditions. All preparations were performed within a Coy anaerobic chamber. A master reactor containing between 100 and 200 mL of solution medium was prepared by combining the electron acceptor and the inoculum in a 250 mL serum bottle. All solutions (except the zinc and manganese stock) were prepared in 10 mM PIPES (pH 6.8). Biotic no-NOM controls were immediately prepared by transferring 10 mL of the suspension into 20 mL amber serum bottles (in at least triplicate). All 20 mL serum bottles were crimp-sealed with Teflon-faced butyl rubber stoppers and aluminum caps. For NOM treatments, biotic controls were also prepared without the metal. Afterwards, zinc or manganese

was incrementally added to the master reactor in an acidified and deoxygenated  $\text{ZnCl}_2$  or  $\text{MnCl}_2$  solution ( $1,000 \text{ mg L}^{-1}$  AAS certified standard) along with an equal volume of  $0.1 \text{ N NaOH}$  (for pH maintenance). At each concentration,  $10 \text{ mL}$  of the suspension was transferred into  $20 \text{ mL}$  amber serum bottles (in triplicate). Five to seven different metal concentrations were usually prepared. Sealed serum bottles were incubated in the dark at  $20^\circ\text{C}$  on orbital shakers outside of the anaerobic chamber. Hydrogen from the anaerobic chamber atmosphere ( $97.5:2.5\% \text{ N}_2:\text{H}_2$ ) was used as the electron donor in all experiments.

#### **4.3.5 Hematite Bioreduction**

Experiments were performed with  $2.0 \text{ g L}^{-1}$  hematite ( $0.0125 \text{ mol Fe}_2\text{O}_3 \text{ L}^{-1}$ ), a final cell density of  $10^8 \text{ cells mL}^{-1}$ , metal concentrations ranging from  $0$  to  $0.229 \text{ mM}$  total zinc or  $0$  to  $1.82 \text{ mM}$  total manganese, and the appropriate NOM (dissolved in  $10 \text{ mM PIPES}$  and added volumetrically). After incubation times of  $5 \text{ d}$ , reactors were sacrificed to measure dissolved and total  $\text{Fe(II)}$ , dissolved and total metal, pH, and planktonic viable cells.

#### **4.3.6 Ferric Citrate Bioreduction**

Experiments were performed in  $10 \text{ mM PIPES}$  containing  $2 \text{ mM}$  ferric citrate (dissolved in  $10 \text{ mM PIPES}$ ),  $4 \text{ mM}$  citric acid, a final cell density of  $10^8 \text{ cells mL}^{-1}$ , variable concentrations of zinc ( $0.02 - 6.88 \text{ mM}$  total zinc), and NOM. Solution pH was maintained at pH  $6.8$  with addition of  $3 \text{ N NaOH}$  or  $3 \text{ N HCl}$ . A  $3:1$  molar ratio of citrate: $\text{Fe(III)}$  was selected to prevent the formation of amorphous ferric hydroxide based on speciation calculations made with MINTEQA2 (Allison et al. 1991). Reactors were prepared in clear glass serum bottles ( $250 \text{ mL}$ ) containing between  $100$  to  $200 \text{ mL}$  of solution medium, crimp-sealed with thick butyl rubber stoppers and aluminum caps, and sealed serum bottles were incubated in the dark at  $20^\circ\text{C}$  on orbital shakers outside of the anaerobic chamber. After incubation times of  $0, 0.5, 1.0, 1.8,$  and

3.8, reactors were sampled within the anaerobic chamber by piercing the septa with a needle and syringe. The withdrawn solution was used to measure dissolved Fe(II), dissolved zinc concentration, and pH.

#### **4.3.7 Nitrate Bioreduction**

Experiments were performed in 10 mM PIPES (pH 6.8) containing 14.4 g L<sup>-1</sup> KNO<sub>3</sub> (20 mg NO<sub>3</sub>-N L<sup>-1</sup>), a final cell density of 10<sup>8</sup> cells mL<sup>-1</sup>, variable concentrations of zinc (0.020 – 0.459 mM total zinc) or manganese (0.020 – 1.82 mM total manganese), and NOM. Reactor preparation and reactor sampling were performed using the same techniques as the ferric citrate experiments. Samples were collected after incubation times of ca. 0, 3.2, 6.5, and 9.2 h and were used to measure nitrate-nitrogen, dissolved metal concentration, and pH.

#### **4.3.8 Analytical Techniques**

Fe(II) was reported as dissolved, total, and adsorbed. For dissolved Fe(II), samples were filtered (0.2 µm cellulose acetate) and Fe(II) was measured by ferrozine (1.96 mM ferrozine in 50 mM HEPES, pH 8.0) in the anaerobic chamber. Solution pH of the filtrate was determined in the anaerobic chamber using a combination pH electrode. For total Fe(II), an unfiltered sample was acidified with HCl to achieve a final solution normality of 0.5 N. The solution was mixed for ca. 24 h, filtered (0.2 µm) and Fe(II) in the filtrate was measured by ferrozine. Adsorbed Fe(II) was calculated as the difference between dissolved and total Fe(II). Dissolved and total metal was measured from the corresponding dissolved and total Fe(II) filtrate samples by flame atomic absorption spectrometry (AAS) after preservation with conc. HNO<sub>3</sub>.

#### **4.3.9 Dialysis**

Equilibrium dialysis was used to quantify the sorption of zinc to SRNOM using methods described previously (Karthikeyan et al. 2000). Spectra/Por 6 dialysis membrane (500 MWCO)

was washed thoroughly with deionized water prior to its placement in a 100 mL glass test tube filled with 10 mM PIPES at pH 6.8. The dialysis cell was filled with external solution without zinc and a volume of concentrated stock SRNOM was added to provide ca. 0, 10, 25, 50, 75, 100, 150, and 200 mg L<sup>-1</sup> SRNOM. Once the cell was sealed, zinc was added to the external solution to give a total system zinc concentration of 0.153 mM. The sealed reactors were agitated in a platform orbital shaker at 70 rpm for 180 days. Concentrations of total and dissolved zinc both inside and outside the dialysis cell were determined by AAS. The quantity of zinc removed from solution was determined from the difference between inside (free and SRNOM bound) zinc and outside (free) zinc concentrations.

#### 4.4 Results

##### 4.4.1 Impact of NOM on Hematite Bioreduction

For this study zinc inhibition was expressed as the decrease in the 5 d extent of hematite bioreduction by *S. putrefaciens* CN32. Total Fe(II) production after 5 d as a function of zinc addition for varied concentrations of IHSS Soil Humic Acid (SHA) and the biotic no-NOM control are presented in Figure 1A. For each SHA concentration, biotic no-SHA no-zinc controls and biotic with-SHA no-zinc controls were also prepared (results not shown). In the absence of zinc, all SHA concentrations stimulated hematite bioreduction compared to their corresponding no-SHA controls. Compared to its corresponding no-SHA control, 250 mg L<sup>-1</sup> SHA stimulated Fe(II) production by 217%.

Low concentrations of zinc stimulated Fe(II) production in the presence and absence of SHA (Fig. 1A). In the no-NOM control samples (open circles), Fe(II) production increased relative to its corresponding no-zinc control for total zinc concentrations up to 0.05 mM. For 15 and 75 mg L<sup>-1</sup> SHA, Fe(II) production increased relative to their no-zinc controls at a total zinc



concentration of 0.02 mM. No stimulatory Fe(II) production effects during zinc addition was observed for 150 and 250 mg L<sup>-1</sup> SHA.

The results in Figure 1B show that SHA addition increased the inhibition of zinc during hematite bioreduction. Inhibition was quantified using methods discussed previously (Stone et al. 2002a) where inhibition was defined as the percent change in the biological output of the system due to zinc addition relative to the corresponding biotic no-zinc control (Sani et al. 2001). The zinc concentration corresponding to a 50% decrease in biological output compared to the no-zinc control was defined as the IC<sub>50</sub>. According to the results presented in Figure 1B, the IC<sub>50</sub> value was 0.211 mM total zinc for the no-NOM control. The two highest SHA concentrations, 150 and 250 mg L<sup>-1</sup>, resulted lowering the IC<sub>50</sub> values to 0.0563 and 0.0245 mM total zinc, respectively. The 15 mg L<sup>-1</sup> SHA concentration resulted in an IC<sub>50</sub> of 0.0784 mM. In other words, higher SHA concentrations increased zinc inhibition. IC<sub>50</sub> values could not be calculated based on free zinc concentrations because NOM-zinc complexation constants were not available. All NOMs decreased the IC<sub>50</sub> between 60 to 88% compared to the no-NOM control. A summary of all zinc IC<sub>50</sub> values for the different NOMs and electron acceptors tested is presented in Table 2.

The addition of IHSS Suwannee River Fulvic Acid (SRFA, 150 mg L<sup>-1</sup>) or IHSS Suwannee River Humic Acid (SRHA, 250 mg L<sup>-1</sup>) also increased the inhibition of zinc during hematite bioreduction (Fig. 2). In the absence of zinc, 150 mg L<sup>-1</sup> SRFA decreased Fe(II) production by 3.3%, while 250 mg L<sup>-1</sup> SRHA increased Fe(II) production by 165% compared to their corresponding no-NOM controls. For SRFA, Fe(II) production increased relative to its no-zinc control at a total zinc concentration of 0.02 mM (Fig. 2A). For SRHA no stimulatory effect

of zinc was observed. The  $IC_{50}$  values for SRFA and SRHA were 0.0685 and 0.0849 mM total zinc, respectively (Fig. 2B).

#### 4.4.2 Impact of Fe(II) Sorption with NOM Addition

Sorbed Me(II) concentrations were calculated as the difference between the total Fe(II) and dissolved Me(II) concentrations. This difference included Me(II) sorbed to both hematite and DMRB, however, there was no means to measure the distribution of Me(II) between these two sorbents. Therefore, sorbed Me(II) concentrations are reported as mM Me(II) per g  $Fe_2O_3$  in all sorption isotherms. A “baseline” Fe(II) sorption isotherm (solid line in Fig. 3A) was developed from a series of hematite bioreduction experiments performed in the absence of any amendment (e.g., zinc, manganese, NOM) (Stone et al. 2002a). The dashed lines in Figure 3A represent 95% confidence intervals associated with the Fe(II) isotherm. The individual data points plotted in Figure 3A represent the sorption of Fe(II) in the presence of the specified NOM concentration and in the absence of zinc. These data were calculated from 5 d hematite bioreduction experiments. The sorption of Fe(II) increased for all four SHA concentrations and the one SRHA concentration, while SRFA did not alter Fe(II) sorption.

A second “baseline” Fe(II) sorption isotherm (solid line in Fig. 3B) was developed from a series of hematite bioreduction experiments performed in the absence of any NOM but in the presence of variable zinc concentrations (0.020 to 0.18 mM total zinc) (Stone et al. 2002a). Zinc was shown to be competitive with Fe(II) and slightly decreased Fe(II) sorption (Stone et al. 2002a). The dashed lines in Figure 3B represent 95% confidence intervals associated with the Fe(II)-in-the-presence-of-zinc isotherm. For the majority of the NOM treatments, the addition of zinc either lowered or did not change the extent of Fe(II) sorption. However, 250 mg  $L^{-1}$  SHA resulted in decreased Fe(II) sorption with increasing zinc, while 75 mg  $L^{-1}$  SHA resulted in

increased Fe(II) sorption. The highest concentration of sorbed Fe(II) occurred at the lowest total zinc concentration for all NOMs. SRFA and SRHA did not substantially alter Fe(II) sorption in the presence of zinc.

A “baseline” Zn(II)-in-the-presence-of-Fe(II) sorption isotherm (solid line in Fig. 3C) was developed from the same no-NOM with-zinc (0.020 to 0.18 mM total zinc) hematite bioreduction experiments (Stone et al. 2002a). The dashed lines in Figure 3C represent 95% confidence intervals associated with this isotherm. In these experiments total Fe(II) concentrations ranged from 0.012 to 0.51 mM. The two lowest SHA concentrations increased zinc sorption for all zinc concentrations, while 250 mg L<sup>-1</sup> SHA always decreased zinc sorption. The highest increase in zinc sorption (155% compared to the no-NOM baseline) occurred with 75 mg L<sup>-1</sup> SHA. SRFA and SRHA did not substantially alter zinc sorption.

#### **4.4.3 SRNOM Equilibrium Dialysis**

The hematite bioreduction results with NOM and zinc revealed that NOM increased zinc inhibition and altered the sorption of both Fe(II) and Zn(II). To demonstrate that these NOMs also altered Me(II) aqueous speciation, a series of equilibrium dialysis experiments were performed with zinc and IHSS Suwannee River NOM (SRNOM). SRFA and SRHA were fractionated from SRNOM and SRNOM was found to contain ca. 95% SRFA. The ability of NOM to complex Me(II) is well established (Randhawa et al. 1965; Matsuda et al. 1970; Mandal et al. 2000), however, an objective of these experiments was to confirm that the Me(II) complexation capacity of a particular NOM could be predicted based on NOM acidity. For example, Stevenson (Stevenson 1994) proposed that Me(II) complexation capacity could be calculated by assuming that 1 mole of Me(II) would consume 2 moles of NOM acidity. Therefore, if the acidity of a NOM is known for the pH of an experiment, then Me(II)

complexation capacity is readily calculated. Results of proton titrations and calculations of acidity as a function of pH (in 10 mM NaCl solution) for several IHSS NOMs, including SRNOM, SRFA, SRHA and SHA, were provided courtesy of Dr. Michael Perdue (Georgia Tech). The results from eight individual dialysis experiments using a constant total zinc concentration of 0.153 mM with SRNOM concentrations ranging from 0 to 200 mg L<sup>-1</sup> are presented in Figure 4. The results indicate that the zinc complexation capacity of SRNOM was 1.89 mM g<sup>-1</sup> (R<sup>2</sup> = 0.99). At pH 6.8 SRNOM acidity was 4.08 meq g<sup>-1</sup> (M. Perdue, personal communication), thus the corresponding Me(II) complexation capacity would be 2.04 mM. Our direct measurements and the estimation technique are in excellent agreement. Therefore, Me(II) complexation capacities for SRFA, SRHA and SHA were estimated as 2.78 mM g<sup>-1</sup>, 1.99 mM g<sup>-1</sup>, and 2.02 mM g<sup>-1</sup>, respectively, based on measured acidity values at pH 6.8 in 10 mM NaCl solution.

#### **4.4.4 Impact on Ferric Citrate Bioreduction**

Bioreduction experiments were performed with ferric citrate to evaluate the effect of NOM on zinc inhibition using a soluble electron acceptor and to determine if these effects differed from those observed with hematite. Previous studies using ferric citrate (Stone et al. 2002a) showed that ferrihydrite could form according to MINTEQA2 calculations (Allison et al. 1991) when using a 3:1 molar ratio of citrate:Fe(III), however, the potential for ferrihydrite formation was deemed inconsequential for our experiments. Higher citrate concentrations (achieved by adding citric acid and neutralizing with NaOH) would have lowered the potential for ferrihydrite formation, however, additional citrate would have led to greater zinc-citrate complexation. Kinetic experiments were performed with ferric citrate and inhibition was calculated based on the decrease in the rate of Fe(II) production (Figure 5). The solid line in

Figure 5 represents the % inhibition-vs.-total zinc concentration for a series of no-NOM ferric citrate controls. The dashed lines represent the 95% confidence intervals associated with the no-NOM inhibition correlation. The  $IC_{50}$  for the no-NOM ferric citrate control was 0.284 mM total zinc (Stone et al. 2002a). The results presented in Figure 5 show that 150 mg L<sup>-1</sup> SRFA significantly decreased the sensitivity of zinc ( $IC_{50}$  232.7 mM total zinc) while 250 mg L<sup>-1</sup> SHA slightly increased zinc inhibition ( $IC_{50}$  0.245 mM total zinc). Free zinc concentrations were not calculated for these experiments because NOM-zinc complexation constants were not available. A summary of the ferric citrate results is presented in Table 2.

#### **4.4.5 Impact on Nitrate Bioreduction**

Bioreduction experiments were performed with nitrate to evaluate the effect of NOM on zinc inhibition with another soluble electron acceptor, this time with one that did not include a high ligand concentration (i.e., citrate). Kinetic experiments were performed with nitrate and inhibition was calculated based upon the decrease in the rate of nitrate reduction (Figure 6.) The solid line represents the % inhibition-vs.-total zinc concentration for a series of no-NOM nitrate controls (Stone et al. 2002a). The dashed lines represent the 95% confidence intervals associated with the no-NOM inhibition correlation. The  $IC_{50}$  for the no-NOM nitrate control was 0.0484 mM total zinc (Stone et al. 2002a). The results presented in Figure 6 show that all NOMs were found to either decrease or completely eliminate zinc inhibition during nitrate bioreduction. The greatest effect occurred for 1000 mg L<sup>-1</sup> SRFA where zinc inhibition was eliminated. The addition of 150 mg L<sup>-1</sup> SRFA increased the  $IC_{50}$  to 0.124 mM total zinc, and 250 mg L<sup>-1</sup> SHA increased the  $IC_{50}$  to 0.373 mM. A summary of the nitrate results is presented in Table 2.

#### 4.4.6 Impact of Manganese Addition

Hematite bioreduction experiments using manganese instead of zinc were performed to determine whether Mn(II), which has similar charge and chemical properties as both Zn(II) and Fe(II), may inhibit hematite bioreduction at similar concentrations as those observed with zinc. The manganese experiments were performed with two NOMs, 150 mg L<sup>-1</sup> SRFA and 250 mg L<sup>-1</sup> SHA, both of which were shown to increase zinc inhibition during hematite bioreduction (Figures 1 and 2, respectively). For the no-NOM control, manganese (0.020 to 1.82 mM) was shown to have little to no inhibitory effect (Figure 7A; IC<sub>50</sub> was 3.06 mM). Only the highest manganese concentration of 1.82 mM decreased Fe(II) production. Even though manganese did not inhibit hematite bioreduction in the absence of NOM, both SRFA and SHA increased manganese inhibition (Fig. 7A). The addition of 150 mg L<sup>-1</sup> SRFA decreased the IC<sub>50</sub> to 0.160 mM total manganese, and 250 mg L<sup>-1</sup> SHA decreased the IC<sub>50</sub> to 0.852 mM.

A “baseline” Fe(II)-in-the-presence-of-manganese sorption isotherm (solid line in Fig. 8A) was developed from a series of hematite bioreduction experiments performed in the absence of any NOM but in the presence of variable manganese concentrations (0.020 to 1.82 mM total manganese) (Stone et al. 2002b). A second “baseline” Mn(II)-in-the-presence-of-Fe(II) sorption isotherm (solid line in Fig. 8B) was also developed from these experiments (in which Fe(II) concentrations ranged from 0.104 to 0.200 mM). The dashed lines in Figures 8A and 8B represent 95% confidence intervals associated with these isotherms. Manganese was shown to be non-competitive with Fe(II), however, Fe(II) was slightly competitive with manganese (Stone et al. 2002b). The addition of SHA increased both Fe(II) and Mn(II) sorption, while the addition of SRFA did not alter Fe(II) sorption. SRFA addition did not alter Mn(II) sorption except for the

two highest dissolved manganese concentrations (0.580 and 1.113 mM) where manganese sorption increased (116%) and decreased (60%), respectively, compared to the no-NOM control.

The impact of manganese and NOMs on the rate of nitrate bioreduction was also examined (Fig. 7B). For the no-NOM control, manganese had no effect on nitrate bioreduction at the Mn(II) concentrations tested (0.020 to 1.82 mM). The addition of SRFA did not promote manganese inhibition of nitrate bioreduction, and was essentially indifferent compared to the no-NOM control. The addition of SHA actually stimulated nitrate bioreduction with increasing manganese.

#### **4.5 Discussion**

The modes for zinc inhibition during the biological reduction of hematite (Stone et al. 2002b) were reported as resulting from either coverage or "passivation" (Fredrickson et al. 2001; Zachara et al. 2001) of the hematite surface or through direct microbial toxicity of the *S. putrefaciens* by free zinc. The motive for this research was to determine if NOM addition would alleviate zinc inhibition previously observed during hematite bioreduction (Stone et al. 2002a). It was proposed that NOM addition would lower both the free and surface bound zinc concentrations through the formation of NOM-zinc complexation reactions. In addition, NOM could complex surface bound Fe(II) which was previously shown as a mechanism controlling the rate of Fe(III) oxide dissolution due to "passivation" of surface reactive sites (Urrutia et al. 1998; Roden et al. 1999).

The ability of NOMs to complex metals is related to the percentage of carboxylic acid present within the NOM structure that can readily exchange protons for divalent metals during ligand exchange reactions. The metal binding capabilities of NOMs are similar to those reported

for EDTA and NTA (Shuttleworth et al. 1993; Urrutia et al. 1999; Roden et al. 2002) where metal binding was accomplished primarily through strongly and weakly coordinated (inner and outer sphere) ligand exchange reactions. The IHSS NOMs used within this study represent a wide variety of physical and chemical characteristics, from a high molecular weight, high aromaticity, terrestrial soil humic acid to a low molecular weight, low acidity, aquatic humic and fulvic acid (SRFA and SRHA). Although the extent of Fe(II) production for hematite reduction varied considerably for the NOM amendments used (Fig. 1A), all amendments increased the sensitivity of zinc during the bioreduction process (Fig. 1B). These results were contrary to our initial hypothesis that NOM-zinc complexation would lessen the inhibitory effects of zinc during hematite bioreduction. All NOMs decreased the total zinc  $IC_{50}$  concentrations (Table 2) compared to controls for hematite bioreduction, with the greatest inhibitory effect occurring with the  $150 \text{ mg L}^{-1}$  SHA treatment. Contrasting these results were the NOM results for the two soluble electron acceptors (nitrate and ferric citrate, Figs. 5, 6), where NOM addition either had no effect (SHA for ferric citrate, Fig. 5) or decreased zinc inhibition (all other treatments, Figs. 5, 6) compared to the no-NOM controls. The decrease in zinc inhibition was mainly attributed to the reduction of “free” zinc concentrations due to NOM-zinc complexation. The difference in the responses for NOM addition between the solid and aqueous phase systems indicated that zinc inhibition for the hematite system (solid phase) was primarily influenced by surface coverage mechanisms and not by direct toxicity of the cells by “free” zinc. While free zinc has been shown to be toxic to DMRB growth (Stone et al. 2002a), had both the solid and aqueous phase experiments displayed similar inhibitory responses for NOM addition, one could conclude that the increased inhibition for NOM was related to direct microbial toxicity by free or non-surface sorbed zinc. The premise for this assumption was due to the fact that DMRB was the only



available sorption site for both NOM and zinc for both aqueous phase experiments (ferric citrate and nitrate). The DMRB surface has been shown to have high metal binding affinities (Ledin et al. 1999) mainly with carboxyl and phosphoryl surface sites on cell walls (Fein et al. 2001). Therefore by lowering the free zinc concentration through NOM complexation, the driving force behind toxicity related to DMRB zinc sorption would be minimized. However, the response of NOM addition for the hematite system actually increased the inhibitory effect of zinc, thus suggesting that surface sorption mechanisms between zinc and NOM appeared to control inhibition under these conditions.

All four SHA concentrations increased zinc inhibition during hematite bioreduction. Further analysis of the SHA results revealed that the degree of metal sorption [Fe(II) and Zn(II)], and in particular, the extent of saturation of the NOM metal complexation capacity, varied considerably for the four SHA concentrations employed. Using the acidity constant correlation (Stevenson 1994; Royer et al. 2002a), the SHA metal complexation capacities ranged from 0.505 mM Me(II) for 250 mg L<sup>-1</sup> SHA to 0.030 mM Me(II) for 15 mg L<sup>-1</sup> SHA (Table 1). Factors that controlled the degree or extent of NOM metal saturation included the concentrations of NOM used and the extent of Fe(II) production relative to the amount of added Me(II). Fe(II) production (Fig. 1A) was highest for 250 mg L<sup>-1</sup> SHA with no added zinc [0.576 mM total Fe(II)], which exceeded the metal complexation capacity [0.504 mM Me(II)] by 13%. Fe(II) sorption under these same conditions (in the absence of zinc, Fig. 3A) resulted in only a slight increase of Fe(II) sorption (21%). The ensuing addition of zinc lowered Fe(II) production (Fig. 1A), but the total concentration of metals present [biogenic Fe(II) plus added Zn(II)] never exceeded the complexation capacity for 250 mg L<sup>-1</sup> SHA. These “under-saturated” conditions resulted in lowering both the Fe(II) (Fig. 3B) and zinc (Fig. 3C) sorption to the cells and

hematite compared to the no-amendment controls. Similar occurrences have been reported in the literature, most notably by Duker et al. (Duker et al. 1995) who found zinc sorption onto goethite decreased in the presence a fulvic acid which was under-saturated with respect to its metal complexation capacity. The reported decrease in zinc sorption onto goethite was attributed to sorbed fulvic acid acting as a physical barrier and preventing additional zinc sorption. The “passifying” or obstruction of hematite surface sites by sorbed SHA has also been reported (Redman et al. 2002).

In contrast, the three lowest SHA concentrations were found to increase both Fe(II) (Fig. 3B) and zinc sorption (Fig. 3C) compared to the no-amendment control. These SHA concentrations had significantly less metal binding capacities due to their lower overall mass (Table 1). The total Fe(II) produced in the absence of zinc (Fig. 1A) exceeded the SHA metal binding capacities by 173 to 600% . As a result, these “over-saturated” SHAs were unable to bind the majority of free and surface sorbed metals in the system, leaving a higher concentration of metals un-complexed and capable of sorbing or remaining in solution. In addition, these SHAs also had a greater affinity to sorb to hematite compared to the other NOMs (Murphy et al. 1990). The higher sorption affinity of SHA, mainly attributed its high aromaticity and lower oxygen-to-carbon ratio, allowed additional sorption of un-complexed or “free” metals through the formation of a ternary SHA complex on the surface of the hematite. This ternary surface complex, as described by Murphy et al. (Murphy et al. 1994), bonds free metals between the hydroxyl site on the hematite and the ionized groups on the NOM. The formation of these complexes therefore explains the increase in Fe(II) and zinc sorption that occurred for the three lowest SHA concentrations. SRFA and SRHA would be expected to have a lower attraction to hematite compared to SHA due to their lower molecular weight, carbon content, and aromaticity

(Murphy et al. 1990). Additionally, both SRFA and SRHA were under-saturated with respect to their metal complexation capacities at zinc concentrations greater than 0.050 mM total zinc.

The results for manganese addition with NOMs (Fig. 6A) was similar to those observed with zinc; NOM addition increased the sensitivity of the metal during hematite bioreduction. The extent of Fe(II) (Fig. 8A) and Mn(II) (Fig. 8B) sorption varied for SHA and SRFA, mainly due to differences associated with their metal complexation capacity. For SHA, the metal complexation capacity [0.505 mM Me(II)] was exceeded for all concentrations of manganese employed, initially as a result of the large concentration of biogenic Fe(II) produced, but later by the addition of manganese. This over-saturated state, coupled with SHA having a high affinity to adhere to hematite, resulted increased Fe(II) and Mn(II) sorption compared to the no-NOM control. It appeared that high concentrations of free Fe(II) and Mn(II) were entrapped within ternary surface complexes (Murphy et al. 1994) on the hematite and cell surfaces, similar to those observed for SHA in the presences of zinc. In contrast, SRFA was both under-saturated (for ca. < 0.364 mM total manganese) with respect to metal binding capacity and had less attraction to hematite, resulting in no change in both Fe(II) and Mn(II) sorption. Mn(II) sorption increased (Fig. 8B) once the SRFA metal binding capacity was exceeded.

Taken together, these results suggest that Zn(II)-NOM and Mn(II)-NOM complexes sorbed to hematite were potent inhibitors of hematite bioreduction. In the absence of zinc or manganese, all NOMs tested significantly enhanced hematite bioreduction which suggested that Fe(II)-NOM complexes did not specifically inhibit bioreduction. In fact, Royer et al. (Royer et al. 2002a) proposed that Fe(II) complexation by NOM reduced the “passivation” of the hematite surface by sorbed Fe(II) and increased the thermodynamic driving force for continued Fe(III) reduction by decreasing the “free” dissolved  $\text{Fe}^{2+}$  concentration. As demonstrated in the nitrate

bioreduction experiments, soluble Zn(II)-NOM and Mn(II)-NOM complexes did not inhibit anaerobic respiration but instead decreased zinc inhibition (Fig. 6) or increased the stimulatory effect of manganese (Fig. 7B). Even in the presence of 6 mM citrate for the ferric citrate system, 150 mg L<sup>-1</sup> SRFA altered zinc speciation (e.g., by forming Zn(II)-SRFA complexes) and decreased zinc inhibition (Fig. 5). Based on the results obtained for the soluble electron acceptors ferric citrate and nitrate, NOMs decreased zinc inhibition by forming Zn(II)-NOM complexes (Fig. 4) and subsequently reducing “free” dissolved Zn<sup>2+</sup> concentrations.

The results for the hematite experiments demonstrated that the NOMs increased the sorption of Fe(II) (Figs. 3A, 3B and 8A), Zn(II) (Fig. 3C) and Mn(II) (Fig. 8B). The humic acids (SHA and SRHA) increased Me(II) sorption more than the fulvic acid (SRFA), however, the highest concentration of SHA (250 mg L<sup>-1</sup>) decreased both Fe(II) and Zn(II) sorption (Figs. 3B and 3C, respectively). Interestingly, in the presence of manganese, 250 mg L<sup>-1</sup> SHA increased both Fe(II) and Mn(II) sorption (Figs. 8A and 8B, respectively). In the absence of NOM, manganese did not inhibit hematite (Fig. 7A) or nitrate bioreduction (Fig. 7B). Manganese is an essential trace nutrient and was selected for these experiments because it did not previously cause toxicity during hematite bioreduction (Stone et al. 2002b). Because NOMs caused an innocuous trace metal [Mn(II)] to become inhibitory to hematite bioreduction and soluble Mn(II)-NOM complexes were not inhibitory to nitrate bioreduction, sorbed Mn(II)-NOM complexes likely caused inhibition of hematite bioreduction.

In the case of zinc, several modes of respiration inhibition are possible. It was reported previously that zinc is directly lethal to *S. putrefaciens* CN32 (Stone et al. 2002a). Ferrozine, a Fe(II)-specific complexant, was used as an amendment in hematite bioreduction experiments to show zinc sorption increased while Fe(II) sorption decreased, and that zinc inhibition increased

(Stone et al. 2002b). This result implied that sorbed zinc (sorbed to either hematite or DMRB surfaces) was a more potent inhibitor of hematite bioreduction than dissolved zinc. In the current experiments with NOM, two separate mechanisms appeared to control zinc inhibition. The increased sorption of zinc that occurred for the over-saturated NOMs indicated that the formation of ternary NOM-zinc complexes was the primary mode of zinc inhibition, primarily through surface “passivation” of the hematite surface or increased exposure to surface bound zinc. For conditions where the NOM was under-saturated with respect to its metal complexation capacity, the decreased zinc sorption indicated that the specific zinc-NOM species formed became more toxic than the “free” zinc for *S. putrefaciens*, although the precise mode of toxicity for these compounds was unresolved.

#### **4.6 Acknowledgments**

Research supported by the Natural and Accelerated Bioremediation Research Program (NABIR), Office of Biological and Environmental Research (OBER), Office of Energy Research, U.S. Department of Energy (DOE), Grants no. DE-FG02-98ER62691 and No. DE-FG02-01ER63180 is gratefully acknowledged.

#### 4.7 Literature Cited

- Ali, M. A. and D. A. Dzombak (1996). "Interactions of copper, organic acids, and sulfate in goethite suspensions." Geochimica et Cosmochimica Acta **60**(24): 5045-5053.
- Allison, J. D., D. S. Brown, et al. (1991). MINTEQA2/PRODEFA2, a geochemical assessment model for environmental systems: Version 3.0 users manual. Athens, GA, U.S. Environmental Protection Agency.
- Chaudri, A. M., B. P. Knight, et al. (1999). "Determination of acute Zn toxicity in pore water from soils previously treated with sewage sludge using bioluminescence assays." Environmental Science & Technology **33**(11): 1880-1885.
- Chaudri, A. M., K. Lawlor, et al. (2000). "Response of a Rhizobium-based luminescence biosensor to Zn and Cu in soil solutions from sewage sludge treated soils." Soil Biology & Biochemistry **32**(3): 383-388.
- Duker, A., A. Ledin, et al. (1995). "Adsorption of zinc on colloidal (hydr)oxides of Si, Al and Fe in the presence of a fulvic-acid." Applied Geochemistry **10**(2): 197-205.
- Fein, J. B., A. M. Martin, et al. (2001). "Metal adsorption onto bacterial surfaces: Development of a predictive approach." Geochimica et Cosmochimica Acta **65**(23): 4267-4273.
- Fredrickson, J. K., J. M. Zachara, et al. (1998). "Biogenic iron mineralization accompanying the dissimilatory reduction of hydrous ferric oxide by a groundwater bacterium." Geochimica et Cosmochimica Acta **62**(19-20): 3239-3257.
- Fredrickson, J. K., J. M. Zachara, et al. (2001). "Biotransformation of Ni-substituted hydrous ferric oxide by an Fe(III)-reducing bacterium." Environmental Science & Technology **35**(4): 703-712.
- Jeon, B. H., B. A. Dempsey, et al. (2001). "Reactions of ferrous iron with hematite." Colloids and Surfaces a-Physicochemical and Engineering Aspects **191**(1-2): 41-55.
- Karthikeyan, K. G. and J. Chorover (2000). "Effects of solution chemistry on the oxidative transformation of 1-naphthol and its complexation with humic acid." Environmental Science & Technology **34**(14): 2939-2946.
- Knight, B. and S. P. McGrath (1995). "A method to buffer the concentrations of free Zn and Cd ions using a cation-exchange resin in bacterial toxicity studies." Environmental Toxicology and Chemistry **14**(12): 2033-2039.
- Ledin, M., C. Krantz-Rulcker, et al. (1999). "Microorganisms as metal sorbents: comparison with other soil constituents in multi-compartment systems." Soil Biology & Biochemistry **31**(12): 1639-1648.
- Mandal, R., M. S. A. Salam, et al. (2000). "Competition of Ca(II) and Mg(II) with Ni(II) for binding by a well-characterized fulvic acid in model solutions." Environmental Science & Technology **34**(11): 2201-2208.
- Matsuda, K. and S. Ito (1970). "Adsorption strength of zinc for soil humus." Soil Science and Plant Nutrition **16**(1): 1-10.
- Murphy, E. M., J. M. Zachara, et al. (1990). "Influence of mineral-bound humic substances on the sorption of hydrophobic organic-compounds." Environmental Science & Technology **24**(10): 1507-1516.

- Murphy, E. M., J. M. Zachara, et al. (1994). "Interaction of hydrophobic organic-compounds with mineral-bound humic substances." Environmental Science & Technology **28**(7): 1291-1299.
- Randhawa, N. S. and F. E. Broadbent (1965). "Soil organic matter-metal complexes: 6. Stability constants of zinc-humic acid complexes at different pH values." Soil Science **99**(6): 362-366.
- Redman, A. D., D. L. Macalady, et al. (2002). "Natural organic matter affects arsenic speciation and sorption onto hematite." Environmental Science & Technology **36**(13): 2889-2896.
- Ritchie, J. M., M. Cresser, et al. (2001). "Toxicological response of a bioluminescent microbial assay to Zn, Pb and Cu in an artificial soil solution: relationship with total metal concentrations and free ion activities." Environmental Pollution **114**(1): 129-136.
- Roden, E. E. and M. M. Urrutia (1999). "Ferrous iron removal promotes microbial reduction of crystalline iron(III) oxides." Environmental Science & Technology **33**(11): 1847-1853.
- Roden, E. E. and M. M. Urrutia (2002). "Influence of biogenic Fe(II) on bacterial crystalline Fe(III) oxide reduction." Geomicrobiology Journal **19**(2): 209-251.
- Royer, R. A., W. D. Burgos, et al. (2002a). "Enhancement of hematite bioreduction by natural organic matter." Environmental Science & Technology **36**(13): 2897-2904.
- Royer, R. A., W. D. Burgos, et al. (2002b). "Enhancement of biological reduction of hematite by electron shuttling and Fe(II) complexation." Environmental Science & Technology **36**(9): 1939-1946.
- Sani, R. K., B. M. Peyton, et al. (2001). "Copper-induced inhibition of growth of *Desulfovibrio desulfuricans* G20: Assessment of its toxicity and correlation with those of zinc and lead." Applied and Environmental Microbiology **67**(10): 4765-4772.
- Shuttleworth, K. L. and R. F. Unz (1991). "Influence of metals and metal speciation on the growth of filamentous bacteria." Water Research **25**(10): 1177-1186.
- Shuttleworth, K. L. and R. F. Unz (1993). "Sorption of Heavy-Metals to the Filamentous Bacterium *Thiothrix* Strain A1." Applied and Environmental Microbiology **59**(5): 1274-1282.
- Stevenson, F. J. (1994). Humus chemistry: genesis, composition, reactions. New York, John Wiley and Sons, Inc.
- Stone, J. J., W. D. Burgos, et al. (2002a). "Impact of zinc on biological Fe(III) and NO<sub>3</sub><sup>-</sup> reduction by *Shewanella putrefaciens* CN32." To be submitted for publication.
- Stone, J. J., W. D. Burgos, et al. (2002b). "Modes of inhibition by zinc on the biological reduction of hematite by *Shewanella putrefaciens* CN32." To be submitted for publication.
- Thorn, K. A., D. W. Folan, et al. (1989). Characterization of the international humic substances society standard and reference fulvic and humic acids by solution state carbon-13 and hydrogen-1 nuclear magnetic resonance spectroscopy, U.S. Geological Survey.
- Urrutia, M. M., E. E. Roden, et al. (1998). "Microbial and surface chemistry controls on reduction of synthetic Fe(III) oxide minerals by the dissimilatory iron-reducing bacterium *Shewanella* alga." Geomicrobiology Journal **15**(4): 269-291.
- Urrutia, M. M., E. E. Roden, et al. (1999). "Influence of aqueous and solid-phase Fe(II) complexants on microbial reduction of crystalline iron(III) oxides." Environmental Science & Technology **33**(22): 4022-4028.

Zachara, J. M., J. K. Fredrickson, et al. (2001). "Solubilization of Fe(III) oxide-bound trace metals by a dissimilatory Fe(III) reducing bacterium." Geochimica et Cosmochimica Acta **65**(1): 75-93.



Table 4.1 Characteristics of NOM

NOM	Source	Organic radical content [spins g <sup>-1</sup> x 10 <sup>17</sup> ] <sup>a</sup>	Acidity @ pH 6.8 [mequiv g <sup>-1</sup> ] <sup>b</sup>	Me(II) complexation capacity [mM Me(II) g <sup>-1</sup> ] <sup>c</sup>	Aromaticity [%] <sup>d</sup>	Carbon Content [%] <sup>a</sup>	O/C ratio <sup>a</sup>
Soil HA	terrestrial	12.9	4.03	2.02	50	58.1	0.586
Suwannee River HA	aquatic	1.15	3.97	1.99	37	52.6	0.809
Suwannee River FA	aquatic	0.54	5.55	2.78	24	53.0	0.828
Suwannee River NOM	aquatic	0.54	4.08	2.04	24	48.8	0.814

a. From IHSS Standard and Reference Collection literature.

b. From Micheal Purdue at Georgia Tech.

c. Me(II) complexation capacity calculated by assuming 1 mole of Me(II) consumes 2 moles of NOM acidity (Stevenson 1994).

d. From Thorn et al.(Thorn et al. 1989).

Table 4.2 Summary of zinc IC<sub>50</sub><sup>a</sup> values for the biological reduction of hematite, ferric citrate, and nitrate by *S. putrefaciens*.

Process	Parameters	Total Me(II) IC <sub>50</sub>
Hematite, no amendments (control)	2 g L <sup>-1</sup> hematite, 10mM PIPES, 10 <sup>8</sup> cells mL <sup>-1</sup> , pH 6.8, 5 d	0.211 mM Zn(II) 3.06 mM Mn(II)
Hematite, 250 mg L <sup>-1</sup> SHA		0.0563 mM Zn(II) 0.852 mM Mn(II)
Hematite, 150 mg L <sup>-1</sup> SHA		0.0245 mM Zn(II)
Hematite, 75 mg L <sup>-1</sup> SHA		0.0625 mM Zn(II)
Hematite, 15 mg L <sup>-1</sup> SHA		0.0784 mM Zn(II)
Hematite, 250 mg L <sup>-1</sup> SRHA		0.0849 mM Zn(II)
Hematite, 150 mg L <sup>-1</sup> SRFA		0.0685 mM Zn(II) 0.160 mM Mn(II)
Ferric citrate, no amendments (control)	2 mM ferric citrate, 4 mM citric acid, 10 <sup>8</sup> cells mL <sup>-1</sup> , pH 6.8	0.283 mM Zn(II)
Ferric citrate, 250 mg L <sup>-1</sup> SHA		0.245 mM Zn(II)
Ferric citrate, 150 mg L <sup>-1</sup> SRFA		232.7 mM Zn(II)
Nitrate, no amendments (control)	20 mg L <sup>-1</sup> NO <sub>3</sub> -N, 10 <sup>8</sup> cells mL <sup>-1</sup> , pH 6.8	0.0484 mM Zn(II) No Mn(II) inhibition
Nitrate, 250 mg L <sup>-1</sup> SHA		0.373 mM Zn(II) No Mn(II) inhibition
Nitrate, 150 mg L <sup>-1</sup> SRFA		0.124 mM Zn(II) No Mn(II) inhibition
Nitrate, 1000 mg L <sup>-1</sup> SRFA		No Zn(II) inhibition

<sup>a</sup> Defined as inhibitory concentration of Me(II) where a 50% reduction of the biological process occurs relative to a no Me(II) control (Sani et al. 2001). The IC<sub>50</sub> was calculated from a least squares line obtained from the data.

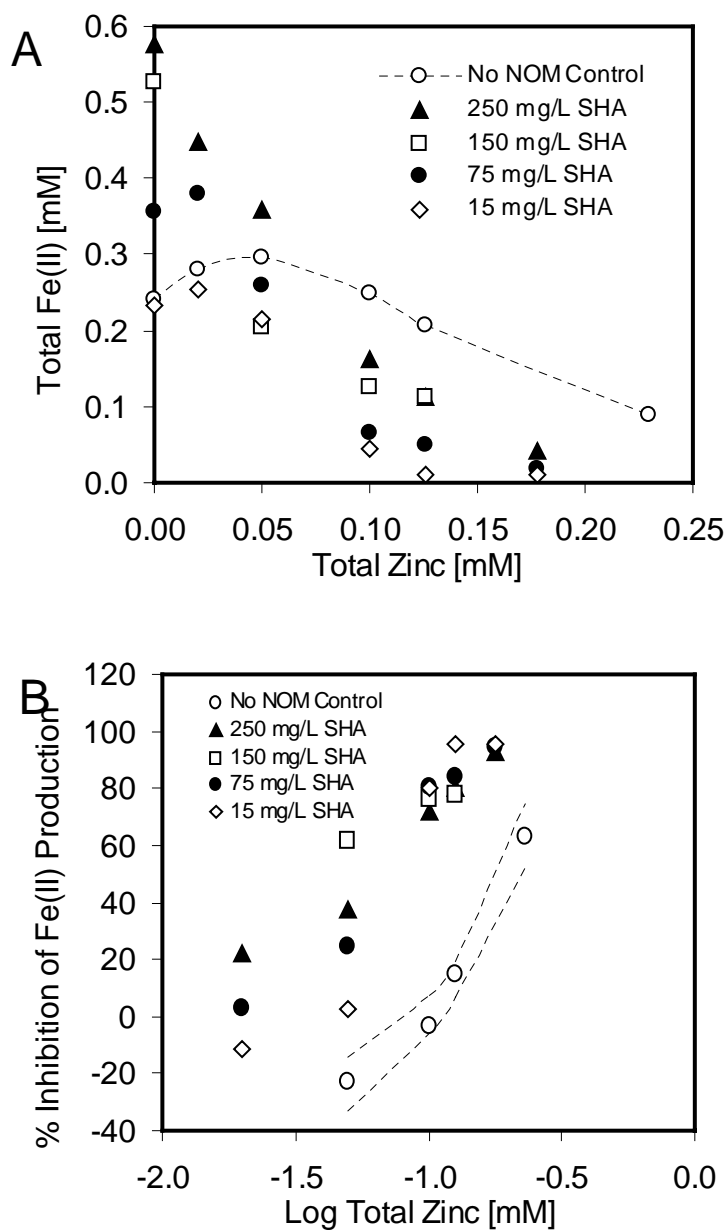


Figure 4.1 (A) Total Fe(II) production and (B) percent inhibition of Fe(II) production as a function of total zinc for (○) no amendment control, (▲) 250 mg L<sup>-1</sup> SHA, (□) 150 mg L<sup>-1</sup> SHA, (●) 75 mg L<sup>-1</sup> SHA, (◇) 15 mg L<sup>-1</sup> SHA. Experiments performed using 2 g L<sup>-1</sup> hematite in 10mM PIPES, pH 6.8, 10<sup>8</sup> *S. putrefaciens* cells mL<sup>-1</sup>, 5 d. Dashed line in (B) represents 95% confidence interval. All values are means of three replicates.

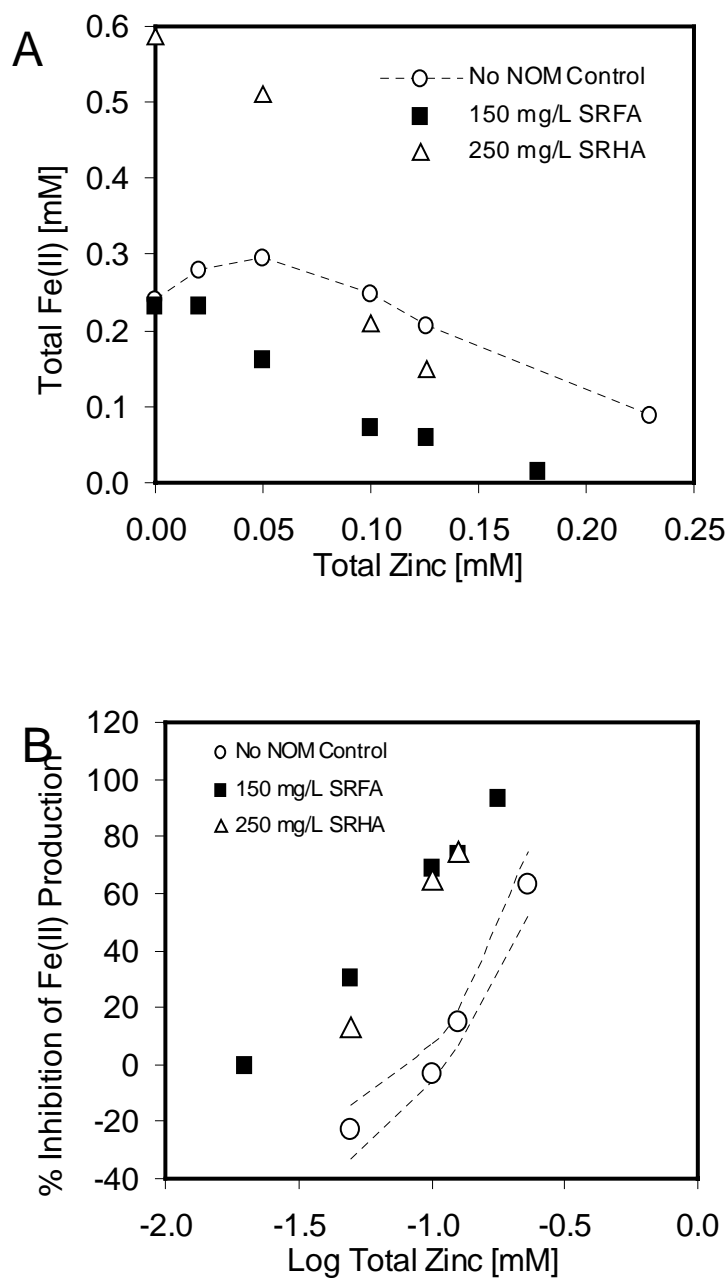


Figure 4.2 (A) Total Fe(II) production and (B) percent inhibition of Fe(II) production as a function of total zinc for (■) 150 mg L<sup>-1</sup> SRFA, (△) 250 mg L<sup>-1</sup> SRHA. Experiments performed using 2 g L<sup>-1</sup> hematite in 10mM PIPES, pH 6.8, 10<sup>8</sup> *S. putrefaciens* cells mL<sup>-1</sup>, 5 d. Dashed line in (B) represents 95% confidence interval. All values are means of three replicates.

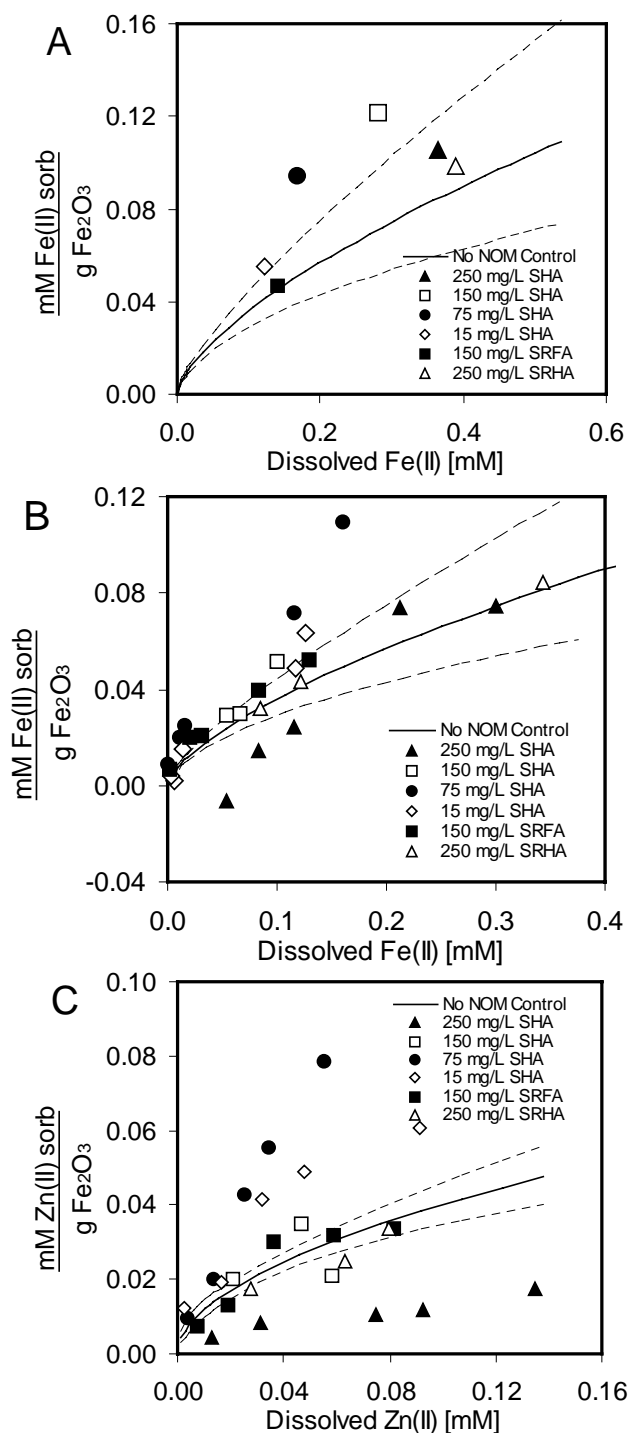


Figure 4.3 The sorption distribution of (A) Fe(II) without zinc, (B) Fe(II) with variable zinc (0.020 to 0.178 mM total zinc), (C) Zn(II) with variable Fe(II) [0.012 to 0.51 mM total Fe(II)] for ( $\blacktriangle$ ) 250 mg L<sup>-1</sup> SHA, ( $\square$ ) 150 mg L<sup>-1</sup> SHA, ( $\bullet$ ) 75 mg L<sup>-1</sup> SHA, ( $\diamond$ ) 15 mg L<sup>-1</sup> SHA, ( $\blacksquare$ ) 150 mg L<sup>-1</sup> SRFA, ( $\triangle$ ) 250 mg L<sup>-1</sup> SRHA addition during the 5 d biological reduction of 2 g L<sup>-1</sup> hematite, 10<sup>8</sup> *S. putrefaciens* cells mL<sup>-1</sup>, pH 6.8. Solid line is Freundlich (non-log) isotherm trend line (for Fe(II):  $R^2 = 0.890$ ,  $K = 0.01156 \text{ mM Fe(II) g}^{-1}$ ,  $1/n = 0.6603$ ; for Zn(II):  $R^2 = 0.894$ ,  $K = 0.01475 \text{ mM Zn(II) g}^{-1}$ ,  $1/n = 0.532$ ) for the no amendment control and dashed line represents 95% confidence interval. Results are 5 d composite samples.

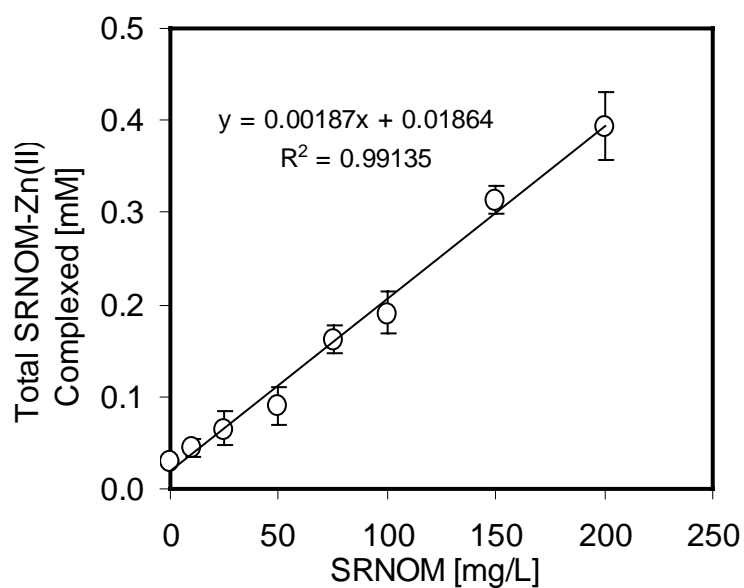


Figure 4.4 The SRNOM zinc complexation isotherm using 500 MWCO dialysis separation at pH 6.8 with 0.153 mM total zinc. Results are 180 d composite samples. SRNOM concentration ranged from 0 mg L<sup>-1</sup> for controls to 200 mg L<sup>-1</sup>. All values are means of three replicates ( $\pm$  standard deviation).

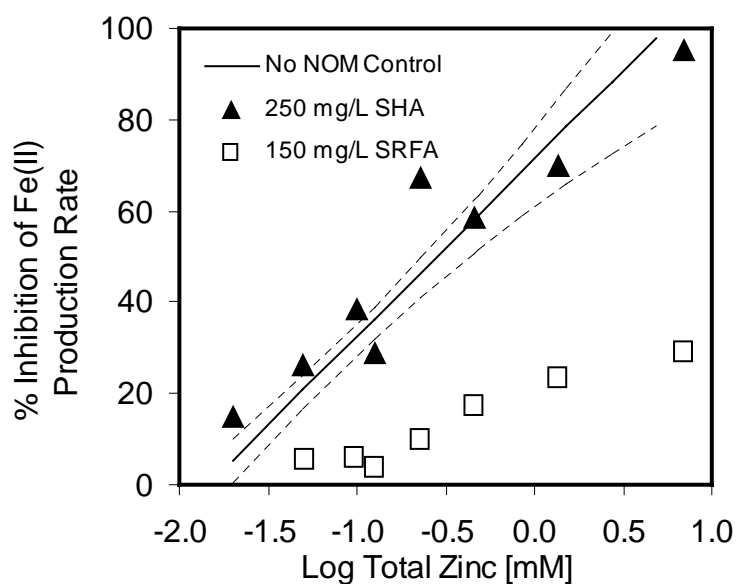


Figure 4.5 The percent of inhibition of the rate of Fe(II) production as a function of log total zinc for the addition of ( $\blacktriangle$ )  $250 \text{ mg L}^{-1}$  SHA, ( $\square$ )  $150 \text{ mg L}^{-1}$  SRFA during the biological reduction of  $2 \text{ mM}$  ferric citrate in  $10 \text{ mM}$  PIPES,  $4 \text{ mM}$  citric acid at pH 6.8. Zinc addition ranged from  $0.020$  to  $6.88 \text{ mM}$  total zinc. Solid line represents the no-NOM control and dashed line the 95% confidence interval. Values are means of three replicates.

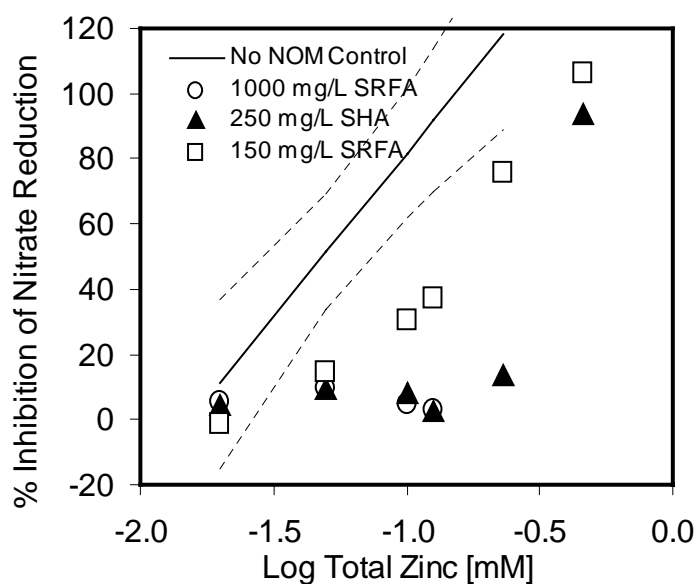


Figure 4.6 The percent inhibition of the rate of nitrate reduction as a function of log total zinc with the addition of ( $\circ$ )  $1000 \text{ mg L}^{-1}$  SRFA, ( $\square$ )  $150 \text{ mg L}^{-1}$  SRFA, ( $\blacktriangle$ )  $250 \text{ mg L}^{-1}$  SHA. Solid line represents the no-NOM control and dashed line the 95% confidence interval. Solutions contain  $10 \text{ mM}$  PIPES,  $14.44 \text{ g L}^{-1}$   $\text{KNO}_3$  (equivalent to  $20 \text{ mg NO}_3\text{-N L}^{-1}$ ),  $10^8 \text{ cells mL}^{-1}$  at pH 6.8. Zinc addition ranged from  $0 \text{ mM}$  for biotic and abiotic controls to  $0.459 \text{ mM}$  total zinc. Values are means of three replicates.



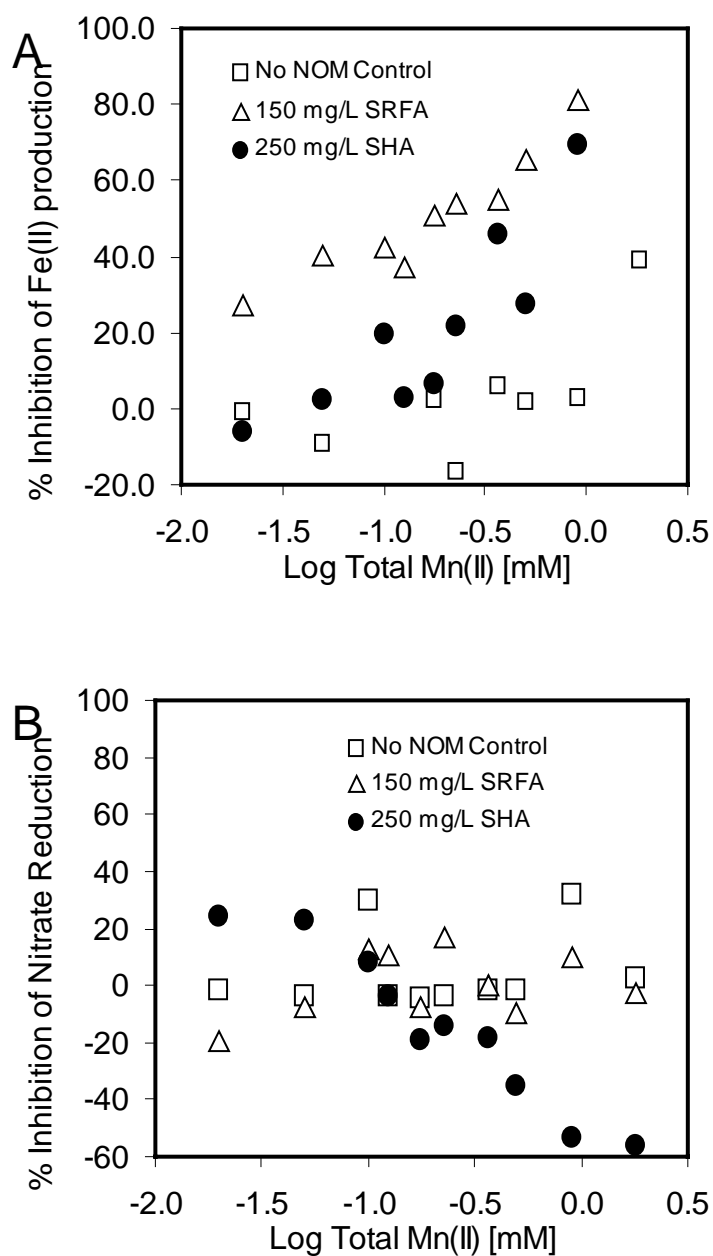


Figure 4.7 The percent inhibition of (A) total Fe(II) production during hematite reduction and (B) rate of nitrate reduction as a function of log total manganese addition for (□) no-NOM control, (△) 150 mg L<sup>-1</sup> SRFA, (●) 250 mg L<sup>-1</sup> SHA addition. All values are means of three replicates.

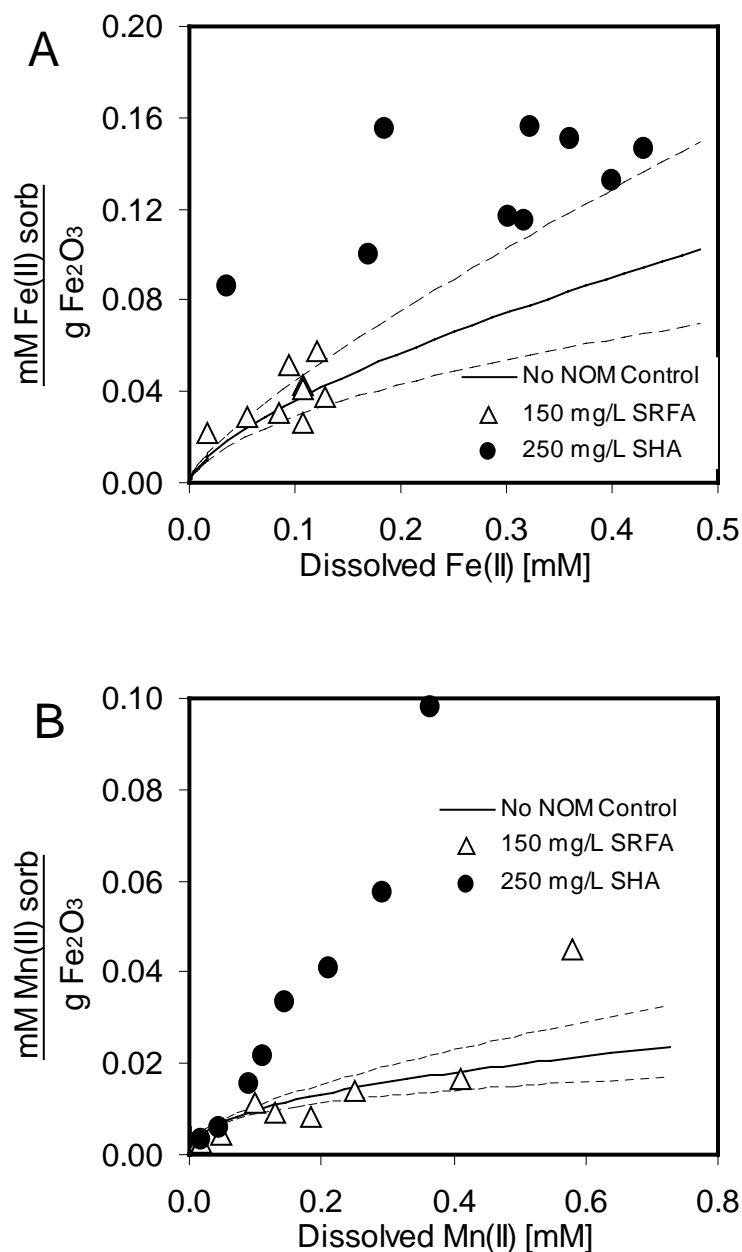


Figure 4.8 The sorption distribution of (A) Fe(II) with variable Mn(II) (0.020 to 0.910 mM total manganese), (B) Mn(II) with variable Fe(II) [0.104 to 0.200 mM total Fe(II)] for ( $\Delta$ ) 150 mg L<sup>-1</sup> SRFA, ( $\bullet$ ) 250 mg L<sup>-1</sup> SHA addition during the 5 d biological reduction of 2 g L<sup>-1</sup> hematite, 10<sup>8</sup> *S. putrefaciens* cells mL<sup>-1</sup>, pH 6.8. Solid line is Freundlich (non-log) isotherm trend line (for Fe(II): R<sup>2</sup> = 0.890, K = 0.01156 mM Fe(II) g<sup>-1</sup>, 1/n = 0.6603; for Mn(II): R<sup>2</sup> = 0.780, K = 0.00452 mM Mn(II) g<sup>-1</sup>, 1/n = 0.448) for the no-amendment control and dashed line represents 95% confidence interval. Results are 5 d composite samples.

# Curriculum Vitae

## James J. Stone, Ph.D., P.E.

### Education:

Ph.D., Environmental Engineering, The Pennsylvania State University, University Park, PA, 2002  
M.S., Environmental Engineering, Virginia Polytechnic Institute and State University, Blacksburg, VA, 1995.  
B.S., Civil Engineering (Environmental), Virginia Polytechnic Institute and State University, Blacksburg, VA 1993.

### Publications:

Stone, J.J., Burgos, W.D., Royer, R.A., Dempsey, B.A. Impact of Zinc on Biological Fe(III) and NO<sub>3</sub><sup>-</sup> Reduction by *Shewanella putrefaciens* CN32. To be submitted to Environmental Science and Technology January 2003.

Stone, J.J., Burgos, W.D., Royer, R.A. Modes of Inhibition by Zinc on the Biological Reduction of Hematite by *Shewanella putrefaciens* CN32. To be submitted to Geomicrobiology Journal January 2003.

Stone, J.J., Burgos, W.D., Royer, R.A., Dempsey, B.A., Unz, R.F. The Effect of Natural Organic Matter on Zinc Inhibition of Hematite Bioreduction using *Shewanella putrefaciens* CN32. To be submitted to Environmental Science and Technology January 2003.

Burgos, W.D., Fang, Y., Royer, R.A., Yeh, G.T., Stone, J.J., Dempsey, B.A. Reaction-Based Modeling of Quinone-Mediated Bacteria Iron(III) Reduction. Submitted to Geochimica Cosmochimica Acta August 2002.

Stone, J.J. Laboratory Studies Using Sodium-Based Waste Simulate ADL 26-94, Masters Thesis, Virginia Polytechnic and State University, 1995.

### Presentations:

Stone, J.J., Burgos, W.D., Royer, R.A. Effects of Reactive Surface Area and DIRB Concentrations on Zinc Inhibition During Dissimilatory Iron Reduction of Hematite. Poster Presentation. The American Society for Microbiology 102<sup>nd</sup> General Meeting, Salt Lake City, UT, May 2002.

Stone, J.J., Burgos, W.D., Royer, R.A. Impact of Zinc on Biological Reduction of Hematite. Oral Presentation. Proceedings of the 6<sup>th</sup> International Conference on the Biogeochemistry of Trace Elements, Guelph, Ontario, Canada, July 2001.

Stone, J.J., Burgos, W.D., Royer, R.A. Impact of Zinc on Biological Reduction of Hematite Using the Dissimilatory Iron Reducing Bacterium *Shewanella putrefaciens*. Poster Presentation. The 11<sup>th</sup> Annual Goldschmidt Conference, Hot Springs, VA, May 2001.

Stone, J.J., Burgos, W.D., Royer, R.A. Impact of Zinc on Biological Reduction of Hematite. Oral Presentation. Allegheny Branch of the American Society for Microbiology Fall Meeting, State College, PA, October 2000.

Dempsey, B.A., Jeon, B.H., Stone, J.J., Royer, R.A., Burgos, W.D. Adsorption of Fe(II) & Zn(II) on Ferric Oxides. Oral Presentation. 74<sup>th</sup> Colloid and Surface Science Symposium, Bethlehem, PA, June 2000.

### Professional Societies:

Registered Professional Engineer, Colorado  
American Society of Civil Engineers  
Water Environment Federation